WARWICK

PKPD Modelling to Assess the Effects of Anti-Cancer Agents on Tumour Volume

ES97N Technical Report

Luke Ross

MSc in Biomedical Engineering

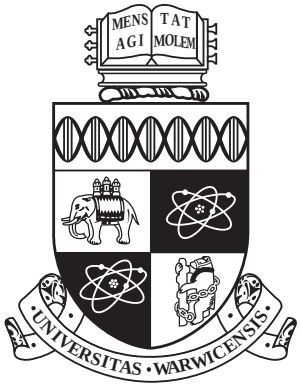

School of Engineering

University of Warwick

Supervisor: Professor Mike Chappell

3rd September, 2024

Declaration Statement

A dissertation submitted in partial fulfilment of the requirements for the MSc in Biomedical Engineering at The University of Warwick.

Acknowledgments

In completing this project I want to extend my gratitude and appreciation to the following individuals:

Honorary Professor at The University of Warwick J Yates who provided valuable insight into the theoretical background of the subject matter, took time to explain the provided data, and answered any questions regarding GlaxoSmithKline's objectives.

My project supervisor Professor M. Chappell, without whose support and encouragement it would not have been such an enjoyable experience. His expertise and suggestions contributed to the completion of this project.

Finally I want to thank my family and friends for their support while carrying out my Masters dissertation.

Abstract

The thesis at hand will assess therapeutics with antiproliferative effects to show how tumour spheroids respond to such anti-cancer agents through mathematical modelling. Implications and vulnerabilities of administering the chemotherapeutics docetaxel and carboplatin separately and in combination are comprehensively addressed through prior works and findings observed in this thesis. Parameter estimates will be conducted with novel pharmacokinetic and pharmacodynamic models which has been validated by means of structural identifiability analysis. GlaxoSmithKline oversaw and provided access to the preclinical dataset utilised to procure performance metrics and visual predictive checks determining the credibility of mathematical models used for simulating tumour growth with various dynamics; specifically when the two chemotherapeutics are administered separately or in combination. Alternatively, a vehicle agent is administered to determine tumour growth with no treatment regimen so comparisons between various therapeutic classes can be assessed. To conclude, forward simulations at various dosing levels are conducted to predict therapeutic windows and doses.

Keywords: structural identifiability, parameter estimates, compartmental modelling, pharmacology, tumours, therapeutics, toxicity.

Abbreviations

ACA Anti-Cancer Agent

ADME Absorption, Distribution, Metabolism, Elimination

AIC Akaike Information Criterion

BIC Bayesian Information Criterion

CHD Coronary Heart Disease

CoV Coefficient of Variation

DAISY Differential Algebra Identifiability of Systems

DDI Drug-Drug Interaction

EAR Exact Arithmetic Rank

GF Growth Factor

GSK GlaxoSmithKline

IBC Invasive Breast Carcinoma

IP Intraperitoneal

IPE Initial Parameter Estimation

IV Intravenous

MLE Maximum Likelihood Estimation

MM Mathematical Model

NLME Non-Linear Mixed Effects

NOS Not Otherwise Specified

ODE Ordinary Differential Equation

PCL Proliferating Cell Line

PD Pharmacodynamic

PDX Patient-Derived Xenografts

PE Parameter Estimation

PK Pharmacokinetic

PKPD Pharmacokinetic-pharmacodynamic

PL Profile Likelihood

RSE Relative Standard Error

SAEM Stochastic Approximation Expectation-Maximisation

SE Standard Error

SIA Structural Identifiability Analysis

STD Standard Deviation

TGM Tumour Growth Model

TS Tumour Spheroid

TW Tumour Weight

UoW The University of Warwick

VPC Visual Predictive Check

Contents

List of Figures

List of Tables

Chapter 1

Introduction

Cancer is the primary cause of death globally surpassing cardiovascular disease, necessitating the need for improved treatments regimens [1], [2]. Mathematical modelling in oncology has provided insight into predicting how tumours grow in response to various Anti-Cancer Agents (ACAs) [3]. The scenarios considered have potential to be multifaceted due to the simulation-based approach however, the practicability of models must be strongly considered [4]. This thesis utilises structural identifiability, pharmacology and compartmental modelling facilitating the analysis of drug mechanisms, optimising therapeutic windows and doses guiding treatment plans for patients. Simulation-based predictions also offer potential for animal experimentation's to conclude by utilising previously collected open-source data, supporting the 3 R's[1] [5].

1.1 Aims

This project strives to model systems delineating compound absorption and the effect this has on drug response with respect to tumour[2] volume in Patient-Derived Xenografts (PDX)[3]. This project was completed in collaboration with GlaxoSmithKline (GSK), a pharmaceutical company based in Stevenage, which has provided access to a preclinical dataset delineating Tumour Weight (TW) over time. Based upon PK[4] models and an appropriate Tumour Growth Model (TGM), the implemented models attempt to characterise tumour growth with respect to selected Anti-Cancer Agents (ACA)s, in an oncological setting. Additionally, the effects of the chemotherapeutics[5] docetaxel and carboplatin are assessed separately and in combination. The model to be administered first is also considered. The aspiration is to determine a robust biomedical system which is adept in predicting accurate and reliable changes in tumour volume over a period of time. This is aimed to be achieved through utilising Structural Identifiability Analysis (SIA)[6] supporting the use of parameter estimates (PE) with greater confidence.

[1] Reduction, refinement, replacement [5].

[2] Abnormal accumulation of tissue from cells which have proliferated more than normal or not died when supposed to.

[3] Tissue grafts obtained from a donor of one species and inserted into an animal of dissimilar species.

[4] A portion of pharmacology which examines the dispersion of drugs within an organism.

[5] Various medications which are used to treat or slow down growth of a manifold of cancers

[6] A methodology which validates whether or not parameters can be uniquely identified from the model's output when provided noise free data.

1.2 Objectives

To successfully fulfil the requirements of this dissertation to the pinnacle of the academic criteria specific objectives were pinpointed.

Core Objectives:

- Fostering a profound understanding of , TGM, Pharmacokinetic-pharmacodynamic (PKPD) and compartmental modelling. Specifically an insight into traditional mathematical models and how they are comparable to each other.
- Investigating prior works which can be utilised, aiding the methodology of this project where results from studies advise the Initial Parameter Estimation (IPE) of the various studies which are carried out. This assists with the simulations for the parameter estimates.
- Developing an understanding of the population PE tool Monolix where familiarity with the syntax will be enhanced so an effective assessment of the provided preclinical data can be carried out. Specifically, comprehension of the functions in the Monolix toolbox, composing mathematical models and reviews of the outputted visuals and plots.
- Extraction, manipulation and sorting of preclinical data to gain insight into the dataset as well as affirming the data are compatible with Monolix and MATLAB.
- Performing SIA when required allowing support for PE within the model. This process offers greater confidence in numerical PE when performed on the relevant preclinical dataset.
- Review of the results attained from Monolix where robustness and precision of various mathematical models and discussing their applicability. This can lead to potential modifications to the model or initial parameter estimates (IPEs). These revisions have the potential to optimise the results of the model by improving the convergence speed, computational cost and avoidance of local minima[7].
- Cultivating a strong project management acumen to manage the academic workload of this project. This comprises time management, verbal and written communication skills, and showcasing successful collaboration between industry and academia.

Desirable Objectives:

[7] A point in a function which is lower than any other point in a neighbourhood but may not be the lowest. This can cause optimisation functions to conclude at such a point hence not being fully optimised.

- Developing an appropriate and reliable mathematical model which illustrates the effects of both chemotherapeutics in combination with one another, specifically reviewing the changes in tumour volume over time.
- Proficient PE using the provided preclinical data and integrating with relevant mathematical models.

1.3 Overview

This report opens with an introduction which showcases the directives set for this project, where the aims, objectives, and overview are conveyed. The literature review delineates established frameworks in drug therapeutics, pharmacology, mathematical modelling and oncology, fostering a foundation to build upon in the latter stages of this report. The background chapter presents the software utilised; featuring MATLAB, Monolix, Mathematica, Excel, and mathematical models. Additionally, ethical concerns in conjunction with preclinical datasets are outlined. Execution of SIA in regards to tumour growth is implemented supporting validation of the credibility of exercised mathematical models in this thesis. The methodology illustrates approaches taken to accumulate results such as integration of data into Monolix and the designing of mathematical models in pursuit of an enhanced fit. Simulations with IPEs were also performed to analyse the conformity to characteristic models delineated in the literature. Results are displayed in a structured manner aided with performance metrics and preliminary observations. Amidst the evaluation and discussion section, observations are built upon and insights are discussed. Limitations and comparability of results are addressed at this juncture. Ultimately, the conclusion highlights the principal findings, the insight garnered, and potential future works.

No fewer than 600 working hours should be committed to this investigation where the key resources utilised have been showcased above and expanded upon in (3). Further to this the The University of Warwick (UoW) comprehensive inventory was also harnessed.

This report follows a structuring of 7 chapters. In chapter 2, the literature review is described highlighting subject knowledge. Chapters 3 and 4 showcased the designs derived and utilised as well as the methodology for this thesis. In chapter 5, results were obtained and observations were made. In chapter 6, performance metrics and visuals are evaluated; forward simulations are performed and discussed. Finally in chapter 7, conclusions and future works are delineated.

Chapter 2

Literature Review

2.1 Therapeutic Agents

During a patient's treatment the period of time, number and degree of the dosages are dependant on the intended aim of the therapeutic. There are three main scenarios in which therapeutics are used; a cure, mitigation or prevention of a disease [6]. In most cases it is widely accepted that developing clinical therapeutics is an expensive and prolonged process, where there are many clinical trials across different phases taking place which involve many participants in control and treatment groups[7].

Engineering effective clinical trials is often directed by PKPD strategies in order to evaluate and competently choose specifications for the dosing regimen and studies which were facilitated by systems engineering and mathematical models [8]. The utilisation of mathematical models to provide robust mechanistic insight into biological problems has become widely adopted over the past decade [9]. Such models offer a system for assessing biological hypotheses which helps to develop experimental designs for clinical trials as well as becoming more commonly used to forecast the potential results and outcomes from a given treatment [9], [10]. Functional relationships between constituents within a mathematical model and the effect they have upon a biological system can be determined by tuning the average tumour weight (TW) for the control and treatment classes where differences are compared. It is important to recognise various species' longevity for the entirety of treatments in the preclincal Patient-Derived Xenograft PDX dataset [11].

A pharmacological compound exhibits four fundamental kinetic processes: Absorption, Distribution, Metabolism, Elimination (ADME). Administration is partitioned into two subclasses; intravascular or extravascular and examples of such are Intravenous (IV)[1], oral, subcutaneous[2] or IP[3] administration where the first showcases intravascular and the latter extravascular [12].

Now that the patient has absorbed the drug the compound is distributed to various regions such as the plasma, tissues or organs. Distribution is known as the process of a reversible flow between the measurement site[4] and other affinities [12].

[1] (Usually an injection or infusion) into or within a vein.
[2] Beneath the skin.
[3] Within the peritoneal cavity, the area which contains the abdominal organs.
[4] This is typically the plasma which represents a fluid which blood cells are suspended in.

Conversely, elimination is an irreversible mechanism where the drug is dissipated from the body via metabolism[5]; this primarily occurs in the liver or via excretion[6] which typically takes place in the kidneys where the compound is chemically unchanged [12].

When designing the dosing regimen for a therapeutic it is vital to find the optimal range of concentrations where the drug exhibits maximal beneficial effects with minimal toxicity[7] where the drug will not be harmful to a patient.
This defines the therapeutic window, where the lower bound highlights the effect required and upper bound the limit for toxicity, Fig (2.1) [13]. This framework should be followed to identify the most favorable dosing regimen where the drug concentration of plasma is robustly limited to this boundary delineated. It is clear that, comprehensive understanding of the pharmacology is essential when determining the dosing regimen because dose is mapped to toxicity and efficacy [12].

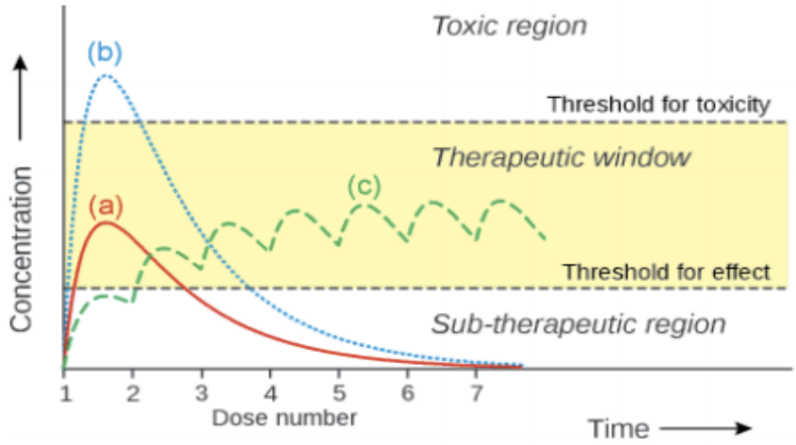

Figure 2.1. *Concentration-time graph after oral administration of a therapeutic compound: (a) single dose, (b) single dose double the quantity of "(a)", (c) divided up dose given over multiple administrations [13].*

[5]Process where a chemical entity is converted to another compound.
[6]Removal of waste products which have built up from metabolic activity.
[7]The degree to which a compound is poisonous.

2.2 Pharmacology

The compartmental models which will be implemented in this research are rooted in two domains of pharmacology: PK and Pharmacodynamic (PD). PD is recognised as the science of drug effect upon the human body, where at the interactive site PK levels produce an effect on the tumour which varies in degree. Conversely, PK is endorsed as the framework delineating what the body does to the drug [13]. This pertains to dose, periodicity, and administration pathway to PK relationships [12] which interlinks temporal contingencies between PK and PD necessitating robust analysis of such biological systems. Notably, PK reviews drug and metabolite[8] dynamics in vivo. This features ADME, which impact the concentrations and dynamics. Alternatively, Anti-Cancer Agent (ACA) interact with biological tissue perturbing TW by application of therapeutic effect [14]. Kinetics which delineate the dynamics of these frameworks are typically not influenced by the size of the dose following first-order kinetics [15] [13]. These mathematical models are utilised by means of; therapeutic dosing regimen computations, interactions between compounds, and novel delivery mechanisms [14]. Insight into therapeutic PK also has a potential to determine the outcome of personalised treatments in the clinic [12].

There are three rudimentary classes of PK models: compartmental, physiologically-based and non-compartmental models. For the formerly mentioned, a compartment delineates tissues with analogous agent propensities, in contrast to selecting distinct anatomical regions. The Second listed form of model, adopts physiological metrics, necessitating pre-existing insight of biological inference such as; the drug uptake of each organ and hemodynamics[9] where such biological insight elevates complexity hindering implementation with practical uses [14]. Regardless of complexity, such a model allows for chemical and physical intuition with characteristics such as; Ph sensitivity or solubility of the therapeutic [16]. The latter model, utilises the average duration of a treatment and PK intensities to determine the pharmacological condition.

It is advised that a PKPD framework is adopted to drive process optimisation of agents where it is indicated that this framework will streamline the workflow, enhancing efficiency [8]. Through administering ACAs, coupled with the TGM advancements of chemotherapeutics can be profoundly enhanced [11]. To conclude, it is evident that insight and utilisation of pharmacology is paramount. Notably, compartmental models are the predominant framework in this field and will be used in this report [3].

[8] A substance formed from a drug through biotransformation, usually occurring in the liver [3].
[9] The flow rates of blood.

2.3 Compartmental Modelling

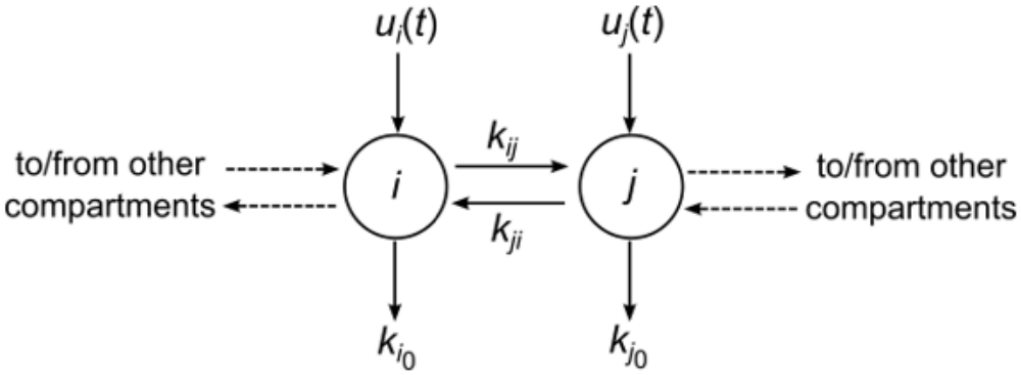

Figure 2.2. *Two-compartment model consisting of compartments i and j interacting with one another and their environment, where k_{ij} represents the flow rate from compartment i to compartment j where u_i and u_j are the inputs to the model; k_{i0} and k_{j0} represent the outflows of compartment i and j respectively [17].*

Compartmental modelling is utilised for delineating multifaceted complex systems in PK and PD separately and in combination. Examples of PK and PD are therapeutic dynamics and chemical kinetics [17]. Fundamentally, a compartmental model is composed of a bounded number of homogeneous[10], lumped elements identified as a compartment which have invariable material exchanges in conjunction with one another and the surroundings [3].
The differential rate of the quantity and concentration of a compound for a distinct compartment can be expressed by first-order Ordinary Differential Equations (ODEs), facilitating the modelling of dynamics of at least one compound. For instance, a therapeutic administered in the plasma reversibly flows to tissues that are characterised by different affinities. A generic model illustrating the simplest form of a compartmental model with 2 compartments i and j, Eq (2.2).

$$\frac{dq_i}{dt} = \left[f_{0i} + \sum_{\substack{j=1 \\ j \neq i}}^{n} f_{ji} q_j \right] - \left[f_{i0} + \sum_{\substack{j=1 \\ j \neq i}}^{n} f_{ij} \right] q_i \quad \text{for } i, j = 1, 2 \tag{2.1}$$

where:

- k_{ij}: Rate constant of exchange from compartment i to j
- q_i and q_j: Quantity in the respective compartments
- f_{ij}: Flow rate from compartment i to j, equal to $k_{ij} \cdot q_j$
- n: Total number of compartments within the model

[10] A structure which has a uniform nature and uses the principle of mass balance.

Whilst compartmental models are perhaps over-simplifications in respect to real-world systems, they provide a good awareness of a steady-state system's feedback regarding small perturbations[11]. Although, by definition quantities and flow rates are physically incapable of being negative, a limitation of this framework [3]. Surroundings of the system, Eq (2.3) are delineated via compartment zero.

2.4 Neoplastic Expansion

Neoplastic expansion is primarily initiated by a limited quantity of abnormally proliferating cells. Moreover, growth of these tumours necessitates transportation of nutrients, particularly glucose, oxygen, and migration of waste from neighbouring tissues to regions where the byproducts can be eliminated; this happens repeatedly [18]. To model the mechanisms of distinct types of tumour growths, various mathematical models have evolved over many years. The weights of untreated in vivo[12] tumours are usually characterised by exponential growth which adheres to linear growth in due course, then a plateau phase is ultimately reached [11]. The Gompertz mathematical model delineates the aforementioned narrative of the TGM [19].

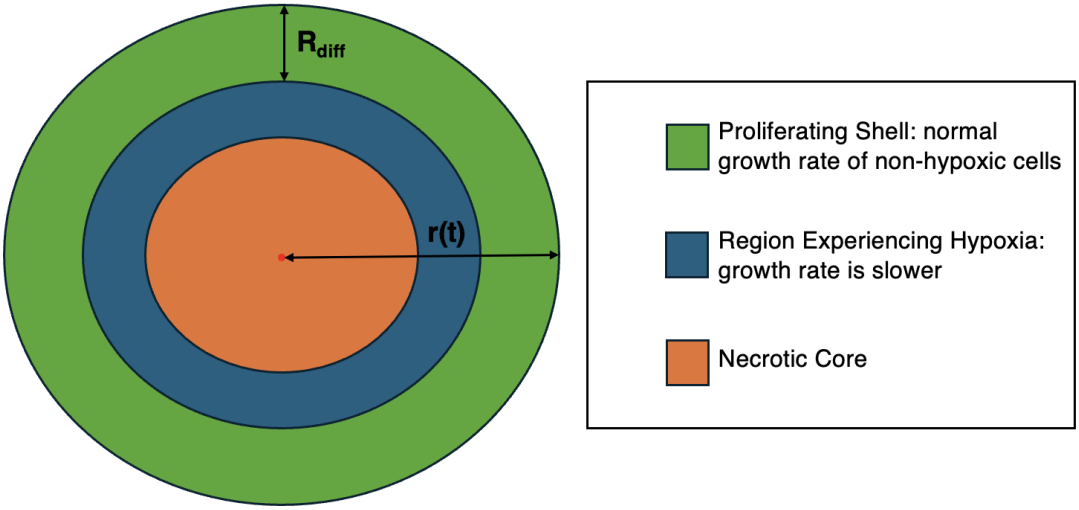

Figure 2.3. *Visualisation of the characteristics of a TS [20].*

A Tumour Spheroid (TS)[13] is believed to comprise of three distinct classes of cells: hypoxic[14], non-hypoxic and necrotic[15]. Growth of hypoxic cells will ultimately turn into necrotic cells

[11] Deviation to a system, moving object, or process from its regular state or path caused by an outside influence [3].

[12] Biological mechanisms which occur within the bodies of living organisms.

[13] Three-dimensional cell cultivation which emulates the structure and environment of a tumour within an organism.

[14] Oxygen-deficient tissue or cells.

[15] Affected or characterised by necrosis: the death of some or all cells in an organ or tissue caused by disease, physical or chemical injury or interference with the blood supply [21].

and die known as apoptosis [22]. Conversely, non-hypoxic cells comply with the generalised-logistic equation for cell proliferation up to the carrying capacity limit. In such cases, the TS will develop bands of tissue forming a proliferative outer layer, with a thickness of a few sheets of cells, lastly followed by a suboptimally oxygenated, hypoxic region. Additional intra-layers exhibit more pronounced oxygen supply deficiency commonly forming a necrotic core, Fig (2.3) [23]. Cells effected by hypoxia commonly have a reduction in their proliferation dynamics and hence are more unyielding to chemotherapeutic agents, which are pursuing cells of brisk proliferation [23]. Notably, the TGM delineated is exclusively an estimation of actual neoplastic expansions.

2.5 Patient-Derived Xenografts

Patient-Derived Xenografts (PDX)[16] are utilised within this thesis due to their capability to preserve tumour structure which accurately mimic in vivo scenarios. Heterogeneity is also showcased; a fundamental characteristic of human tumours. Albeit such benefits, there are humanitarian concerns because of the usage of human tissue which are deployed into various species for testing. It is vital that the 3R's; replacement, reduction, and refinement are considered and followed which is advocated though the utilisation of simulation based predictions [5]. It is highlighted that, as systems engineering and applied mathematics continues to improve, aspiring towards the potential for further PDX experiments to become an unnecessary perquisite. Alternatively, Proliferating Cell Lines (PCLs) could be utilised because of their capability to permanently expand, provided there is an available void for the cells to occupy [24]. PCLs have by no means unjust humanitarian practices, contrary to PDX. However, the aforementioned PDX properties make PDX a preeminent choice for determination of optimal dosing levels which offers significance to this project. This is owing to a PDX's coherence with human tissue arguing that PDX facilitates transferability from preclinical to clinical more adeptly than alternatives.

2.6 Structural Identifiability

Structural identifiability is the process of determining whether it is possible to uniquely identify the unknown parameters of a model based on the given system observations or outputs with the aspiration of showing the corresponding model is structurally globally identifiable [25]. Adhering to PE criteria, SIA should be conducted before the model is leveraged in the majority of scenarios [26]. Contrary to the requirements of PE, SIA cannot always be implemented due to the complexity of some mathematical models necessitating significant symbolic computational

[16] Utilised in cancer research where cancerous tissue is taken from a patient and implanted into an animal species.

power.

2.6.1 Symbolic Representation

Considering $p \in \Omega \subset \mathbb{R}^m$ defines the entirety of unknown parameters within the model where Ω represents an open set of valid vectors. It is shown that the output, $y(t,p)$, is determined via the unknown parameter vector defined. Moving forward, it is known a model that produces identical outputs implies $p, \bar{p} \in \Omega$ are identical:

$$y(t,p) = y(t,\bar{p}) \quad \forall t \geq 0 \implies p \sim \bar{p} \tag{2.2}$$

For generic $p \in \Omega$, the parameter p_i is *locally identifiable* if there is a neighbourhood, N, of p such that

$$\bar{p} \in N, \quad p \sim \bar{p} \quad \implies \quad \bar{p}_i = p_i \tag{2.3}$$

If $N = \Omega$ by (2.3) p_i must be globally identifiable. Further to this, if $N(p_i) \subset \Omega$ a parameter is shown to be locally identifiable by 2.3. However, p_i is unidentifiable if an uncountable number of sets are required [27], [25].

A mathematical model is considered structurally globally identifiable (SGI) if and only if $\forall p_i$ are globally identifiable. A model is locally structurally identifiable if $\forall p_i$ are locally identifiable and no fewer than one is not uniquely identifiable. Only one parameter has to be unidentifiable for the entirety of the model to be structurally unidentifiable [27], [28], [25]. Fundamentally SIA validates whether or not unknown parameters can be uniquely identified given that there is input-output insight available for the model [29]. Ordinary Differential Equation (ODE)s in biomedical disciplines especially benefit from a SIA due to having various parameters which need to be distinctly identified where data is not in excess.

2.6.2 Taylor Series

This report utilises the Taylor series approach where the output is expanded about the point $t = 0$ resulting in (2.4)-(2.5) [28].

$$y(t,p) = y(0,p) + \dot{y}(0,p)t + \cdots + y^{(n)}(0,p)\frac{t^n}{n!} + \cdots \tag{2.4}$$

where

$$y^{(n)}(0,p) = \lim_{t \to 0} \frac{d^n y}{dt^n}(t,p) \tag{2.5}$$

It has been established that coefficients of the Taylor series expansion are unique allowing unknown parameters identifiability to be determined with this approach expressed via (2.6) [27].

If $p, \bar{p} \in \Omega$ are identical then,

$$y(0,p) = y(0,\bar{p}), \quad y^{(n)}(0,p) = y^{(n)}(0,\bar{p}) \quad \forall n > 0. \tag{2.6}$$

If $\bar{p} = p$ where there is a countable number of coefficients the approach has shown the mathematical model is structurally globally identifiable (SGI). If $\bar{p} = p$ cannot be reached this necessitates dependencies between parameters to be determined so the quantity of Taylor series coefficients required to establish structural identifiability is bounded [27]. In this case, the model is structurally unidentifiable.

2.7 Docetaxel

2.7.1 Genesis

Docetaxel[17] is a frequently employed chemotherapeutic which was established through experiments with taxanes[18] and platinum-based compounds for cancer treatments. The hybrid-synthetic docetaxel is comparable to Paclitaxel[19] since they both belong in the taxane class [34]. Paclitaxel exhibited a distinct effect where microtubules[20] are maintained and cell proliferation inhibited aiding significant advancements with cancer therapies [35], [36]. Albeit effective, the agent Paclitaxel has limited accessibility leading to challenges commercialising such a treatment regimen. Conversely, docetaxel which was created in the 1980s was identified to inherit similar properties to Paclitaxel such as microtubule stabilisation while the potency and solubility was also amplified facilitating marketisation dissimilar to Paclitaxel [34].

2.7.2 Mechanisms of Agent

Docetaxel influences tumour growth and hence TW through hindering microtubule dynamics which is a fundamental requirement for a cell to divide [36]. By means of affinity towards the β-tubulin[21] docetaxel promotes a stable environment for the creation of robust microtubule clusters

[17] A Compound formed by utilising a progenitor molecule which resides in the needles of a European yew tree (Taxus baccata) [30].

[18] Type of diterpenes which is a type of chemical compound formulated from plants. They are noted for stabilising microtubules [31].

[19] Natural compound "extracted from the bark of the Pacific yew tree (Taxus brevifolia)" [32], [33].

[20] Tubular infrastructure composed of protein sub-units [35].

[21] Building block of microtubules [37].

[37]. This mitigates mitotic spindle[22] formation and provokes apoptosis[23]. Notably, attacking the mitotic spindle demonstrates why docetaxel is impactful against aggressive tumour growth [38], [34].

2.7.3 Pharmacokinetics and Pharmacodynamics

PK are facilitated by a triphasic plasma concentration[24] the first phase diminishes after IP administration where there is expeditious distribution. After this distribution phase, the therapeutic eventually adheres to a protracted elimination state. The potency of the agent is responsive to dose variation where a larger dose leads to a more profound antiproliferative effect, however, this also corresponds to higher toxicity [40], [39].

2.7.4 Clinical Efficacy

Docetaxel has showcased numerous clinical studies for solid tumours. Principally, this therapeutic is used for treating breast cancer showcasing the importance of assessing variants such as Invasive Breast Carcinoma (IBC). Other classifications are also treated with this chemotherapeutic inducing: non-small cell lung cancer (NSCLC), prostate cancer, gastric cancer, and head and neck cancer [41], [37].

When treating IBC, docetaxel is commonly used in combination with other chemotherapeutics like doxorubicin[25], capecitabine[26] or carboplatin[27]. Combining such therapeutics has shown to improve a patient's response to therapy and overall life expectancy [42], [41]. Albeit that it has potential, docetaxel with the combined affect of another drug such as carboplatin has yet to become standard practice, exemplifying the significance of this report. On the other hand, docetaxel has become a confirmed standard for the secondary treatment of NSCLC [43]. Similarly, docetaxel and prednisone in combination are utilised to treat hormone-rectory prostate cancer exemplifying the potential combined therapeutic effects that they have for solid tumour therapies [44].

2.7.5 Adverse Effects and Patient Considerations

Despite clinical significance there are various adverse effects associated with the toxicity of docetaxel. Neutropenia[28] is a common side effect of such a chemotherapy leading to shortcomings

[22] Structure composed of microtubules [37].
[23] Programmed cell death which happens in multicellular organisms.
[24] This includes three phases: the absorption phase, distribution phase and elimination phase [39].
[25] An antibiotic widely utilised in chemotherapy.
[26] An orally administered chemotherapeutic.
[27] Chemotherapeutic with a platinum core.
[28] A class of white blood cells which are in abnormally low quantity in the respective individual.

such as a minimisation of the therapeutic window[29], elevated likelihood of infection and peripheral nephropathy [30] [45], [46]. Additional impactful side effects are alopecia[31], stomatitis[32] and hypersensitivity reactions, since the latter adverse effects commonly require preemptive medication with corticosteroids[33] [47], [48].

A patient's hepatic aberration profoundly impacts the dosing regimen which can be safely administered to the individual because of the altered PKs leading to heightened toxicity. This reinforces the necessity to review a patient's liver function prior to and during therapy. It is vital that toxicokinetics[34] are monitored in any individual with a comorbid[35] disorder. Ultimately, attention to personalised needs of patients facilitates optimal clinical results.

2.8 Carboplatin

2.8.1 Genesis

Carboplatin is the next generation of platinum derived chemotherapeutics refined from cisplatin[36] [49], [50]. Albeit cisplatin has significant efficacy upon solid tumours, the exceptionally narrow therapeutic window contributed to dangerous dosing regimens causing nephrotoxicity[37], neurotoxicity[38] and ototoxcity[39] [51]. Necessitating a safer toxicity profile induced the discovery of carboplatin in the 1970s [52]. Academics worked to substitute the chloride[40] ligands[41] with bidentate cyclobutane-dicarboxylate[42] ligand because the double bonding upon the central metal minimised the responsiveness of the platinum core. This gave rise to an agent with a similar antiproliferative[43] behaviour with a profoundly diminished toxicological profile providing a safer form of treatment for patients diagnosed with solid tumours [34].

[29] Interval of dose levels where the desired response is observed while there are no adverse effects.
[30] Condition, where the peripheral nerves are damaged causes, can come from exposure to toxins.
[31] Condition where hair is lost on the individuals scalp or other regions of the body.
[32] Condition where the mucous membranes become inflamed.
[33] A steroid hormone procured in the adrenal gland which reduces inflammation as well as inhibiting a patients immune system.
[34] Applying the notion of pharmacokinetics to toxic compounds.
[35] An individual who has one or more additional conditions adjacent to a primary disease
[36] A platinum-derived compound established in the 1960s where solid tumour responded effectively to the chemotherapeutic.
[37] Kidney damage.
[38] Damage of the nervous system.
[39] Damage leading to hearing loss.
[40] Represents a negatively charged ion developed by chlorine acquiring an electron.
[41] Molecules that can donate no fewer than one pair of electrons creating a dative bond with a central ion in a complex.
[42] Represents a ligand which forms two bonds with a central metal ion in a coordinate complex.
[43] An agent which inhibits the proliferation of living cells.

2.8.2 Mechanisms of Agent

Similar to alternative platinum-derived chemotherapeutics, carboplatin deploys an antiproliferative effect via the process of DNA complexes[44] which result in crosslinking of nucleotide chains[45] [53]. This prompted DNA transcription and replication to be hindered which eventually led to programmed apoptosis of briskly proliferating cells.

The activation energy required for DNA to interact with carboplatin necessitates aquation[46] [54]. Notably, carboplatin is not as responsive as cisplatin however, carboplatin's capability to produce DNA crosslinks leads to similar results for both therapeutics therapeutically [53].

2.8.3 Pharmacokinetics and Pharmacodynamics

Carboplatin and cisplatin have dissimilar PKs because of the variation in chemical structure. carboplatin quickly disperses in an organism where binding to plasma proteins is not as prominent compared to Cisplatin which is showcased by their disparate therapeutic windows [55]. Contrasting docetaxel, approximately 70% of carboplatin is excreted via the kidneys, over a 24 hour period [56]. Renal clearance is explicitly connected to an individual's glomerular filtration rate (GFR) showcasing the importance of nephric[47] function when ascertaining an appropriate dosing regimen [56], [57]. It should be acknowledged that the AUC[48] framework has become a benchmark for personalised dosing regimens of carboplatin [56].

2.8.4 Clinical Efficacy

Carboplatin showcases notable clinical efficacy, especially when administered in combination with an alternative class chemotherapeutic, namely, carboplatin, which has been pivotal in therapies for ovarian cancer particularly when exhibiting a combined effect with Paclitaxel[49] where prognostic rates were elevated [58], [59]. Furthermore, carboplatin is noteworthy in addressing childhood cancers due to a toxicity profile which can be tolerated by paediatrics unlike cisplatin [60]. Carboplatin offers a favourable balance between toxicity and efficacy showcasing its dominance within the antiproliferative platinum-based agents [49].

[44] Substances which are constructed from the binding of two or more molecules conjugated via chemical forces.

[45] The fundamental building blocks of nucleic acids like DNA and RNA. Nucleotides are assembled from three constituents: a phosphate group, a five-carbon sugar and a nitrogenous base.

[46] A technique where a platinum ion is hydrated.

[47] Represents the kidneys

[48] Area under the curve

[49] Identified as a taxane. A type of chemotherapeutic which has a platinum core.

2.8.5 Adverse Effects and Patient Considerations

Although carboplatin has less intense undesirable effects than cisplatin, complications such as myelosuppression[50] especially thrombocytopenia[51] restricts the dosage level which can be administered [61]. Consequently, it is an imperative for patients with impaired hematopoiesis[52] or those undergoing concomitant[53] treatment are monitored closely for indicators of myelosuppression. Carboplatin may still induce nausea, vomiting and electrolyte asymmetries, but this is often less profound for cisplatin.

2.9 Previous Studies

2.9.1 "How translational modelling in oncology needs to get the mechanism just right" by JWT

This report provides an understanding of the difficulties of translating the insights which can be gained through oncological simulations of a preclinical dataset to a clinical environment. It provides crucial points on how to make sure that even when a model is theoretically correct it must also be ensured that the model is clinically significant. Detailing the importance of maintaining a balance between complexity and practicality. If the model is too complex it will become increasingly difficult to carry out PE and sensitivity analysis[54] and draw conclusions from how ACAs affect TW [62].

2.9.2 "Compartmental models and their application" by KPC

Godfrey et al facilitates a prime foundation for understanding PKPD models and how compartmental modelling is crucial in the field of pharmacology. It shows how compartmental models can be applied to preclinical data to simulate how ACAs affect TW. This book gives a range of different biological models and methods which can be adapted for oncological simulations. Furthermore, the analysis of novel models from 1983 gives a good understanding of the fundamental models used and how they can be developed for future research by using empirical and theoretical knowledge. The book also gives applications where PKPD is utilised. PKPD is essential for analysis of TGMs with respect to the ACA being applied [3].

[50] Condition where the activity of bone marrow declines.
[51] A reduction in platelets.
[52] Process of blood cell formation.
[53] Something that occurs while having another condition.
[54] A procedure carried out to assess how varying the values of the independent variable impact a distinct dependant variable

2.9.3 "A Spatially Resolved Mechanistic Growth Law for Cancer Drug Development Predicting Tumour Growth Fractions" by AN

This thesis gives an in-depth analysis of a spatially resolved mechanistic law which is crucial in understanding and developing our insights on how ACAs affect tumour growth. The TGM proposed via Nasim et al [63] considers space and tumour heterogeneity; spatial consideration is required in TGM because the proliferation of tumours does not occur in isolation hence spatiality impacts diffusion gradients affecting nutrient levels which are a determinant of tumour growth. The latter variable accounts for neoplastic expansion where a spectrum of genetic mutations commonly occurs. This novel model could be more accurate than traditional models as discussed by Godfrey. There is potential to advance this model due to its fresh perspective in analysing these cancer growths [20].

Chapter 3

Background

For the duration of this project, various software tools were implemented to facilitate a better understanding and analysis of the data provided, as well as for performing simulations and PE. Their functions and applications are outlined below.

3.0.1 MATLAB

MATLAB created by MathWorks is a numerically-based computational environment scripted in Java and C/C++. MATLAB's main focus is on performing matrix manipulations, utilisation of functions and plotting data uploaded into MATLAB [64]. Furthermore, forward simulations were conducted in MATLAB for this thesis through utilisation of ODEs delineating the carboplatin PK model to better understand how the concentrations in each compartment change with respect to time. MATLAB was obtained with an academic license held by the UoW, leading to no further expenses.

3.0.2 Monolix

Monolix was accessed by submitting a request form to obtain an academic license free of charge. Monolix's framework is a source for developing therapeutics primarily used to perform PE of Non-Linear Mixed Effects (NLME)[1]. The SAEM approach pursues population parameters which optimise the likelihood estimates utilising the exploratory and smoothing phase to maximise these results [65]. Results can be visually evaluated through VPCs and other illustrative diagnostic plots [66].

3.0.3 Mathematica

Mathematica is a computational software system cultivated by Wolfram Research and is predominately written in C and Wolfram Language [67]. This software is sophisticated in symbolic computation and capable of deriving Taylor series expansions[2] for complex functions which is a traditional method for determining the SIA of a nonlinear system.

[1] Nonlinear mixed effects is a statistical technique which uses both fixed effects and random effects.

[2] A function where at a single point a manifold of derivatives are computed and used to create an infinite sum [28].

3.0.4 Microsoft Excel

The spreadsheet editor Microsoft Excel was utilised to establish a better awareness of the data given via GSK. The preliminary data was initially of a large quantity however Excel was leveraged to determine columns of significance through the use of the built-in filter function. An additional column named "Regressor"[3] was also created in Excel in order to reliably estimate the initial TW for studies on the preclinical data. Then the raw dataset was reduced to a more manageable size within Excel aiding the avoidance of syntax errors when converting the Excel spreadsheet to a ".csv" file and uploading to Monolix. Microsoft Excel was attained freely through the use of a student license.

[3]Model which predicts the value of another variable.

3.1 Definition of Models

3.1.1 Docetaxel Model

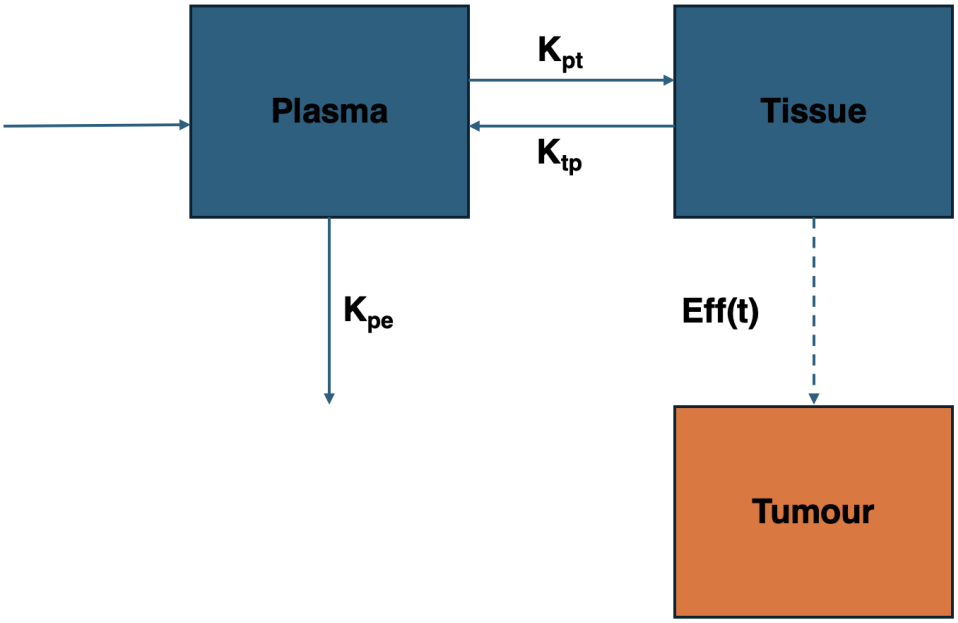

Figure 3.1. *PK, two-compartmental model delineating drug distribution after IP administration for docetaxel [68].*

ODEs Defining the Docetaxel Model

The compartmental model is defined mathematically using two ODEs. These have been taken from the work of Evans et al [68].

$$\frac{dq_P(t)}{dt} = -(K_{pe} + K_{pt}) \cdot q_P(t) + K_{tp} \cdot q_T(t) \tag{3.1}$$

$$\frac{dq_T(t)}{dt} = K_{pt} \cdot q_P(t) - K_{tp} \cdot q_T(t) \tag{3.2}$$

$$C_P = \frac{q_P(t)}{V_P} \tag{3.3}$$

Explanation of Parameters in (3.1)-(3.3)

- q_P: Drug quantity in the "Plasma" compartment [μmol]
- q_T: Drug quantity in the "Tissues" compartment [μmol]

- V_P: Drug volume in "Plasma" compartment $[kg^{-1}]$
- K_{pe}: Flow rate leaving the model from the "Plasma" $[h^{-1}]$.
- K_{pt}: Flow rate from "Plasma" compartment to "Tissues" compartment $[h^{-1}]$.
- K_{tp}: Flow rate from "Tissues" compartment to "Plasma" compartment $[h^{-1}]$.
- C_p: Concentration of drug in the "Plasma" [μmol/kg].

Parameters values for the model defined in (3.1)-(3.3)

Parameter [units]	**Value**	**SDLN**[4]	**5%**[5]	**95%**[6]
K_{pe} [h^{-1}]	0.382	0.49	0.169	0.860
K_{pt} [h^{-1}]	0.523	0.80	0.140	1.950
K_{tp} [h^{-1}]	0.196	0.48	0.090	0.430
V_p [kg^{-1}]	1.30	0.57	0.508	3.323

Table 3.1. *PE for the PK of docetaxel [68].*

Forward Simulation of the Pharmacokinetic Model for Docetaxel

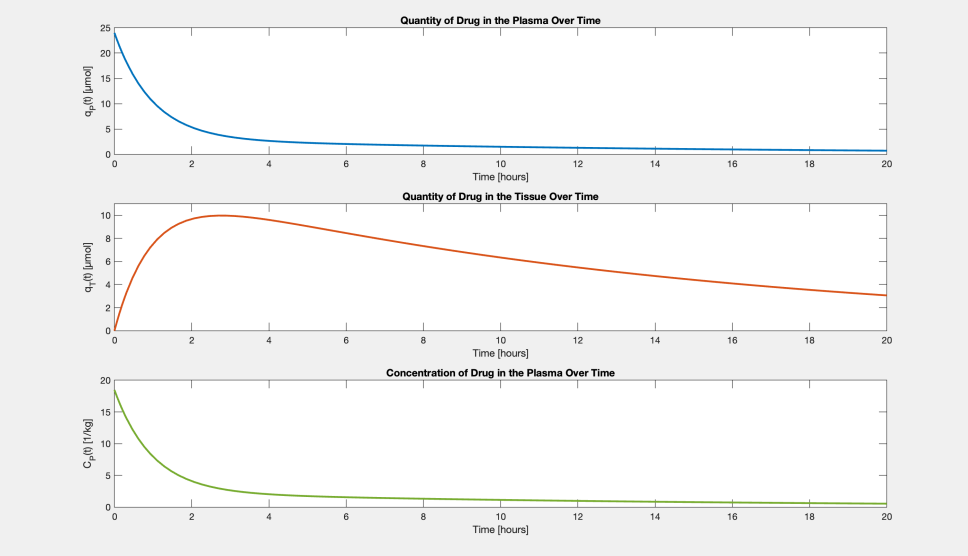

Figure 3.2. *Simulation of docetaxel with the provided PEs 3.1 and compartmental model by Evans et al [68].*

As time progresses, the concentration and quantity of the therapeutic docetaxel in the plasma compartmental reduces where the initial levels are the highest values obtained for plasma. This

[4]Standard Deviation of the Log-Normal distribution representing the variability of the model parameters on the logarithmic scale.

[5]Highlights 5% of the parameter values are anticipated to have values below the respective values.

[6]Highlights 95% of the parameter values are anticipated to have values below the respective values.

is due to distribution and elimination of the drug, eventually the curves flatten indicating the rate of outflow and transfer to the tissue compartment has reduced and the amount of drug in the plasma compartment has nearly fully depleted.

Conversely, the initial value in the tissue compartment is minimal reflecting the absence of a therapeutic in the tissues to begin with. As time goes on, the drug is redistributed highlighted by the flow rate into the tissue compartment where over time, a peak amount is reached. Dissimilar to the plasma compartment, after the peak amount is reached the rate of decrease is gradual potentially because the tissues act as a drug reservoir where the rate of removal is much slower than in other affinities.

3.1.2 Carboplatin Model

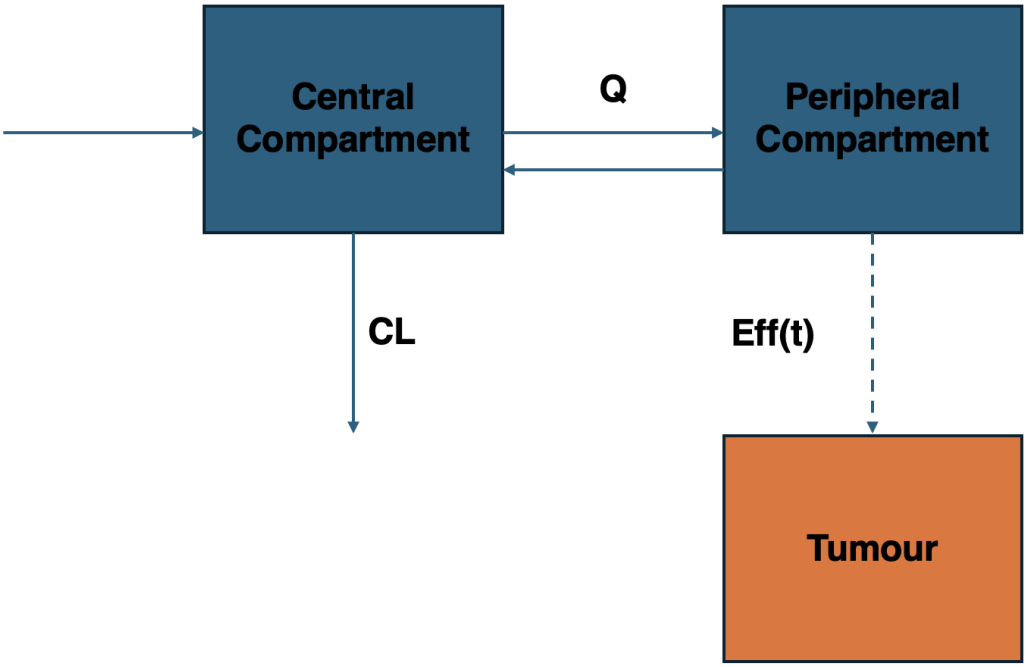

Figure 3.3. *PK, two-compartment model delineating drug distribution after IP administration for carboplatin [69].*

ODEs Defining the Carboplatin Model

The compartmental model is defined mathematically using two ODEs. These have been derived from the work of Zandvliet et al [69], [68].

$$\frac{dq_P(t)}{dt} = -(K_{pe} + K_{pt}) \cdot q_P(t) + K_{tp} \cdot q_T(t) \tag{3.4}$$

$$\frac{dq_T(t)}{dt} = K_{pt} \cdot q_P(t) - K_{tp} \cdot q_T(t) \tag{3.5}$$

$$C_P = \frac{q_P(t)}{V_P} \tag{3.6}$$

where

$$K_{pt} = \frac{CL_{inter}}{V_P} \tag{3.7}$$

$$K_{tp} = \frac{CL_{inter}}{V_C} \tag{3.8}$$

$$K_{pe} = \frac{CL}{V_P} \tag{3.9}$$

Explanation of Parameters in (3.4)-(3.6)

- q_P: Drug quantity in the central compartment representing the plasma [μmol].
- q_T: Drug quantity in the peripheral compartment representing the tissues [μmol].
- V_C: Drug volume in central compartment [l].
- V_P: Drug volume in peripheral compartment [l].
- C_p: Concentration of drug in the "Plasma" [μmol/l].
- CL: Amount of drug which is removed from the central compartment [h^{-1}].
- CL_{inter}: Amount of drug which is distributed from the central to peripheral compartment and vice versa [h^{-1}].

Parameters values for the model defined in (3.4)-(3.6)

Parameter [units]	**Estimate**	**RSE**[7]	**IIV**[8]	**RSE**[9]
Clearance [h^{-1}]	0.76+1.5	0.05	13%	0.27
Volume of Central Compartment [l]	15.5	0.19	54%	1.46
Intercompartmental Clearance [h^{-1}]	3.46	0.18	46%	0.39
Volume of Peripheral Compartment [l]	9.86	0.11	31%	0.41

Table 3.2. *Parameter estimates for the PK of carboplatin [69]*

3.1.3 Tumour Growth Model

The proposed model utilised from Yates et al [62] will be tested for SIA. Then PE are evaluated to test the applicability of the proposed model in predicting TW where a key insight will be testing the accuracy of the model predictions compared to the observed preclinical data. An extension to the model is the inclusion of the growth factor; a novel predictor of tumour proliferation dynamics.

Defined by Assuming a Tumour Spheroid Without a Therapeutic Administered

First, the ODE describing TW is given by:

$$\frac{dV}{dt} = V\left((\beta - \mu_P)\,\text{GF} - \mu_Q(1 - \text{GF})\right); \quad V(0) = V_0 \tag{3.10}$$

where

$$\text{GF} = 1 - \left(1 - \frac{R_{\text{diff}}}{r}\right)^3 \tag{3.11}$$

Explanation of Parameters in (3.10) and (3.11)

- $V(t)$: Tumor volume at time t [cm^3].
- β: Proliferation rate [d^{-1}].
- μ_P: Rate of cell death in the proliferating compartment [d^{-1}].
- μ_Q: Rate of cell death in the quiescent compartment [d^{-1}].
- GF: Growth fraction, the proportion of tumour cells which are proliferating [$dimensionless$].
- R_{diff}: Depth of the proliferating compartment into the tumor [cm].
- r: Radius of the tumor spheroid [cm].
- V_0: Initial tumor volume [cm^3].

Coupling of Tumour Volume and Growth Factor Dynamics without a Therapeutic Administered

$$\frac{dGF}{dt} = m(\text{GF} - \text{GF}_\infty)\left((1 - \text{GF}) - (1 - \text{GF})^{\frac{2}{3}}\right); \quad \text{GF}(0) = \text{GF}_0 \tag{3.12}$$

$$\frac{dV}{dt} = mV(\text{GF} - \text{GF}_\infty); \quad V(0) = V_0 \tag{3.13}$$

[7] Residual standard error of the estimates.

[8] Known as inverse variance weighting; a methodology to concatenate multiple estimates of a parameter to improve accuracy.

[9] The residual standard error for the inverse variance weighting.

where

$$m = \beta - \mu_P + \mu_Q \tag{3.14}$$

and

$$\text{GF}_\infty = \frac{\mu_Q}{m} \tag{3.15}$$

Explanation of Further Parameters in (4.22)-(4.26)

- $GF(t)$: Growth fraction at time t [$dimensionless$].
- m: Effective growth rate, defined as $\beta - \mu_P + \mu_Q$ [d^{-1}].
- GF_∞: Growth fraction when the tumor size plateaus, defined as $\frac{\mu_Q}{m}$ [$dimensionless$].
- GF_0: Initial growth fraction [$dimensionless$].

The Parameter m is Revised when a Treatment is Applied to Take the Form:

$$m = \beta\,(1 - Eff(t)) - \mu_P - K_{\text{kill}} C_p + \mu_Q \tag{3.16}$$

Explanation of Further Parameters in (3.16)

- K_{kill}: Rate at which tumour cells are killed [d^{-1}].
- Eff(t): Effect the drug has on the TW where there are four traditional effects delineated below in Eq (3.17).

$$Eff(t) = \begin{cases} I_{max} C_P & \text{if a Linear effect} \\ I_{max} C_P^2 & \text{if a Quadratic effect} \\ \frac{I_{max} C_P}{IC_{50} + C_P} & \text{if a Michaelis-Menten effect} \\ \frac{I_{max} C_P^n}{IC_{50} + C_P^n} & \text{if a Hill type effect} \end{cases} \tag{3.17}$$

Explanation of Further Parameters in (3.17)

- I_{max}: Maximum effect ranging between $[0, 1]$ [$dimensionless$].
- IC_{50}: Half-maximal effective concentration ranging between $[0, 1]$ [$dimensionless$].
- C_p: Concentration of drug in the "Plasma" [$\mu mol/kg$].

Adapted m Expression

When estimating parameter values the initial effects from (3.17) showcased a strong divergence from the observed data when analysing the individual fits. This led to an adaptation of equation (3.16) to take the form:

$$m = \beta\left(1 + Eff(t)\right) - \mu_P - K_{\text{kill}} C_p + \mu_Q \tag{3.18}$$

Revised C_P accounting for the additive combination of docetaxel and carboplatin

$$Ct_P = Cd_P + Cc_P \tag{3.19}$$

Ct_P is substituted for C_P in 3.17 and 3.18 to perform the results obtained in 5.4.

Explanation of Parameters in (3.19)

- Ct_P: Additive combination of the C_P's of docetaxel and carboplatin [$\mu mol/kg$].
- Cd_P: C_P of docetaxel [$\mu mol/kg$].
- Cc_P: C_P of carboplatin [$\mu mol/kg$].

The model proposed in Nasim's paper [20] was also acknowledged but due to there still being current evaluations of the proposed model's effectiveness and accuracy the model from Yates et al [62] was selected moving forward. However, it should be noted that testing of Nasim's model with a preclinical dataset is further work which could bring valuable insight into oncology and pharmacology.

3.2 Initial Forward Simulations

3.2.1 The Literature

Proceeding with insight acquired from the Yates et al model's forward simulations can be performed of the TGM with a vehicle agent and treatment plan [62]. Credibility of the anticipated results will be determined using initial benchmark parameter values prior to a more comprehensive parameter approximation. Such forward simulations will be conducted in the coding language MATLAB [64].

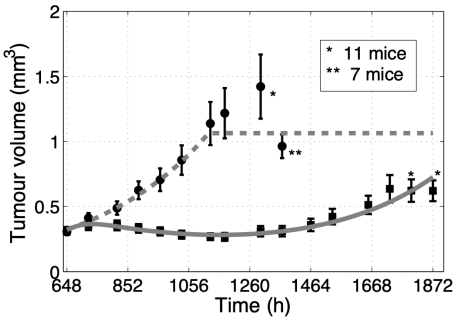

(a) Illustrated tumour growth in mice where a treatment regimen is compared with the control [68].

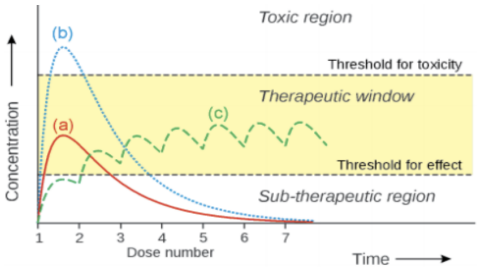

(b) Depiction of PK and the therapeutic window [13].

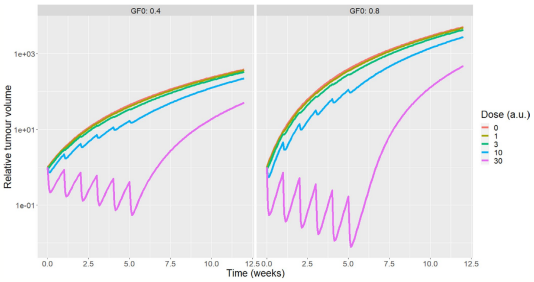

(c) Tumour growth showcased in literature by Yates [62].

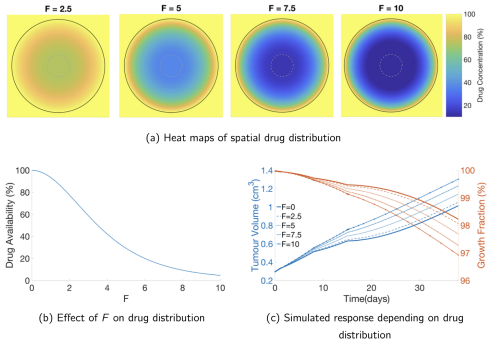

(d) Tumour progression and growth fraction showcased in literature by Nasim [63].

Figure 3.4. *Various visuals from the literature which depict anticipated simulations for; tumour weights, growth fraction, and PK of the administered therapeutic.*

The aim is to observe the characteristics as seen in the literature, e.g., figures 3.4(b) and 3.4(c) for tumour growth where the control commonly starts slowly following an exponential growth phase then decelerates eventually adhering to a plateau following a Gompertz model [19]. Furthermore when a therapeutic is administered a desirable simulation should show the tumour responds to the drug by decreasing in weight and then start to grow again until another dose is administered, Fig 3.4(c) [62]. The PK is absorbed via IP administration, distributed from plasma to the body's tissues and eliminated via the kidneys. Contrary to ADME in Fig 2.1, metabolic activity is not defined via the compartmental models $3.1 - 3.3$ and $3.4 - 3.6$ since metabolic activity had minimal effect upon the pharmacokinetics of docetaxel and carboplatin [40], [54], [70].

3.2.2 The Simulations

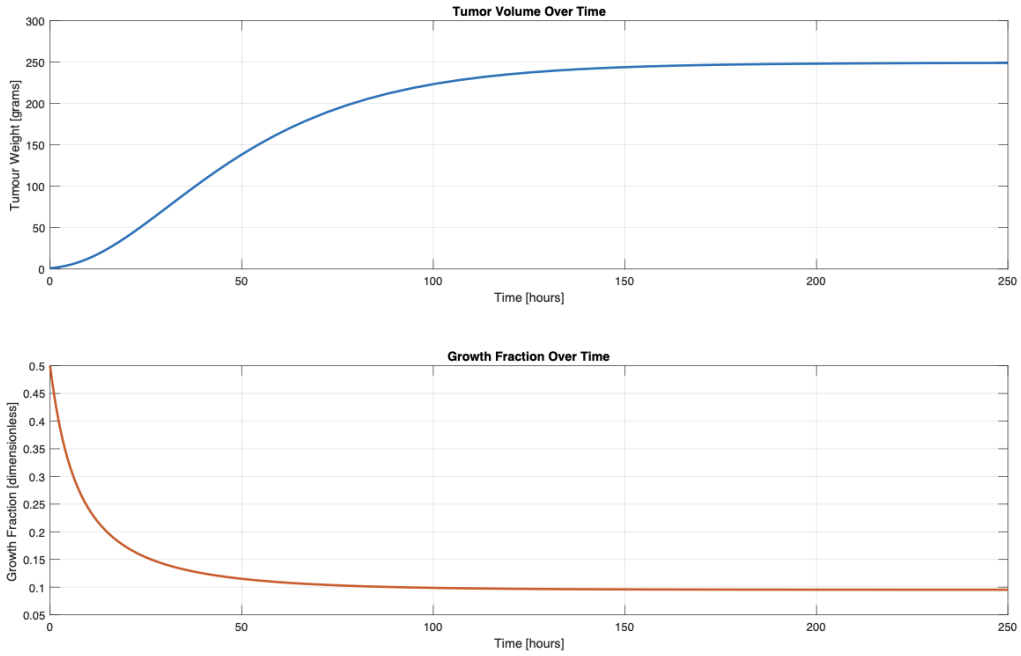

(a) Initial forward simulation of tumour growth without a treatment regimen employed.

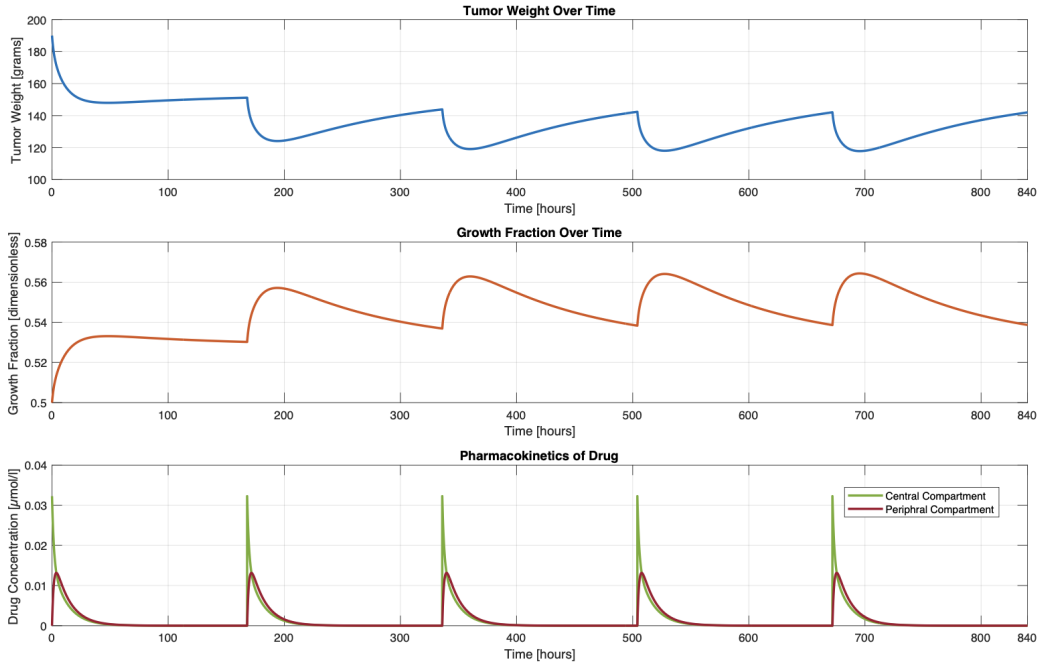

(b) Initial forward simulation of tumour growth and PK when a drug is administered at periodic intervals.

Figure 3.5. *Various visuals from the literature which depict anticipated simulations for; tumour weights, growth fraction, and PK of the administered therapeutic.*

Dissimilar to PD only treatment data such as carboplatin will have PD to examine. Additionally to the aforementioned PDs it is essential that the PD adheres the core literature [13].

The vehicle agent group (3.5(a)) highlighted the simulation procured similar dynamics to the literature (3.4(a)), (3.4(d)). Specifically the characteristics of a decreasing growth factor while TW grows 3.4(d).

The showcased figure (3.5(b)) illustrates similar characteristics to academic material (3.4(c)), (3.4(b)) where a reduction in TW is observed when effective therapeutics are administered such as carboplatin[62].

3.3 Preclinical Dataset

3.3.1 Overview of Data

The preclinical dataset was provided via project collaborators at GSK for docetaxel and carboplatin separately and in combination, which showcased a primary focus upon patient-derived xenografts which corresponded to Invasive Breast Carcinoma (IBC). Notably, a fraction of the database constructed was a Not Otherwise Specified (NOS) form of breast cancer, showcasing that a handful of breast cancers are challenging to partition into further subsections such as IBC for enhanced specificity. A spectrum of cancer cell lines had been grafted onto host tissue where their volumes were measured over time. A portion of the treatments such as docetaxel, carboplatin were administered separately and in combination. Some of these ACAs were given a placebo, showcased as the control group, and others the chemotherapeutic. The dosage level for docetaxel and carboplatin in the preclinical dataset was $20mg/kg$ and $50mg/kg$ respectively. Similarly, in combination, a dosage of $20mg/kg$ was given. For all the studies which are being evaluated from the preclinical dataset an intraperitoneal (IP) bolus administration was used. The control groups weren't administered with treatment of any dosage level or a vehicle agent was applied.

A definition of the columns provided with the preclinical dataset as well as added columns to aid PE computed in Monolix is as follows:

- "AgentName" - Identifies the drug being administered.
- "Patient_ID" - Identifies the code showcasing specific patients.
- "Animal_ID" - Delineates the specific animal identified in the study.
- "ID" - Code identifying the ID.
- "OBS_DAY" - Showcases the day an observation of TW is taken.

- "TUMOR_WT" - Showcases the size of the TW.
- "SDC_Diagnosis_Description" - Identifies the cell line.
- "Study" - Highlights the study selected.
- "Group" - Identifies the code showcasing the group an animal belongs to.
- "Dose Level" - The amount of drug administered.
- "Unit" - Showcases the unit for the dose level.
- "Route" - Delineates how the drug is administered.
- "Frequency" - Showcases how often a drug is administered to a patient.
- "Regressor" - Showcases the initial values of the TWs in the data. This was an addition to the raw dataset provided by GSK.

There were 20, 11, 19 and 7 studies in the preclinical PDX database corresponding to; the control where no therapeutic or a vehicle agent was administered, docetaxel, carboplatin, docetaxel and carboplatin in combination respectively. Additionally, a dosing level of $50mg/kg$ was employed for carboplatin as well as $20mg/kg$ used for both docetaxel separately and in combination with carboplatin.

3.3.2 Ethical, Legal, Social, and Professional Considerations

Due to the fact that the data used was publicly available and related to animal studies the project does not meet the conditions for requiring ethical approval, however due to the scope of the report there should still be a reflection on the standard of welfare. Although, data collection was not a technique for this project, the preclinical secondary data collection, which GSK was fully approved for, must still be assessed. Currently by law animals do not have the legal status that humans do leading, to the debate as to whether consent can be dismissed or should ethical concerns in research and testing be scrutinised further. Throughout this project concerns regarding the welfare of animals and the effect this has upon the pharmaceutical industry has been acknowledged. For instance the controversial case which delineated the harmful experiments undergone in the Silver Spring Monkeys study [71] was compared with the long term benefit which has come from preclinical testing, questioning if testing is justified if the results are significant enough [72]. This project pivots on such a question, where derivation of a reliable mathematical model, can over time, minimise the amount of animals affected by testing and still reach a positive outcome [73]. This methodology demonstrates the use of the 3 R's[10] a widely accepted strategy internationally when designing an approach for humane animal testing and research [74], [73]. Emphasis has been put upon the use of mathematical models and

[10]Replacement, Refinement, and Reduction.

simulations in order, in the future, to replace animals being used in clinical studies [74], [73].

The therapeutics being researched in separation and combination are carboplatin and docetaxel with a focus on treating IBC one of the leading causes of mortality and government expense in the UK [75], [76].

Chapter 4

Methodology

4.1 Analysis of Preclinical Data

Prior to conducting PE preliminary analysis of the preclinical data was performed. This provided a beneficial overview of the dataset where trends and similarities between studies within the dataset could be examined allowing for an informed judgment to be made as to which studies should be analysed further in this project. The dataset was scrutinised so that potential outliers or potential challenges with estimations could be spotted in the early stages of the project. There were varied strategies used to diagnose the aforementioned shortcomings.

The control dataset which has been partitioned into its corresponding studies is showcased in Appendix (A.2.1). It is clear that the study **HCI-023** is an outlier within the data. Further to this the distinct observational period of the TW running up to 120 days, where most studies concluded at 30 days, highlighted a clear disparity in this study to the others. It was deemed necessary to remove this study to minimise unfavourable performance metrics and results.

Alongside this it is necessary to remove all studies in other datasets such as docetaxel which do not appear within the control dataset. From these datasets which extend from Appendix (A.2) the studies **HCI-001, HCI-002, HCI-016, HCI-019** were removed from the docetaxel dataset. Further to this, studies should be kept to a distinct time period for consistency and comparability between the studies and to reduce noise. For this reason the studies **15008-TG9, HCI-027-TG5, HCI-030-TG5** were removed from the docetaxel and carboplatin in the combination dataset used, where docetaxel was administered first.

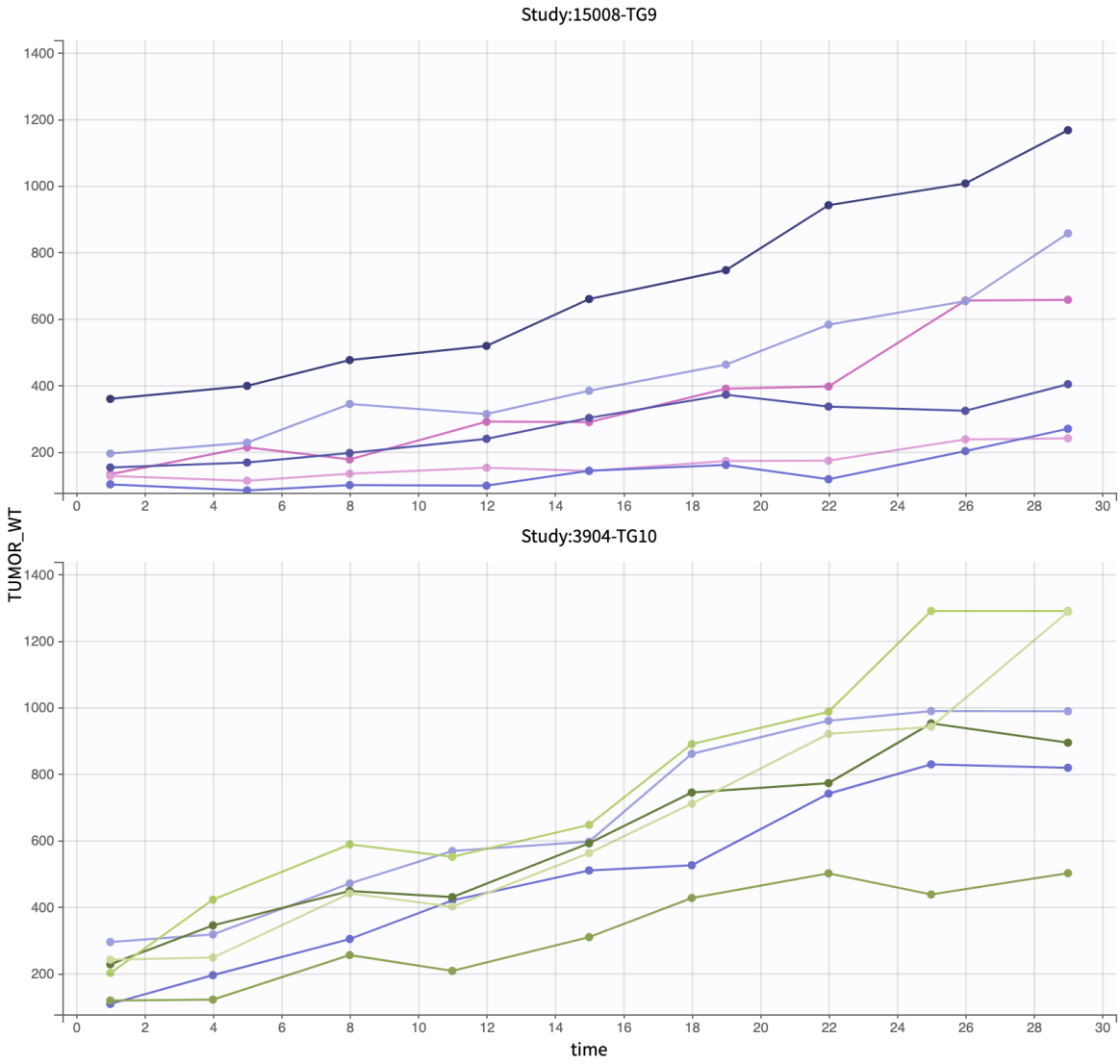

Figure 4.1. *Visual of tumour weights over time for the studies 15008-TG9 and 3904-TG10*

Homing in on specific studies such as **15008-TG9** and **3904-TG10** Fig (4.1) shows discrepancies in their characteristics. Study **15008-TG9** illustrates this with a slightly higher rate of increase showcasing a marginally elevated TW by the end of the concluded time. It is worth noting that this study has a steady trend and minimal fluctuations. Conversely, study **3904-TG10** showcases a more inconsistent trend where **3904-TG10** follows a cycle of rapid growth which then evolves into a slower progression.

Another key aspect is the relative dissimilarities between the data when observing the same studies but with treatments, such as docetaxel and carboplatin, with the aforementioned control dataset. This can be seen by referring to Appendix A.2 where attention is directed towards the steady-states and declining growth rates. In particular study **3904-TG10**, where carboplatin is administered, manifests a steady-state during its observational period. Conversely, compared to the majority of the control studies this steady-state illustrates carboplatin's ability to sustain a

fairly consistent TW demonstrations to carboplatin's effectiveness for this study.

4.2 Manipulation of Preclinical Data

4.2.1 Implementation of a Regressor

The initial TW (Vt_0) was determined by means of a regressor constructed in Excel, which can be referred to in Appendix A.1.1 and integrated into the Monolix model. The regressor utilised from the Monolix toolbox performed effective predictive capabilities for the parameter Vt_0 where a unique TW was not available. It is worth noting that the regressor was used for all the control and treatment groups and the corresponding Mlxtran code can be found in Appendix B.1 specifically lines 6 and 11 in Appendix B.1.1; code which will be found in all Mlxtran scripts.

4.2.2 Detection and Removal of Influential Cases

Further to this, the built-in Excel filter function was used to remove unwanted studies where their influence masked true relationships between terms within the models. For instance, **HCI-023** lasted longer than the majority studies inducing an unfavourable influence on the results. Furthermore tumour weights have not been collected in their entirety, Fig 4.2.

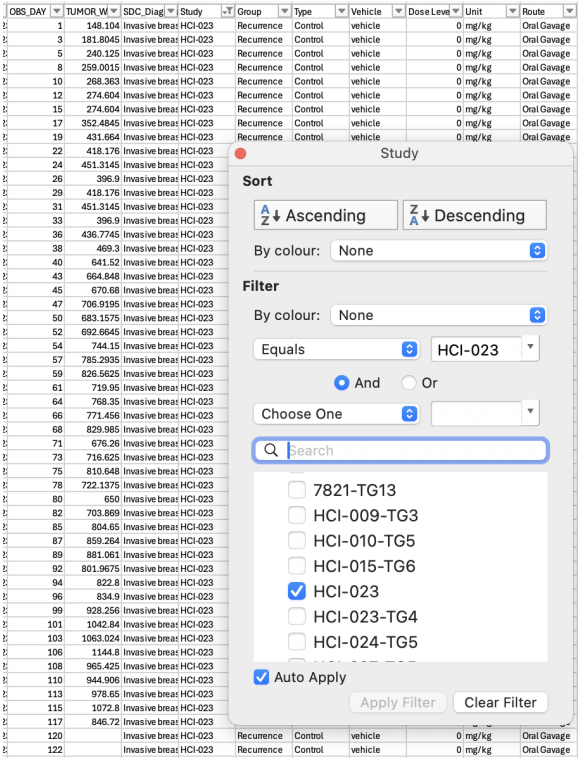

Figure 4.2. *Demonstration of the in-built filter function within Excel to remove outliers.*

4.3 Structural Identifiability Analysis

4.3.1 Revised Tumour Growth Model

The proposed TGM defined by Eqs (3.10) can be refined where R_{diff} is expressed in terms of V Eqs (4.1)-(4.6) as follows:

Tumour Volume

$$\frac{dV}{dt} = V\left((\beta - \mu_P)\,\text{GF} - \mu_Q\,(1 - \text{GF})\right); \quad V(0) = V_0 \tag{4.1}$$

and Growth Fraction

$$\text{GF} = 1 - \left(1 - \frac{R_{\text{diff}}}{r}\right)^3 \tag{4.2}$$

where (4.2) can be rearranged to give:

$$\left(1 - \frac{R_{\text{diff}}}{r}\right)^3 = 1 - \text{GF} \implies 1 - \frac{R_{\text{diff}}}{r} = (1 - \text{GF})^{\frac{1}{3}} \tag{4.3}$$

$$\implies \frac{R_{\text{diff}}}{r} = 1 - (1 - \text{GF})^{\frac{1}{3}} \tag{4.4}$$

$$\implies \frac{R_{\text{diff}}}{1 - (1 - \text{GF})^{\frac{1}{3}}} = r = \left(\frac{3V}{4\pi}\right)^{\frac{1}{3}} \tag{4.5}$$

since the tumour is assumed to be spherical
Therefore, $\frac{dV}{dt}$ can be expressed as:

$$\frac{dV}{dt} = V\left((\beta - \mu_P)\left(1 - \left(1 - \frac{R_{\text{diff}}}{\left(\frac{3V}{4\pi}\right)^{\frac{1}{3}}}\right)^3\right) - \mu_Q\left(1 - \left(1 - \frac{R_{\text{diff}}}{\left(\frac{3V}{4\pi}\right)^{\frac{1}{3}}}\right)^{\frac{1}{3}}\right)\right) \tag{4.6}$$

Yields an ODE solely in terms of the observed variable $V(t)$

4.3.2 Taylor Series Approach

Now that the Growth Factor (GF) Eqs (4.2) has been utilised to show that the radius can be expressed in terms of TW via Eqs (4.6) it is possible to use the Taylor series approach for SIA of TGM.

The Taylor series approach is effective at dealing with nonlinear models and hence an appropriate and reliable choice to determine structural ineffability for the TGM.

4.3.3 Validation of Tumour Growth Model for Control

Structural identfiability analysis will be determined for Eqs (3.10) where the m expression is defined by 3.14.
The unknown parameters for the control are defined as:

$$p = (\beta,\ \mu_P,\ \mu_Q)^T \tag{4.7}$$

with output given by

$$y(t,p) = V_t(t,p).$$

Consider the Taylor series coefficients of the TGM for control given the system of observations is given by $y = V(t)$:

$$y(0) = V(0) = V_0$$

$$\dot{y}(0) = \dot{V}(0) = V_0(\beta - \mu_p + \mu_Q)\left(\frac{2^{2/3}\left(\frac{\pi}{3}\right)^{1/3} \cdot R_{diff}}{V_0^{\frac{1}{3}}} - \frac{\mu_Q}{\beta - \mu_p + \mu_Q}\right) \tag{4.8}$$

$$\ddot{y}(0) = \ddot{V}(0) = (\beta - \mu_p + \mu_Q)\left(\frac{4 \cdot 2^{2/3}\left(\frac{\pi}{3}\right)^{1/3} \cdot R_{diff}}{3V_0^{\frac{1}{3}}} - \frac{\mu_Q}{\beta - \mu_p + \mu_Q}\right) \tag{4.9}$$

$$\dddot{y}(0) = \dddot{V}(0) = -\frac{2}{9V_0^{\frac{4}{3}}} \cdot 2^{2/3}\left(\frac{\pi}{3}\right)^{1/3}(\beta - \mu_p + \mu_Q) \cdot R_{diff} \tag{4.10}$$

Then combining (4.8) and (4.9),

$$\dot{y}(0) - \frac{3}{2}\ddot{y}(0) = \frac{1}{2}\mu_Q \tag{4.11}$$

Highlighting, μ_Q is unique from (4.11) which allows $\beta - \mu_p$ to be shown to be unique via (4.10). Therefore, it can be seen that μ_Q is uniquely identifiable however the other parameters β and μ_p only there difference is unique. This shows that the model is not globally structurally identifiable for the TGM of the control.

4.3.4 Validation of Tumour Growth Model for Treatment

Structural identfiability analysis will be determined for (3.10) where the m expression is defined by 3.16.
The unknown parameters for the treatment are defined as:

$$p = (\beta,\ \mu_P,\ \mu_Q,\ K_{kill},\ I_{max}, IC_{50})^T \tag{4.12}$$

with output given by

$$y(t,p) = V_t(t,p).$$

Consider the Taylor series coefficients of the TGM for treatment:

$$y(0) = V(0) = V_0 \tag{4.13}$$

$$\dot{y}(0) = \dot{V}(0) = \left(C_pK_{kill} + \left(1 - \frac{C_pI_{max}}{C_p + IC_{50}}\right)\beta - \mu_p + \mu_Q\right) \times$$

$$\left(\frac{2\cdot 2^{2/3}\left(\frac{\pi}{3}\right)^{1/3}\cdot R_{diff}}{V_0^{\frac{1}{3}}} - \frac{\mu_Q}{C_pK_{kill}+\left(1-\frac{C_pI_{max}}{C_p+IC_{50}}\right)\beta-\mu_p+\mu_Q}\right) \tag{4.14}$$

$$\ddot{y}(0) = \ddot{V}(0) = -\frac{2\cdot 2^{2/3}\left(\frac{\pi}{3}\right)^{1/3}\cdot R_{diff}}{3V_0^{\frac{1}{3}}}\left(C_pK_{kill} + \left(1 - \frac{C_pI_{max}}{C_p + IC_{50}}\right)\beta - \mu_p + \mu_Q\right) +$$

$$\left(C_pK_{kill} + \left(1 - \frac{C_pI_{max}}{C_p+IC_{50}}\right)\beta - \mu_p + \mu_Q\right)\left(\frac{2\cdot 2^{2/3}\left(\frac{\pi}{3}\right)^{1/3}\cdot R_{diff}}{V_0^{\frac{1}{3}}} - \frac{\mu_Q}{C_pK_{kill}+\left(1-\frac{C_pI_{max}}{C_p+IC_{50}}\right)\beta-\mu_p+\mu_Q}\right) \tag{4.15}$$

$$\dddot{y}(0) = \dddot{V}(0) = -\frac{2\cdot 2^{2/3}\left(\frac{\pi}{3}\right)^{1/3}\cdot R_{diff}}{9V_0^{\frac{4}{3}}}\left(C_pK_{kill} + \left(1 - \frac{C_pI_{max}}{C_p + IC_{50}}\right)\beta - \mu_p + \mu_Q\right) \tag{4.16}$$

The equations delineated in $(4.13)-(4.16)$ showcase a common factor $C_pK_{kill}+\left(1 - \frac{C_pI_{max}}{C_p+IC_{50}}\right)\beta-\mu_p + \mu_Q$ hence by grouping this combination together where:

$$F = C_pK_{kill} + \left(1 - \frac{C_pI_{max}}{C_p + IC_{50}}\right)\beta - \mu_p + \mu_Q \tag{4.17}$$

Then, the equations $(4.3.4) - (4.16$ can be simplified where F is a unique term:

$$\dot{y}(0) = \dot{V}(0) = F\left(\frac{2\cdot 2^{2/3}\left(\frac{\pi}{3}\right)^{1/3}\cdot R_{diff}}{V_0^{\frac{1}{3}}} - \frac{\mu_Q}{F}\right) \tag{4.18}$$

$$\ddot{y}(0) = \ddot{V}(0) = F\left(\frac{4\cdot 2^{2/3}\left(\frac{\pi}{3}\right)^{1/3}\cdot R_{diff}}{3V_0^{\frac{1}{3}}} - \frac{\mu_Q}{F}\right) \tag{4.19}$$

$$\dddot{y}(0) = -F\left(\frac{2\cdot 2^{2/3}\left(\frac{\pi}{3}\right)^{1/3}\cdot R_{diff}}{9V_0^{\frac{4}{3}}}\right) \tag{4.20}$$

Then combining (4.18) and (4.19),

$$\dot{y}(0) - \frac{3}{2}\ddot{y}(0) = \frac{1}{2}\mu_Q \tag{4.21}$$

Highlighting, μ_Q is unique from (4.21) hence only the combination $C_p K_{kill} + \left(1 - \frac{C_p I_{max}}{C_p + IC_{50}}\right)\beta - \mu_p$ is identifiable via (4.20). This implies that only this combination and μ_Q should be parameterised in Monolix. However, insight by Yates et al [62] suggests PEs of the parameters separately is still of significance.

4.3.5 Considerations

In both cases considered, calculating further derivatives, Taylor series coefficients, will not help with identifying any other parameters for the control and treatment TGMs aforementioned. Therefore, additional techniques such as STRIKE-GOLDD[1] and Exact Arithmetic Rank (EAR)[2] should be performed to determine if further parameters are unique with the objective of proving the model is structurally globally identifiable.

4.4 Steady-State Analysis

Steady-state analysis will be performed generically allowing the insight acquired to be applied to the results obtained for the PEs. This aids the evaluation of individual fits which have diverged from the anticipated fits. Specifically, fits which have a close neighbourhood around the steady-state point with the potential of seeing more fluctuations between growth and decay in the individual fits.

4.4.1 Conditions for Steady-States

For GF to be a steady-state set $\frac{dGF}{dt} = 0$:

$$\frac{dGF}{dt} = m(GF - GF_\infty)\left((1 - GF) - (1 - GF)^{\frac{2}{3}}\right); \quad GF(0) = GF_0 \tag{4.22}$$

For V to be a steady-state set $\frac{dV}{dt} = 0$:

$$\frac{dV}{dt} = mV(GF - GF_\infty); \quad V(0) = V_0 \tag{4.23}$$

where, for the control:

$$m = \beta - \mu_P + \mu_Q \tag{4.24}$$

for the treatment:

$$m = \beta\,(1 + Eff(t)) - \mu_P - K_{\text{kill}} C_p + \mu_Q \tag{4.25}$$

[1] A structural identifiability tool made to run in MATLAB [77].

[2] A type of structural identifiability analysis which can be accessed by request from the Fraunhofer Charmans Centre.

and

$$GF_{\infty} = \frac{\mu_Q}{m} \tag{4.26}$$

4.4.2 Steady-States Occurring from Tumour Volume, Growth Fraction or the m Expression

Case 1:

When $GF = GF_{\infty}$ a steady-state will be reached implying that the growth fraction is at its equilibrium level $GF_{\infty} = \frac{\mu_Q}{m}$.

Case 2:

When $(1 - GF) - (1 - GF)^{\frac{2}{3}} = 0$ when GF tends to either 1 or 0:

- At a value of 1 the growth factor is maximised emphasised by the tumour being fully saturated.
- At a value of 0 growth factor has been fully exhausted potentially suggesting apoptosis.

Case 3:

For the control when $m = \beta - \mu_P + \mu_Q = 0$ a steady-state will be reached hence the evaluation of the parameter β, μ_P and μ_Q.

Case 4:

For the treatment when $m = \beta\,(1 + Eff(t)) - \mu_P - K_{kill}C_p + \mu_Q = 0$.

4.5 Parameter Estimation

4.5.1 Delineation of Model in Monolix

The specialised modelling language Monolix was utilised for computing PEs of all mathematical models delineated in this project and written in Mlxtran [66]. For example, carboplatin and docetaxel in both separation and combination had their parameters estimated in Monolix. These aforementioned treatments were simulated no less than four times as their were four fundamental effects which were of significance to the tumour response when a drug was applied. Depending on the treatment regimen being estimated there were varied responses from the studies caused by the distinct effects. The control group was independent of these effects because there was no therapeutic administered for an effect to occur. For each treatment strategy the spectrum of models were: linear effect, quadratic effect, Michaelis-Menten effect, Hill type

effect. It should be highlighted that it is only the effect function which changes across all of the treatments for the pharmacodynamics, however a notable point is the Hill type effect could not be fitted for docetaxel and carboplatin in combination.

Dissimilar to the pharmacodynamics of the various Monolix models curated, the PK varied across all of the mathematical models. As stated prior both carboplatin and docetaxel are modelled via a two-compartmental model with outflows both coming from the central compartment however are unique through their different parameter values. As no drug is applied to the control there are no PK simulations in this system. The complexity of the model is amplified with the two chemotherapeutics combined as it is necessary for the combined effect of these two drugs to be determined also.

The Mlxtran code for all the models starts with a "$DESCRIPTION$:" block explaining what each model does aiding individuals unfamiliar with this modelling software and providing a better understanding of the effect applied to the administered drug being estimated. Moving forward, the "$[LONGITUDINAL]$" block is where the model resides. Parameters which need to be estimated are scripted into the "$input = \{\}$" variable prior to the PK block which delineates the PK model. Subsequently, the "$depot(target = \dots)$" is used to identify the compartment which the therapeutic is administered to. Furthermore, "$\{use = regressor\}$" was integrated so initial values of Vt_0 could be successfully identified by Monolix. The "$EQUATION$:" block delineates the entirety of the mathematical equations which describe the model being used, including their initial conditions. Finally, the "$OUTPUT$:" block determines what modelled outputs are fitted to the observed preclinical data.

4.5.2 Initial Parameter Estimation

Running of the SAEM protocol is supported with IPE in Fig 4.3 were facilitated prior allowing the SAEM algorithm to compute estimates more timely and reliably because of the guidance of the IPEs. Monolix illustrates both the predicted parameter values and the observed data with the fitted model on the same visual in the IPE interface. The intention of this preliminary phase is to observe trends within the fitted model which resemble the observed data to a degree. Known parameters which were provided from mathematical and pharmaceutical literature were fixed in the initial parameter interface. On the contrary, unknown parameters were calculated through the utilisation of the Maximum Likelihood Estimation (MLE)[3]. To begin with IPEs for the control dataset were performed as this was to least complex computation as there were fewer parameters to be estimated compared to the treatment group. Inference of these parameters β, μ_P and μ_Q were obtained relatively quickly from the SAEM algorithm. The of estimates procured for the control were then used to aid further approximations in the treatment groups where

[3]The likelihood function is a measure of how effectively a model is able to observe,in this case the preclinical data, when parameter values are varied. The algorithm attempts to maximise this value.

the values for the fixed effect and random effects guiding the starting values for docetaxel and carboplatin both in separation and combination. Notably, estimation of the treatment groups was also more challenging as the literature did not advise on initial values for the varied effects such as the linear effect and Hill type effect.

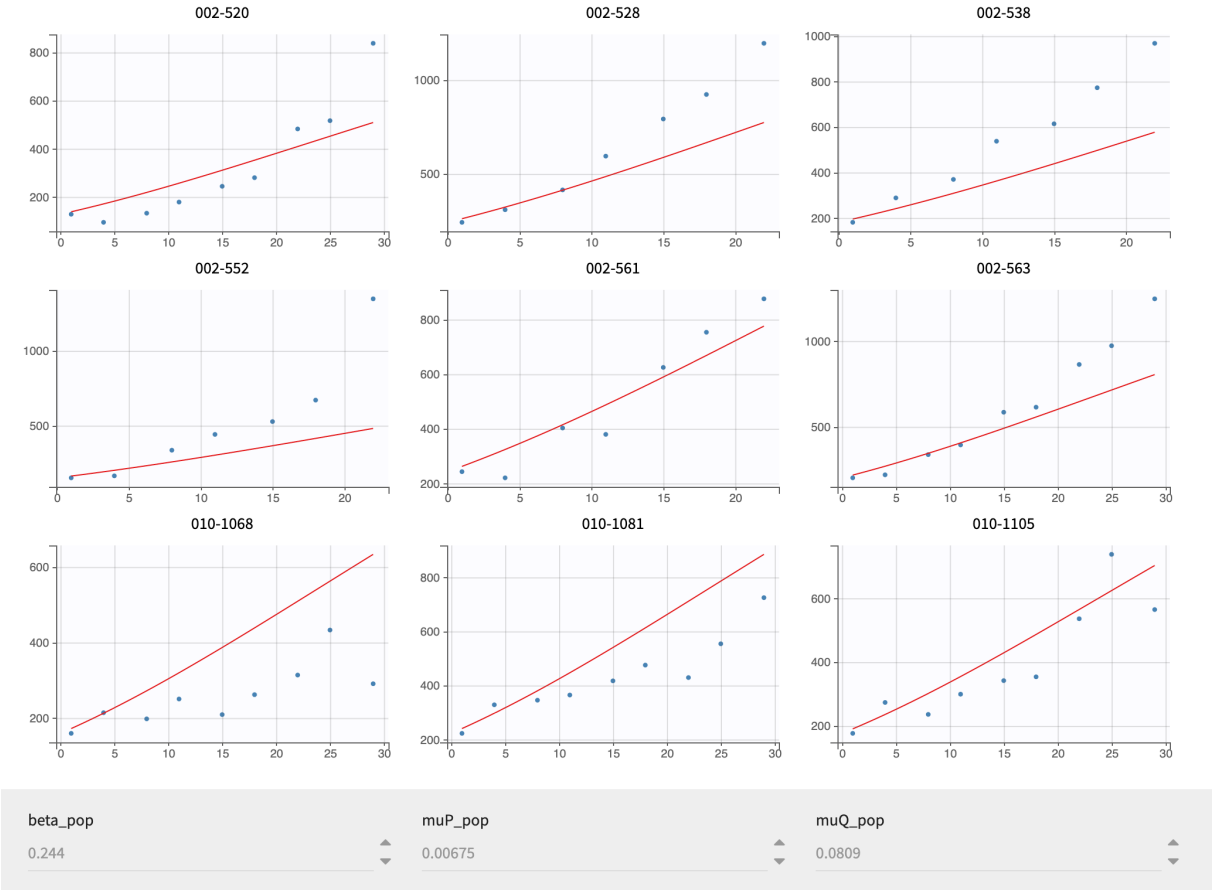

Figure 4.3. *Initial PEs for studies* $HCI-002$ *and HCI-010.*

Chapter 5

Results

This section presents results both visually and quantitatively with individual fits illustrated as well as performance metrics such as the Standard Error (SE)[1], the Relative Standard Error (RSE)[2] and the Coefficient of Variation (CoV)[3] and the error model defined in tables adapted from the modelling language Monolix output [66].

Furthermore, there were four fundamental error models which could be performed in Monolix such as; the constant error model[4], the proportional error model[5] and two types of combined error models[6]. The error model utilised to produce the presented results was the combined model from Appendix F.1.3 which demonstrated the best fit in comparison to other accessible error models.

The linearisation approach was performed to fit the preclinical PDX datasets to various mathematical models where, the stochastic approach was not utilised.

[1]Highlights the variability of the sample mean from the true population mean mathematically shown by, Eq F.5.

[2]Delineates the standard error with respect to the magnitude of the sample shown mathematically by, Eq F.6.

[3]Delineates the relationship between the standard deviation and mean as a percentage shown by, Eq F.7

[4]The simplest error model where the error remains constant no matter the predicted value shown in Appendix F.1.1.

[5]The error model shown in Appendix F.1.2 rises proportionally with the predictor f.

[6]The combined error models in Monolix are shown in Appendix F.1.3 and F.1.3.

5.1 Control Group

PEs were performed on the TGM (3.9)-(3.12) where no therapeutic was administered. This was performed on the preclinical PDX data where the entirety of the studies for the dataset are referred to in Appendix A.2.1.

Parameter	**VALUE**		**S.E.**	**R.S.E. (%)**
Fixed Effects				
beta_pop	0.19		0.0088	4.65
muP_pop	0.00084		0.00044	53.2
muQ_pop	0.05		0.0059	12.0
Parameter	**VALUE**	**C.V.(%)**	**S.E.**	**R.S.E. (%)**
Standard Deviation of the Random Effects				
omega_beta	0.3	30.28	0.032	10.8
omega_muP	1.8	498.47	0.43	23.8
omega_muQ	0.55	58.88	0.11	19.8
Error Model Parameters				
a	6.71		2.58	38.4
b	0.12		0.009	7.39

Table 5.1. *Parameter estimates of the control group simulated in Monolix [66].*

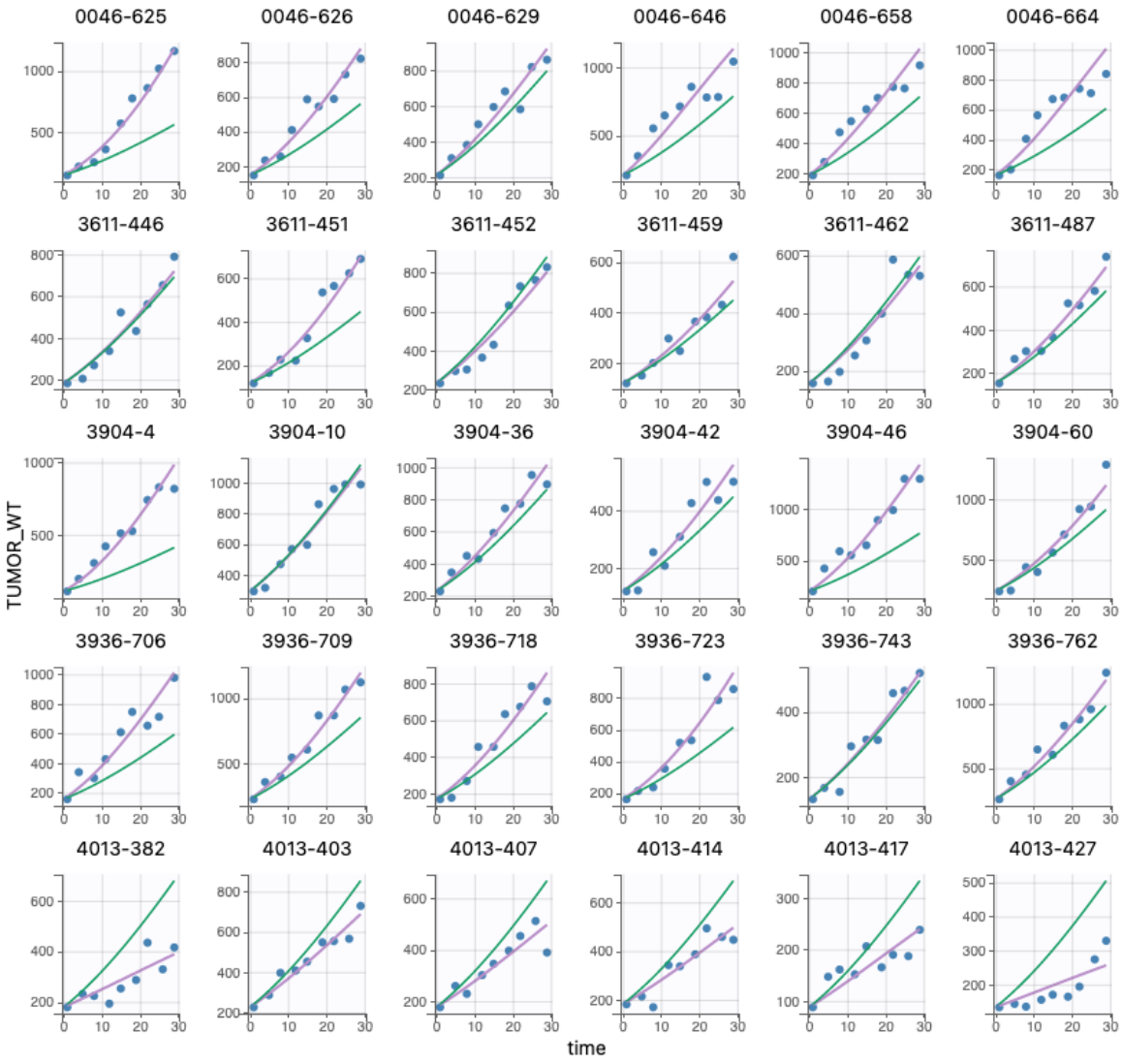

Figure 5.1. *Individual fits of the control group simulated in Monolix, figure 2 [66].*

5.2 Docetaxel Group

PEs were performed on the TGM $(3.9), (3.10), (3.12)$ and the m expression (3.13). The therapeutic docetaxel was administered and defined by the Eqs $(3.1) - (3.3)$. The effects which are applied in (5.2.1)-(5.2.2) and (E.1.1) can be referred to in Eqs (3.17). Results were performed on preclinical PDX data where the entirety of the studies for the dataset are referred to in Appendix A.2.2.

5.2.1 Linear Effect

Parameter	**VALUE**		**S.E.**	**R.S.E. (%)**
Fixed Effects				
beta_pop	0.32		0.046	14.0
muP_pop	0.015		0.03	207
muQ_pop	0.000042		0.00013	322
K_kill_pop	0.2		0.04	20.5
I_max_pop	0.44		0.13	30.7
Parameter	**VALUE**	**C.V.(%)**	**S.E.**	**R.S.E. (%)**
Standard Deviation of the Random Effects				
omega_beta	0.42	44.41	0.11	24.9
omega_muP	1.13	160.52	2.77	245
omega_muQ	3.24	19251.8	2.33	71.9
omega_K_kill	0.36	36.78	0.14	40.3
omega_I_max	0.46	48.67	0.26	55.3
Error Model Parameters				
a	8.65		2.01	23.2
b	0.14		0.019	13.4

Table 5.2. *Parameter estimates of docetaxel group with the linear effect term simulated in Monolix [66].*

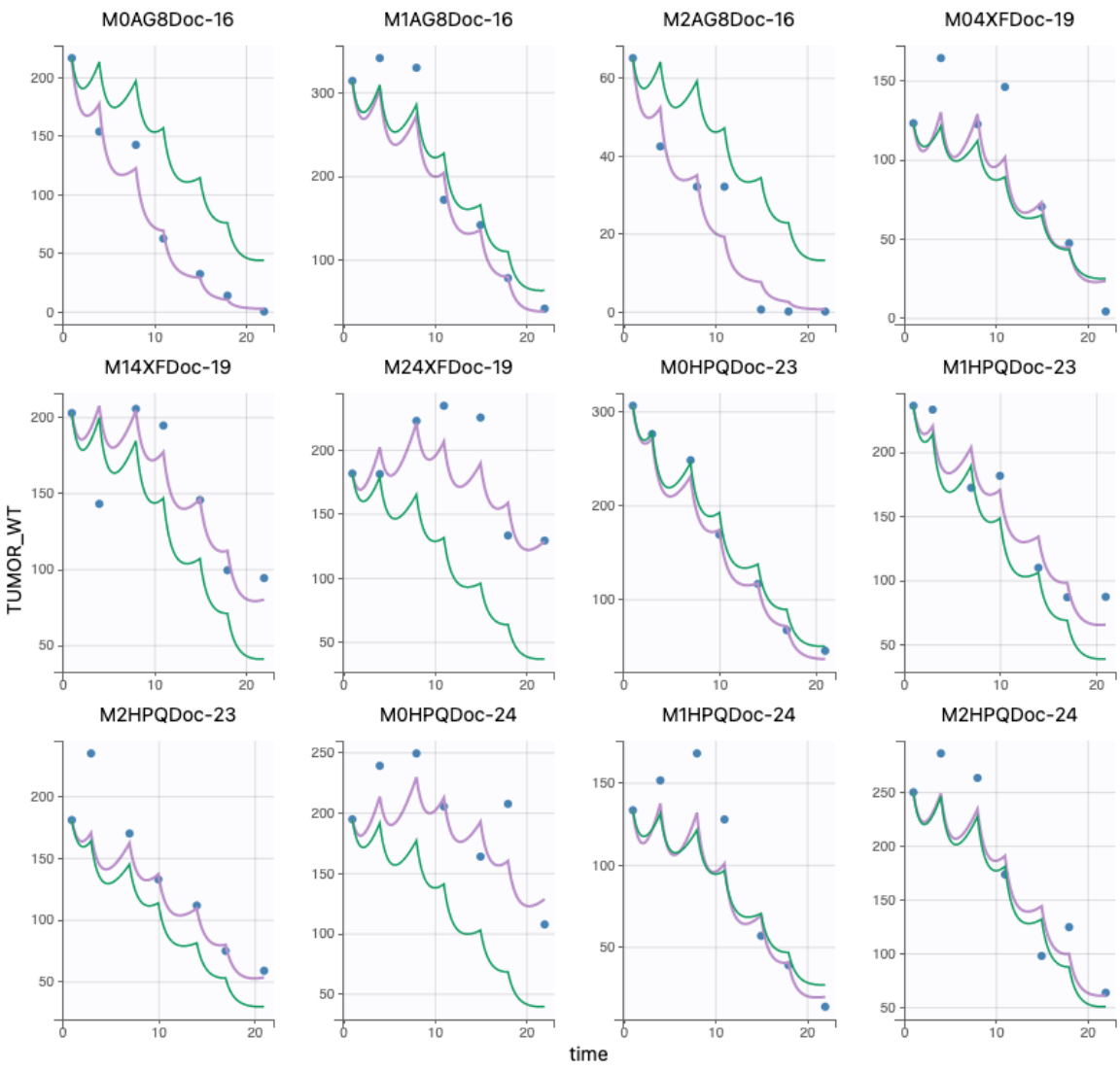

Figure 5.2. *Individual fits of the docetaxel treatment group with the linear effect simulated in Monolix, figure 2 [66].*

5.2.2 Michaelis-Menten Effect

Parameter	VALUE		S.E.	R.S.E. (%)
Fixed Effects				
beta_pop	0.19		0.045	23.5
muP_pop	0.0028		0.0098	353
muQ_pop	0.059		0.04	68.4
K_kill_pop	0.04		0.0057	14.3
I_max_pop	0.5		0.22	42.8
IC_50_pop	1.83		0.22	12.1
Parameter	**VALUE**	**C.V.(%)**	**S.E.**	**R.S.E. (%)**
Standard Deviation of the Random Effects				
omega_beta	0.28	28.12	0.08	25.4
omega_muP	2.06	828.56	3.71	180
omega_muQ	0.3	31.08	0.98	323
omega_K_kill	0.34	35.02	0.086	25.3
omega_I_max	0.39	40.03	0.21	53.3
omega_IC_50	0.071	7.11	0.099	140
Error Model Parameters				
a	10.99		2.23	20.3
b	0.11		0.019	17.1

Table 5.3. *Parameter estimates of docetaxel group with the Michaelis-Menten effect simulated in Monolix [66].*

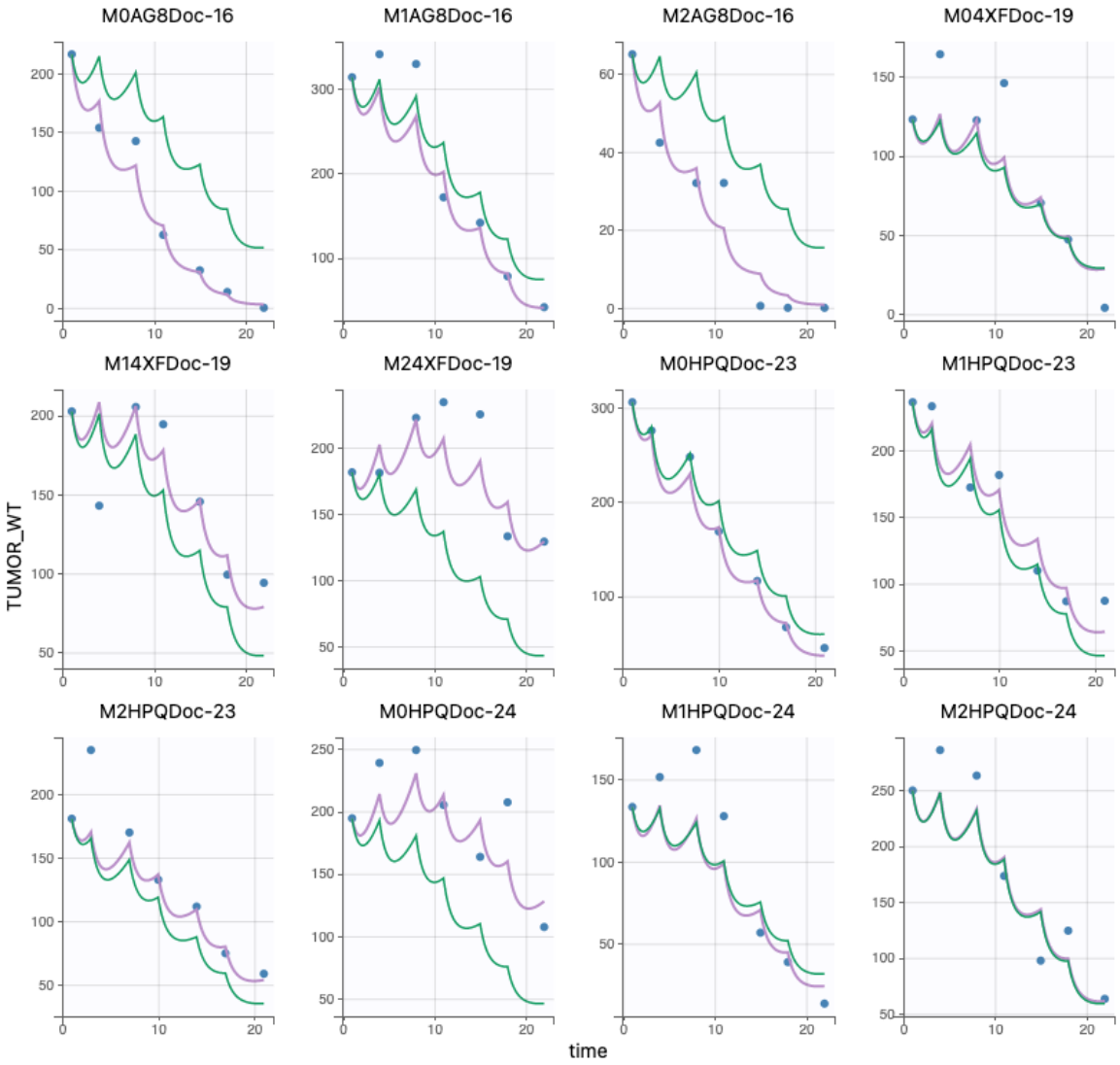

Figure 5.3. *Individual fits of the docetaxel treatment group with the Michaelis-Menten effect simulated in Monolix, figure 2 [66].*

5.3 Carboplatin Group

PEs were performed on the TGM $(3.9), (3.10), (3.12)$ and the m expression (3.13). The therapeutic carboplatin was administered and defined by the Eqs $(3.4) - (3.6)$. The effects which are applied in $(5.3.1) - (5.3.4)$ can be referred to in Eqs (3.17). Results were performed on preclinical PDX data where the entirety of the studies for the dataset are referred to in Appendix A.2.3.

5.3.1 Linear Effect

Parameter	VALUE		S.E.	R.S.E. (%)
Fixed Effects				
beta_pop	0.33		0.034	10.3
muP_pop	0.01		0.0083	81.8
muQ_pop	0.18		0.033	18.7
K_kill_pop	0.19		0.035	18.4
I_max_pop	0.55		0.1	18.3
Parameter	**VALUE**	**C.V.(%)**	**S.E.**	**R.S.E. (%)**
Standard Deviation of the Random Effects				
omega_beta	0.027	2.72	0.17	639
omega_muP	1.62	359.62	0.59	36.2
omega_muQ	0.42	44.25	0.085	20.1
omega_K_kill	0.15	15.35	0.086	56.1
omega_I_max	0.13	12.78	0.12	92.5
Error Model Parameters				
a	10.46		1.83	17.5
b	0.1		0.0093	9.20

Table 5.4. *Parameter estimates of carboplatin group with the linear effect simulated in Monolix [66].*

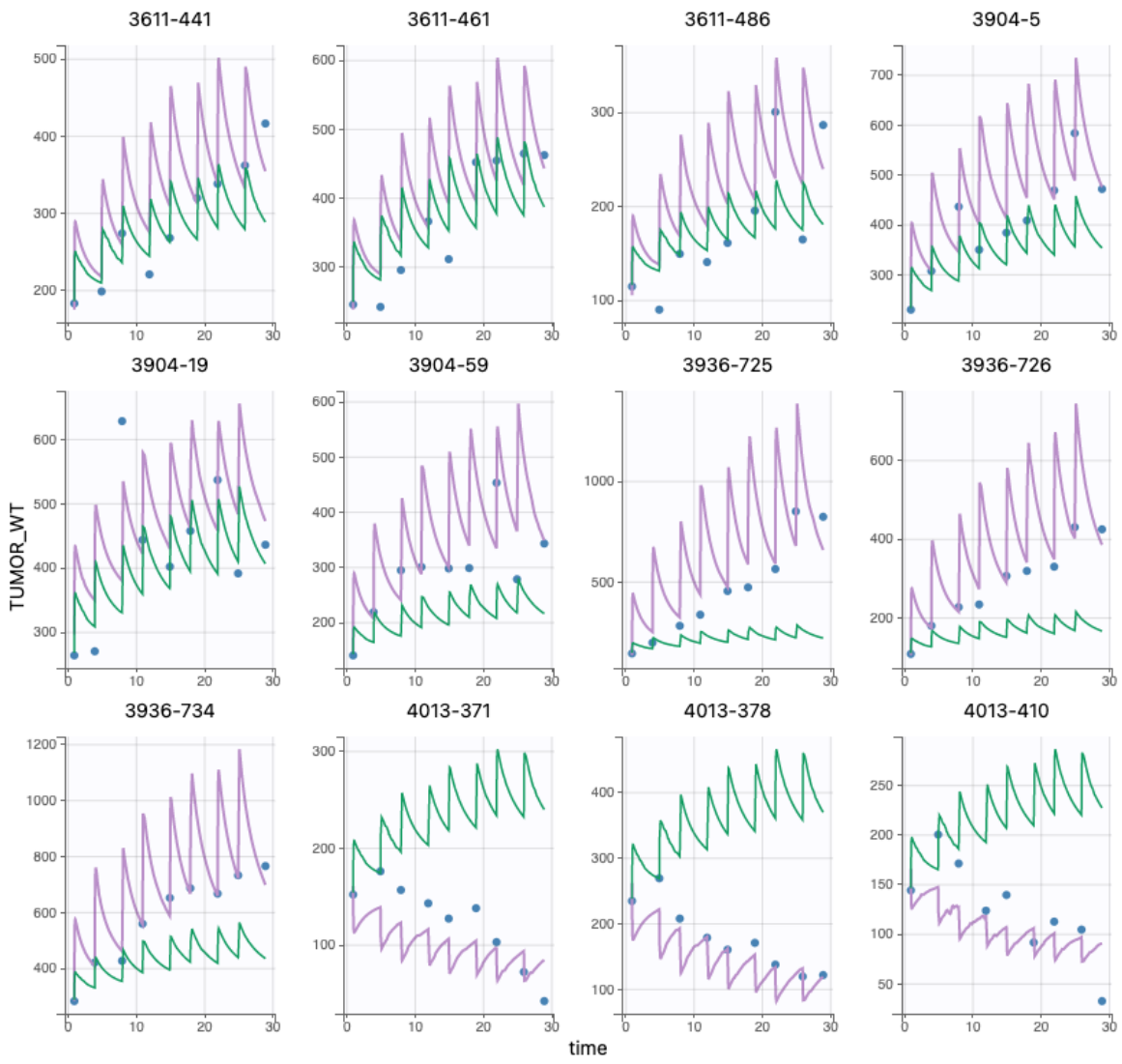

Figure 5.4. *Individual fits of the carboplatin treatment group with the linear effect simulated in Monolix, figure 3 [66].*

5.3.2 Michaelis-Menten Effect

Parameter	VALUE		S.E.	R.S.E. (%)
Fixed Effects				
beta_pop	0.26		0.029	11.1
muP_pop	0.19		0.028	14.8
muQ_pop	0.037		0.0079	21.2
K_kill_pop	0.013		0.003	23.4
I_max_pop	0.48		0.16	32.5
IC_50_pop	0.07		0.08	114
Parameter	**VALUE**	**C.V.(%)**	**S.E.**	**R.S.E. (%)**
Standard Deviation of the Random Effects				
omega_beta	0.12	12.34	0.087	70.5
omega_muP	0.22	22.45	0.1	47.3
omega_muQ	0.23	23.12	0.16	70.0
omega_K_kill	1.21	181.48	0.16	13.7
omega_I_max	0.17	17.2	0.6	350
omega_IC_50	1.16	168.83	0.84	72.4
Error Model Parameters				
a	10.83		1.93	17.9
b	0.1		0.0098	9.40

Table 5.5. *Parameter estimates of carboplatin group with the Michaelis-Menten effect simulated in Monolix [66].*

5.3.3 Quadratic Effect

Parameter	VALUE		S.E.	R.S.E. (%)
Fixed Effects				
beta_pop	160.7		1.76	1.10
muP_pop	0.0094		0.0021	22.4
muQ_pop	149.56		2.14	1.43
K_kill_pop	3.08		0.57	18.4
I_max_pop	0.011		0.0021	18.5
Parameter	**VALUE**	**C.V.(%)**	**S.E.**	**R.S.E. (%)**
Standard Deviation of the Random Effects				
omega_beta	0.038	3.78	0.011	28.0
omega_muP	0.93	116.61	0.17	17.9
omega_muQ	0.068	6.82	0.011	16.6
omega_K_kill	1.31	213.56	0.13	9.99
omega_I_max	1.29	207.79	0.13	10.3
Error Model Parameters				
a	18.01		3.41	18.9
b	0.12		0.016	13.7

Table 5.6. *Parameter estimates of carboplatin group with the quadratic effect simulated in Monolix [66].*

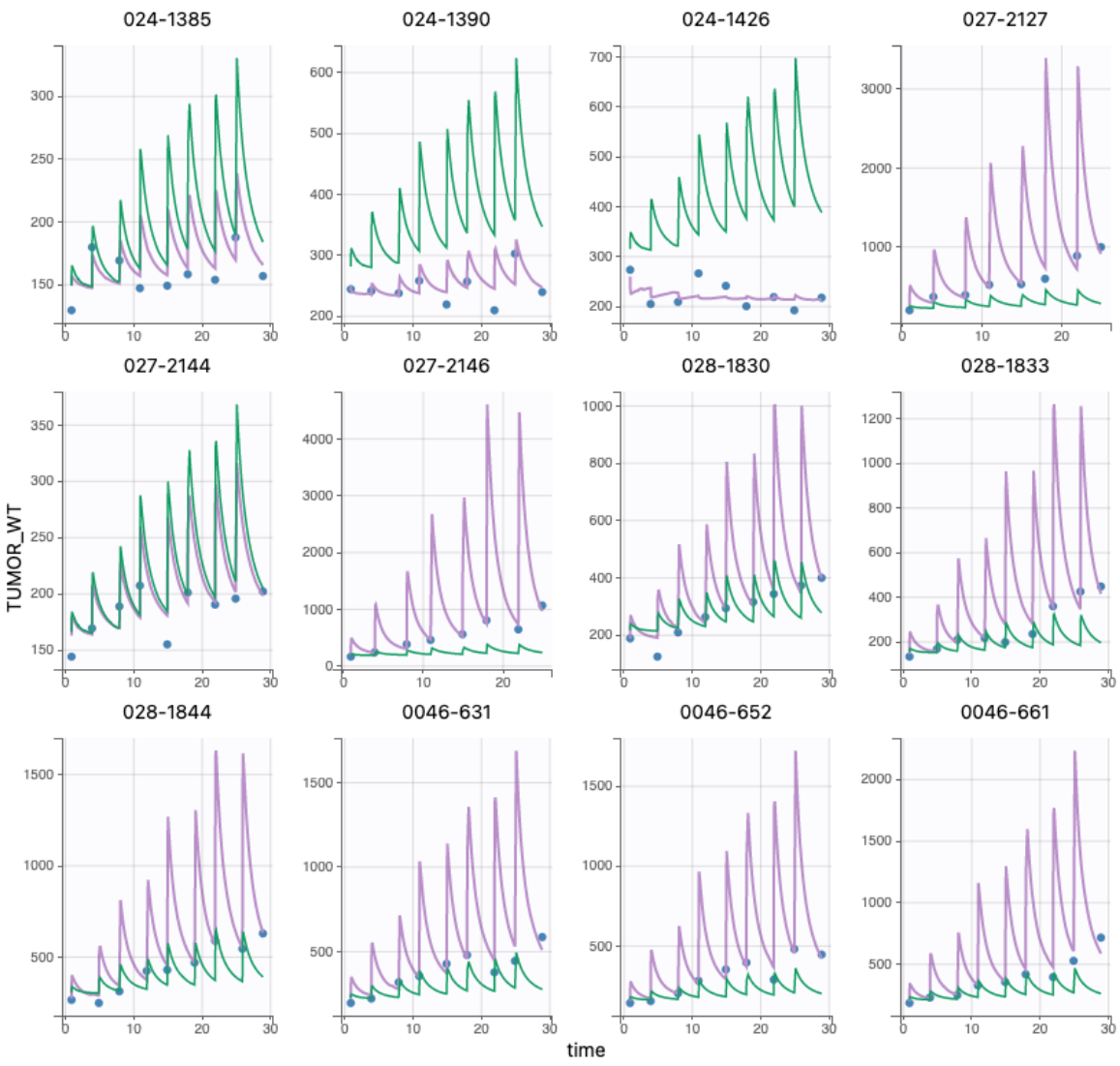

Figure 5.5. *Individual fits of the carboplatin treatment group with the quadratic effect simulated in Monolix, figure 2 [66].*

5.4 Docetaxel and Carboplatin in Combination

PEs were performed on the TGM $(3.9), (3.10), (3.12)$ and the m expression (3.13). The therapeutics docetaxel and carboplatin were administered and defined by Eqs $(3.1) - (3.3)$ and $(3.4) - (3.6)$ respectively. The therapeutic effects which are applied in (5.4.1)-(5.3.3) can be referred to in Eqs (3.17) which are performed on both carboplatin and docetaxel where their effects are then summed together, Eqs 3.19. Results were performed on preclinical PDX data where the entirety of the studies for the dataset are referred to in Appendix A.2.4.

5.4.1 Additive Drug Combination with Linear Effect

Parameter	**VALUE**		**S.E.**	**R.S.E. (%)**
Fixed Effects				
beta_pop	39.67		2.02	5.10
muP_pop	9.75		1.25	12.8
muQ_pop	30.11		2.11	7.00
K_kill_pop	1.56		0.18	11.4
I_max_pop	0.0068		0.0049	72.1
Parameter	**VALUE**	**C.V.(%)**	**S.E.**	**R.S.E. (%)**
Standard Deviation of the Random Effects				
omega_beta	0.15	14.9	0.038	25.8
omega_muP	0.38	38.96	0.097	25.9
omega_muQ	0.2	20.42	0.053	26.3
omega_K_kill	0.37	37.85	0.082	22.5
omega_I_max	2.05	810.32	0.53	26.0
Error Model Parameters				
a	46.93		8.28	17.6
b	0.0019		0.032	1.71e+3

Table 5.7. *Additive drug combination with the linear affect for docetaxel and carboplatin in combination [66].*

5.4.2 Additive Drug Combination with Quadratic Effect

Parameter	VALUE		S.E.	R.S.E. (%)
Fixed Effects				
beta_pop	42.26		2.59	6.13
muP_pop	4.61		1.05	22.8
muQ_pop	18.84		1.19	6.32
K_kill_pop	0.91		0.15	16.1
I_max_pop	0.049		0.022	44.7
Parameter	**VALUE**	**C.V.(%)**	**S.E.**	**R.S.E. (%)**
Standard Deviation of the Random Effects				
omega_beta	0.18	18.03	0.045	25.4
omega_muP	0.57	61.66	0.18	32.3
omega_muQ	0.18	17.99	0.047	26.4
omega_K_kill	0.37	37.85	0.12	22.5
omega_I_max	1.1	154.63	0.32	31.8
Error Model Parameters				
a	25.66		8.98	35.0
b	0.19		0.033	28.6

Table 5.8. *Parameter estimates of the additive combination of docetaxel and carboplatin with the Michaelis-Menten effect expression simulated in Monolix [66].*

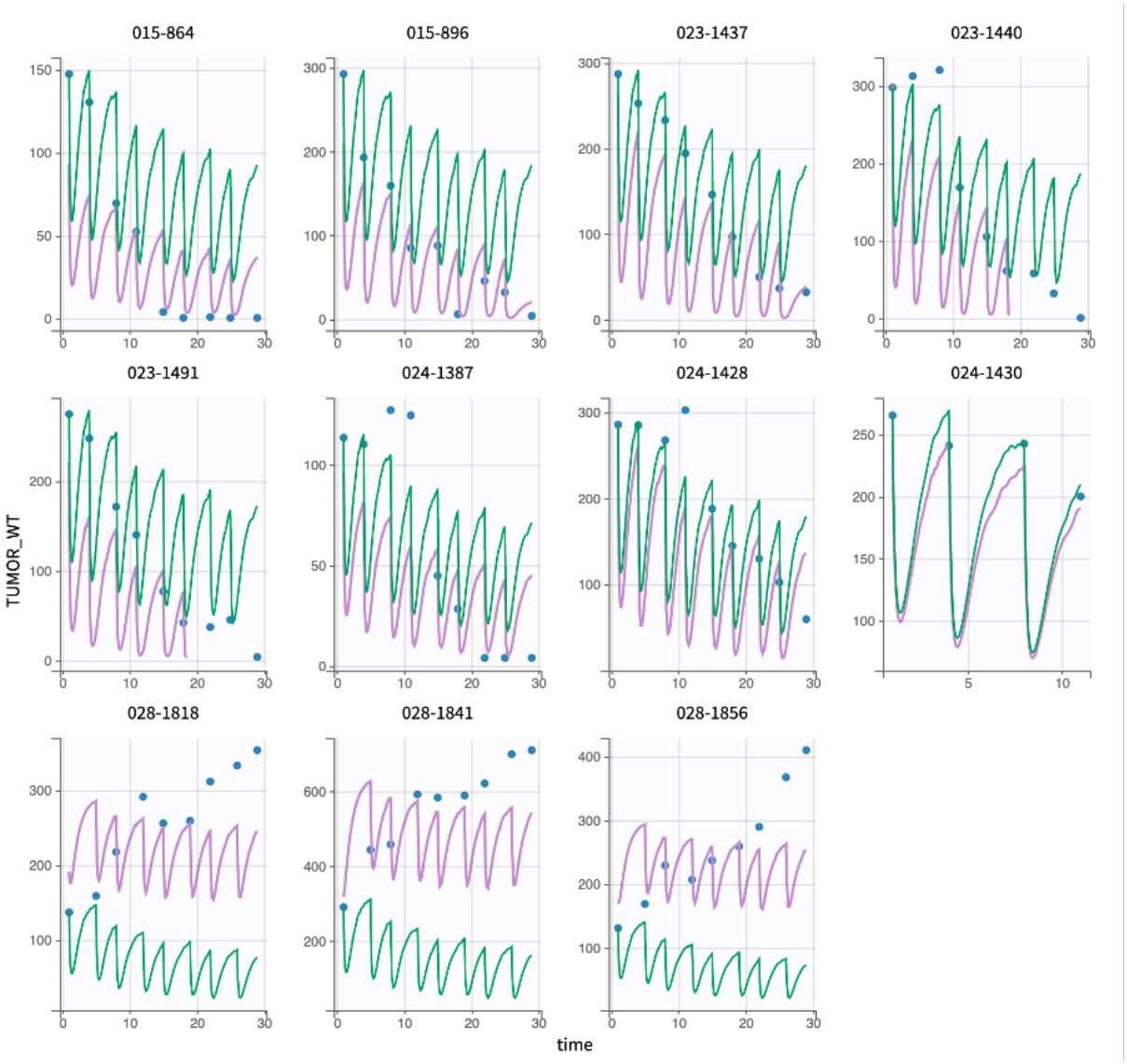

Figure 5.6. *Individual fits of the additive drug combination with the quadratic affect for docetaxel and carboplatin in combination [66].*

5.4.3 Additive Drug Combination with Michaelis-Menten Effect

Parameter	VALUE		S.E.	R.S.E. (%)
Fixed Effects				
beta_pop	34.82		3.75	10.8
muP_pop	3.3		0.97	29.5
muQ_pop	15.2		1.76	11.6
K_kill_pop	0.72		0.16	22.5
I_max_pop	0.049		0.023	46.7
IC_50_pop	0.038		0.017	43.6
Parameter	**VALUE**	**C.V.(%)**	**S.E.**	**R.S.E. (%)**
Standard Deviation of the Random Effects				
omega_beta	0.31	32.19	0.08	25.4
omega_muP	0.74	86.08	0.23	31.5
omega_muQ	0.33	34.4	0.086	25.8
omega_K_kill	0.68	77.32	0.16	23.9
omega_I_max	0.93	118.03	0.41	43.5
omega_IC_50	0.87	106.55	0.34	39.2
Error Model Parameters				
a	18.55		7.9	42.6
b	0.22		0.052	23.9

Table 5.9. *Additive drug combination with the linear effect term for docetaxel and carboplatin in combination [66].*

Chapter 6

Evaluation and Discussion

The Monolix software appropriately colours relative standard error(RSE)[1] values in accordance with the degree of accuracy, where yellow, orange and red are used for values upward of 50, 100 and 200 respectively. This is a pivotal illustration of how effective Monolix has been at estimating the necessary parameters for the given model and data. Substantial RSE values impact on the credibility of the parameter estimates making any predictions conducted ineffective for pharmaceutical insight. It is crucial that such parameters are thoroughly examined to yield performance metrics which indicate that the mathematical models have successfully fitted to the datasets provided.

6.1 Review of Results

6.1.1 Performance Metrics

For the carboplatin treatment the quadratic effect yields the smallest RSE values, Table (5.8), indicating that this effect produced the best fit and was most resilient to the biological variability from the studies in this treatment regimen because the linear effect (5.4), Michaelis-Menten effect (5.6) and Hill type effect terms (E.2) all yielded parameter estimates with higher RSE values. Namely, the Hill type effect performed poorly for all groups in this investigation hence further analysis was stopped.

For the docetaxel treatment the linear effect and Michaelis-Menten effect terms yielded the smallest RSE values, tables $(5.3) - (5.2)$, where the Michaelis-Menten effect was capable of more robustly estimating the fixed effects, however Michaelis-Menten significantly underperformed in relation to the RSEs of the random effects compared to the linear effect.

For docetaxel and carboplatin in combination the quadratic effect yielded the smallest RSE values, table (5.8), indicating this effect produced the best fit. It should be noted that the Michaelis-Menten effect also produces some significant results with minimal RSE values highlighting a robust model for this treatment strategy, table (5.9). The linear effect term produced promising results for the fixed effects and random effects parameters however the performance metrics for the error within the model demonstrated major shortcomings for this model table (5.7). This

[1] Statistical metric which is used to review the precision of an estimate. The mathematical formula is referred to in F.6.

was concluded by not integrating the linear effect term into the forward simulations used to assess the effects of varied dosing regimens from the treatment plans parameterised effectively. Initial parameter estimates for the Hill type effect term were not influential enough for SAEM to be performed on this model so no parameter estimates can be observed for this framework.

6.1.2 Error Models

Whilst the combined error model in Appendix F.1.3 produced results with the lowest RSE values overall, table (5.7), the proportionality constant "b" with a RSE of $1.71e+3\%$ conflicts this. The metrics obtained in this case suggest a different error model would be an optimal choice, for instance, the constant error model in Appendix (F.1.1) where the proportionality constant is not a term of the model. Table (5.7) was a rare case in this investigation hence the combined error model in Appendix (F.1.3) continued to be used. However scenarios such as model $(5.4.1)$ should be interpreted with caution.

The entirety of the structural models for the treatment and control groups aside from the metrics delineated in table (5.7) for the error model showed all their results for error model components to be below 50%. This was illustrated by none of the RSE values being highlighted in red, orange or green.

6.1.3 Individual Fits

Docetaxel illustrated individual fits for the Michaelis-Menten effect and linear effect, Fig (D.1.3) and (D.1.2) respectively. The figures presented the most aggressive responses to tumours where administration of this therapeutic not only induced an antiproliferative effect but also the weight of tumours declined considerably. Further to this, the population fits followed closely to the trends of the individual fits highlighting the consistencies between the entirety of studies and individuals reinforcing the credibility of the model.

Carboplatin displayed considerably less coherence with the individual and population fits suggesting there was more biological variability for this therapeutic. Potentially caused via the larger number of stuides investigated for this group illustrated by Appendix A.2.3 compared to docetaxel. Furthermore, large disturbances can be observed at points of administration becoming more pronounced when the quadratic effect is performed. This indicates further inspection upon the TGM or error model is warranted potentially followed by reparameterisation.

6.1.4 Visual Predictive Checks

VPC was performed upon model $(5.4.1)$ where the error model in Appendix F.1.3 computed a large RSE value. The VPC shown in Appendix D.32 emphasises the error aforementioned in table (5.7) where the confidence interval is large in comparison to the VPC for the control group shown in Appendix D.31. Furthermore, the presence of outliers highlighted by red circles on a VPC warrants additional investigation reflecting the potential need for some models to be reparameterised.

6.2 AIC and BIC Analysis

Further to the aforementioned results the values for the Akaike Information Criterion (AIC)[2] and Bayesian Information Criterion (BIC)[3] illustrate the quality of the fits for the various models constructed. A review of the AIC and BIC has not been undertaken for the Hill type effect due to the significantly high RSEs which were mentioned previously.

Chemotherapeutic	Model	AIC	BIC
Control	No Effect	8731.14	8751.14
	Quadratic Effect	*	*
	Linear Effect	*	*
	Michaelis-Menten Effect	*	*
Carboplatin	No Effect	*	*
	Quadratic Effect	5888.74	5911.92
	Linear Effect	4842.11	4865.29
	Michaelis-Menten Effect	4869.73	4896.78
Docetaxel	No Effect	*	*
	Quadratic Effect	1926.8	1939.34
	Linear Effect	1933.98	1946.52
	Michaelis-Menten Effect	1911.84	1929.98
Docetaxel & Carboplatin in Combination	No Effect	*	*
	Quadratic Effect	5888.74	5911.92
	Linear Effect	1273.95	1278.73
	Michaelis-Menten Effect	1405.7	1411.27

Table 6.1. *AIC and BIC values for different models and chemotherapeutics considered.*

The findings shown in Table (6.1) were anticipated to a degree because it is expected that the AIC and BIC values augment with larger datasets [78]. This is demonstrated by the treatment

[2] A statistical tool which aids in finding the balance between simplicity and goodness of fit. AIC formula is shown in Eq F.8.

[3] A statistical tool which aids in finding the balance between simplicity and goodness of fit although has a bigger penalty compared to AIC for the number of parameter used in a model. BIC formula is shown in Eq F.9.

regimens with progressively smaller datasets such as; control, carboplatin, docetaxel, carboplatin and docetaxel in combination.

However, it should be noted that for docetaxel and carboplatin in combination with the quadratic effect, the values obtained contrast the other effects in the treatment group. Whilst, both chemotherapeutics illustrate a good fit with the quadratic effect separately it is seen that when combined the model lacks the same effectiveness.

In summary, the linear effect term produced the best results for the carboplatin and docetaxel fits best with the Michaelis-Menten effect term where the quadratic effect was the second best for this treatment. Additionally, the Michaelis-Menten effect was also the optimal choice for docetaxel and carboplatin in combination when assessing these performance metrics. This was also observed for both the AIC and BIC measures.

6.3 Forward Simulations

In light of some notable of the PEs aforementioned, a systematic review of forward simulations for various treatment regimens was performed and assessed. This section will focus on testing a number of different dosing levels to evaluate the most effective dose for the respective treatment strategies. The administration of the therapeutics has been simulated with a weekly interval adhering to the preclinical dataset. It is important to note that docetaxel has not been simulated because of how aggressively the tumours responded to this therapeutic at a standard dose in the studies which were performed [68].

6.3.1 Analysis of Tumour Dynamics and Growth Fraction when Carboplatin is Administered at Various Dose Levels and Intervals

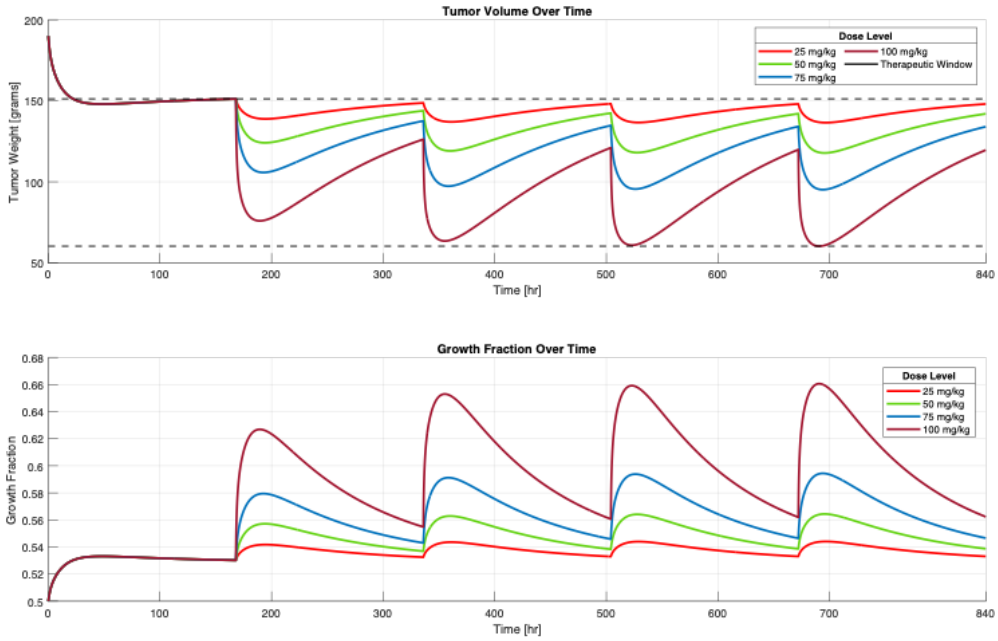

Figure 6.1. *Forward predictions of tumour volume and growth fraction when the chemotherapeutic carboplatin is administered weekly at various dose levels.*

Figure (6.1) shows the effects that carboplatin has upon TW for various dose levels. It is evident that as the dose increases reduction in TW intensifies. Furthermore, steady-states occur at the same time points and a cyclical trend is observed where tumour weight declines significantly upon administration, then continues to rise until the next IP administration. Albeit the potency attributed to a dose level, toxicity of each regimen must be evaluated through the PKs of carboplatin.

6.3.2 Pharmacokinetic Analysis when Carboplatin is Administered at Various Dose Levels and Intervals

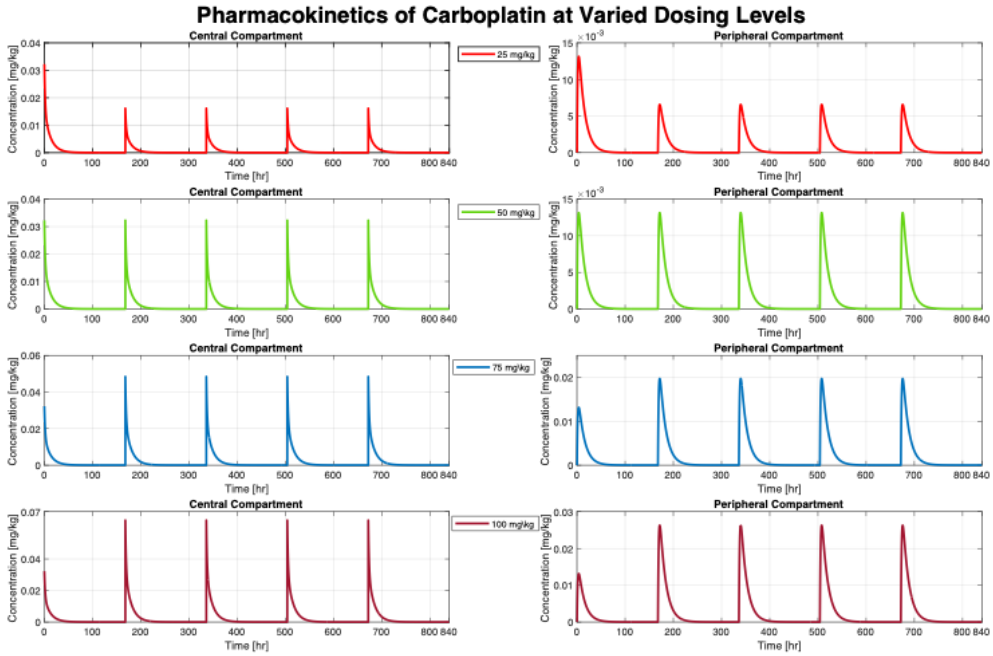

Figure 6.2. *Forward predictions regarding the distribution of the chemotherapeutic carboplatin between two affinities. Namely, the plasma and tissues corresponding to the central and peripheral compartments respectively; administered weekly at various dose levels.*

Figure (6.2) illustrates the PKs of carboplatin at various dosing levels ranging from $25mg/kg$ to $100mg/kg$ with an administration on a weekly basis. The central compartment for each dose shows that only a portion of the administered dose culminates in this compartment at approximately 64% where the rest is dissipated to unintended sites.

The simulations in Figure (6.2) demonstrate a weekly dosing regimen ensures that a minimal trace of the therapeutic is left within both the central and peripheral compartment. The degree to which the steady-state is maintained at this minimal trace level indicates a shorter time to administration over the same time period has the potential to elevate the antiproliferative effect on the tumour, while adhering to the same toxicological profile as a weekly dose shown in, Fig (C.1), (C.2).

Chapter 7

Conclusions and Future Work

7.0.1 Conclusions

This research utilised datasets docetaxel and carboplatin separately and in combination performed in Monolix. Performance metrics such as RSE's and the information criteria were evaluated to optimise; the structural model, studies from the datasets and the error model so a robust and credible model for the control and treatment data can be obtained. Furthermore, quantitative analysis was conducted by comparing PEs; β, μ_P, μ_Q, K_{kill}, I_{max} and IC_{50} as well as VPC analysis.

It was found that 3 of the 4 effects, Fig (3.17) were able to reliably perform fits with the linearisation approach. Namely, the Hill type effect in Appendix E could not produce credible performance metrics. Following this, the docetaxel treatment group demonstrated the most reliable individual fits while carboplatin delineated the best performance metrics but the individual fits responded more aggressively than anticipated. Albeit producing the best performance metrics, the quadratic effect dramatically elevated this aggression to an unrealistic response, Fig (5.5).

Thus, with optimal effects chosen from the framework aforementioned, forward simulations were conducted predicting how tumour weights would respond to varied dosing levels from the chemotherapeutics focusing on the administration of carboplatin. The priority of carboplatin stemmed from docetaxel illustrating an aggressive tumour response showing a considerable decline in weight suggesting no need to alter the standard dosing level; contrary to carboplatin where the antiproliferative effect was not so impactful.

7.0.2 Future Works

It is suggested that some more data should be collected, enough to adequately validate the forward predictions conducted for various dosing levels enhancing the credibility of results.

Whilst the PK models, Eqs $(3.1) - (3.6)$ utilised have been shown to accommodate PKs where there is optimal kidney function the models cannot provide accurate regimen proposals for patients with comorbidities where there is a decline in renal function. This suggests PKPD models can be further personalised to a patients needs providing an enhanced insight into potential

treatments. However, by focusing on personalised simulation to aid more individually-based treatment regimens will potentially necessitate additional preclincal data opposing the 3R's [5], [60].

Moreover, combining therapies necessitates Drug-Drug Interactions (DDIs) to be considered. For instance, the intersection of cardiovascular disease and cancer follows a cyclic trend of treating one disease while aggravating the other [79]. Common regimens for Coronary Heart Disease (CHD) comprise of antiplatelet drugs[1] and statins[2] which are known for interacting with anti-cancer agents and causing efficacy to decline. This is commonly because of the interference CHD drugs have on chemotherapeutics metabolic activity [79], [80]. Following this, it is vital combinations of therapeutics are not evaluated in isolation to a singular disease but anticipation of other comorbidities and the treatments induced should be considered also. This leads back to the argument of personalised medicine especially in the elderly where the associated risks with various diseases are significantly higher [81]. Although notably, the number of individuals also affected in their midlife stage for cancer has rose dramatically over the recent years [2].

[1] A drug known for mitigating blood clots by preventing platelets from clumping together.
[2] A drug which lowers a patients cholesterol levels.

Bibliography

[1] *Cancer Statistics - NCI*. [Online]. Available: https://www.cancer.gov/about-cancer/understanding/statistics#.

[2] G. R. Dagenais, D. P. Leong, S. Rangarajan, *et al.*, "Variations in common diseases, hospital admissions, and deaths in middle-aged adults in 21 countries from five continents (PURE): a prospective cohort study," *The Lancet*, vol. 395, no. 10226, pp. 785–794, Mar. 2020, ISSN: 1474547X. DOI: 10.1016/S0140-6736(19)32007-0. [Online]. Available: http://www.thelancet.com/article/S0140673619320070/fulltext%20http://www.thelancet.com/article/S0140673619320070/abstract%20https://www.thelancet.com/journals/lancet/article/PIIS0140-6736(19)32007-0/abstract.

[3] K. Godfrey, *Compartmental Models and their Application*. London: Academic Press, 1983.

[4] S. Motta and F. Pappalardo, "Mathematical modeling of biological systems," *Briefings in Bioinformatics*, vol. 14, no. 4, pp. 411–422, Jul. 2013, ISSN: 1467-5463. DOI: 10.1093/BIB/BBS061. [Online]. Available: https://dx.doi.org/10.1093/bib/bbs061.

[5] R. C. Hubrecht and E. Carter, "The 3Rs and Humane Experimental Technique: Implementing Change," *Animals : an Open Access Journal from MDPI*, vol. 9, no. 10, Oct. 2019, ISSN: 20762615. DOI: 10.3390/ANI9100754. [Online]. Available: /pmc/articles/PMC6826930/%20/pmc/articles/PMC6826930/?report=abstract%20https://www.ncbi.nlm.nih.gov/pmc/articles/PMC6826930/.

[6] D. Schwartz and J. Lellouch, "Types of intervention and their development," *Journal of Chronic Diseases*, vol. 20, no. 8, pp. 637–648, Jun. 2015, ISSN: 00219681. DOI: 10.1016/0021-9681(67)90041-0. [Online]. Available: https://www.ncbi.nlm.nih.gov/books/NBK305514/.

[7] C. A. Umscheid, D. J. Margolis, and C. E. Grossman, "Key Concepts of Clinical Trials: A Narrative Review," *Postgraduate Medicine*, vol. 123, no. 5, p. 194, Sep. 2011, ISSN: 00325481. DOI: 10.3810/PGM.2011.09.2475. [Online]. Available: /pmc/articles/PMC3272827/%20/pmc/articles/PMC3272827/?report=abstract%20https://www.ncbi.nlm.nih.gov/pmc/articles/PMC3272827/.

[8] R. Gieschke and J.-L. Steimer, "Pharmacometrics: modelling and simulation tools to improve decision making in clinical drug development," *European Journal of Drug Metabolism and Pharmacokinetics*, vol. 25, no. 1, pp. 49–58, Mar. 2000, ISSN: 0378-7966. DOI: 10.1007/BF03190058.

[9] H. M. Byrne, "Dissecting cancer through mathematics: from the cell to the animal model," *Nature Reviews Cancer*, vol. 10, no. 3, pp. 221–230, 2010.

[10] A. Daşu, I. Toma-Daşu, and M. Karlsson, "The effects of hypoxia on the theoretical modelling of tumour control probability," *Acta Oncologica*, vol. 44, no. 6, pp. 563–571, 2005, ISSN: 0284186X. DOI: 10.1080/02841860500244435.

[11] M. Simeoni, P. Magni, C. Cammia, *et al.*, "Predictive pharmacokinetic-pharmacodynamic modeling of tumor growth kinetics in xenograft models after administration of anticancer agents," *Cancer research*, vol. 64, no. 3, pp. 1094–1101, Feb. 2004, ISSN: 0008-5472. DOI: 10.1158/0008-5472.CAN-03-2524. [Online]. Available: https://pubmed.ncbi.nlm.nih.gov/14871843/.

[12] M. Rowland and T. N. Tozer, *Clinical Pharmacokinetics: Concepts and Applications, Philadelphia: Lea & Febiger*. 1980.

[13] S. H. Curry and R. Whelpton, *Introduction to Drug Disposition and Pharmacokinetics, Chichester: John Wiley & Sons, 2017.*

[14] Thorsteinn Loftsson, "Essential pharmacokinetics : a primer for pharmaceutical scientists," *Amsterdam: Academic Press*, 2015.

[15] R. Mehvar, "Principles of Nonlinear Pharmacokinetics," *American Journal of Pharmaceutical Education*, vol. 65, pp. 178–184, 2001.

[16] T. Kerbusch, "Implementation of a transit compartment model for describing drug absorption in pharmacokinetic studies," *Journal of Pharmacokinetics and Pharmacodynamics*, Jan. 2007. [Online]. Available: https://www.academia.edu/87465495/Implementation_of_a_transit_compartment_model_for_describing_drug_absorption_in_pharmacokinetic_studies.

[17] M. Chappell and N. Evans, *Seminar: ES4A4 Biomedical Systems Modelling*.

[18] Y. Jiang, J. Pjesivac, and J. Freyer, "A Cellular Model for Avascular Tumor Growth," 2002.

[19] K. M. Tjørve and E. Tjørve, "The use of Gompertz models in growth analyses, and new Gompertz-model approach: An addition to the Unified-Richards family," *PloS one*, vol. 12, no. 6, Jun. 2017, ISSN: 1932-6203. DOI: 10.1371/JOURNAL.PONE.0178691. [Online]. Available: https://pubmed.ncbi.nlm.nih.gov/28582419/.

[20] K. Adams, "Modelling Anti-Cancer Drug Kinetics and their Therapeutic Effects on Xenografted Tumour Cell Lines in Mice ES327 Technical Report," Tech. Rep.

[21] *BIOLOGICAL DISORDERS — Richards on the Brain*. [Online]. Available: https://www.richardsonthebrain.com/biological-disorders/.

[22] B. Ribba, E. Watkin, M. Tod, *et al.*, "A model of vascular tumour growth in mice combining longitudinal tumour size data with histological biomarkers," *European journal of cancer (Oxford, England : 1990)*, vol. 47, no. 3, pp. 479–490, 2011, ISSN: 1879-0852. DOI: 10.1016/J.EJCA.2010.10.003. [Online]. Available: https://pubmed.ncbi.nlm.nih.gov/21074409/.

[23] M. R. Owen, H. M. Byrne, and C. E. Lewis, "Mathematical modelling of the use of macrophages as vehicles for drug delivery to hypoxic tumour sites," *Journal of Theoretical Biology*, vol. 226, no. 4, pp. 377–391, Feb. 2004, ISSN: 00225193. DOI: 10.1016/j.jtbi.2003.09.004. [Online]. Available: https://pubmed.ncbi.nlm.nih.gov/14759644/.

[24] A. Ulrich and P. Pour, "Cell Lines," *in Encyclopedia of Genetics, Academic Press*, pp. 310–311, 2001.

[25] C. Cobelli and J. J. DiStefano, "Parameter and structural identifiability concepts and ambiguities: a critical review and analysis," *https://doi.org/10.1152/ajpregu.1980.239.1.R7*, vol. 8, no. 1, pp. 7–24, 1980, ISSN: 03636119. DOI: 10.1152/AJPREGU.1980.239.1.R7. [Online]. Available: https://journals.physiology.org/doi/10.1152/ajpregu.1980.239.1.R7.

[26] A. F. Villaverde, A. Barreiro, and A. Papachristodoulou, "Structural Identifiability of Dynamic Systems Biology Models," *PLOS Computational Biology*, vol. 12, no. 10, e1005153, Oct. 2016, ISSN: 1553-7358. DOI: 10.1371/JOURNAL.PCBI.1005153. [Online]. Available: https://journals.plos.org/ploscompbiol/article?id=10.1371/journal.pcbi.1005153.

[27] R. Bellman and K. J. Åström, "On structural identifiability," *Mathematical Biosciences*, vol. 7, no. 3-4, pp. 329–339, Apr. 1970, ISSN: 0025-5564. DOI: 10.1016/0025-5564(70)90132-X.

[28] John R.Taylor, "An Introduction to Error Analysis. The study of uncurtainties in the physical measurments," p. 329, 1982.

[29] J. Karlsson, M. Anguelova, and M. Jirstrand, "An Efficient Method for Structural Identifiability Analysis of Large Dynamic Systems," *IFAC Proceedings Volumes*, vol. 45, no. 16, pp. 941–946, Jul. 2012, ISSN: 1474-6670. DOI: 10.3182/20120711-3-BE-2027.00381.

[30] T.-S. Kam, K.-Y. Loh, and C. Wei, "Conophylline and Conophyllidine: New Dimeric Alkaloids from Tabernaemontana divaricata," *Journal of Natural Products*, vol. 56, no. 11, pp. 1865–1871, Nov. 1993, ISSN: 0163-3864. DOI: 10.1021/np50101a001.

[31] E. K. Rowinsky and R. C. Donehower, "Paclitaxel (Taxol)," *New England Journal of Medicine*, vol. 332, no. 15, pp. 1004–1014, Apr. 1995, ISSN: 0028-4793. DOI: 10.1056/NEJM199504133321507.

[32] M. C. Wani, H. L. Taylor, M. E. Wall, P. Coggon, and A. T. Mcphail, "Plant antitumor agents. VI. The isolation and structure of taxol, a novel antileukemic and antitumor agent from Taxus brevifolia," *Journal of the American Chemical Society*, vol. 93, no. 9, pp. 2325–2327, May 1971, ISSN: 0002-7863. DOI: 10.1021/JA00738A045. [Online]. Available: https://pubmed.ncbi.nlm.nih.gov/5553076/.

[33] C. Carmona and J. Servando Publisher, "MOLECULAR AND BIOMOLECULAR-BASED NANOMATERIALS: TUBULIN AND TAXOL AS MOLECULAR CONSTITUENTS Item Type text; Electronic Dissertation," 2009. [Online]. Available: http://hdl.handle.net/10150/195413.

[34] B. Xue, J. Zhao, Y. Fan, *et al.*, "Synthesis of Taxol and Docetaxel by Using 10-Deacetyl-7-xylosyltaxanes," *Chemistry & Biodiversity*, vol. 17, no. 2, e1900631, Feb. 2020, ISSN: 1612-1880. DOI: 10.1002/CBDV.201900631. [Online]. Available: https://onlinelibrary.wiley.com/doi/full/10.1002/cbdv.201900631%20https://onlinelibrary.wiley.com/doi/abs/10.1002/cbdv.201900631%20https://onlinelibrary.wiley.com/doi/10.1002/cbdv.201900631.

[35] P. B. Schiff, J. Fant, and S. B. Horwitz, "Promotion of microtubule assembly in vitro by taxol [19]," *Nature*, vol. 277, no. 5698, pp. 665–667, 1979, ISSN: 00280836. DOI: 10.1038/277665A0.

[36] *Docetaxel - NCI*. [Online]. Available: https://www.cancer.gov/about-cancer/treatment/drugs/docetaxel.

[37] B. Ramaswamy and S. Puhalla, "Docetaxel: A tubulin-stabilizing agent approved for the management of several solid tumors," *Drugs of Today*, vol. 42, no. 4, pp. 265–279, Apr. 2006, ISSN: 16993993. DOI: 10.1358/dot.2006.42.4.968648.

[38] M. C. O. Da Rocha, P. B. Da Silva, M. A. Radicchi, *et al.*, "Docetaxel-loaded solid lipid nanoparticles prevent tumor growth and lung metastasis of 4T1 murine mammary carcinoma cells," *Journal of Nanobiotechnology*, vol. 18, no. 1, pp. 1–20, Mar. 2020, ISSN: 14773155. DOI: 10.1186/S12951-020-00604-7/FIGURES/12. [Online]. Available: https://jnanobiotechnology.biomedcentral.com/articles/10.1186/s12951-020-00604-7.

[39] O. Tacar, P. Sriamornsak, and C. R. Dass, "Doxorubicin: an update on anticancer molecular action, toxicity and novel drug delivery systems," *Journal of Pharmacy and Pharmacology*, vol. 65, no. 2, pp. 157–170, Dec. 2012, ISSN: 0022-3573. DOI: 10.1111/J.2042-7158.2012.01567.X. [Online]. Available: https://dx.doi.org/10.1111/j.2042-7158.2012.01567.x.

[40] P. Jeffrey and S. Summerfield, "The Future of ADME in Drug Design and Development," *Pharmacology for Chemists: Drug Discovery in Context*, pp. 316–342, Oct. 2017. DOI: 10.1039/BK9781782621423-00316. [Online]. Available: https://books.rsc.org/books/edited-volume/1832/chapter/2249578/The-Future-of-ADME-in-Drug-Design-and-Development.

[41] A. Montero, F. Fossella, G. Hortobagyi, and V. Valero, "Docetaxel for treatment of solid tumours: a systematic review of clinical data," *The Lancet. Oncology*, vol. 6, no. 4, pp. 229–239, Apr. 2005, ISSN: 1470-2045. DOI: 10.1016/S1470-2045(05)70094-2. [Online]. Available: https://pubmed.ncbi.nlm.nih.gov/15811618/.

[42] A. S. Zandvliet, J. H. Schellens, C. Dittrich, J. Wanders, J. H. Beijnen, and A. D. Huitema, "Population pharmacokinetic and pharmacodynamic analysis to support treatment optimization of combination chemotherapy with indisulam and carboplatin," *British Journal of Clinical Pharmacology*, vol. 66, no. 4, p. 485, Oct. 2008, ISSN: 03065251. DOI: 10.1111/J.1365-2125.2008.03230.X. [Online]. Available: /pmc/articles/PMC2561111/%20/pmc/articles/PMC2561111/?report=abstract%20https://www.ncbi.nlm.nih.gov/pmc/articles/PMC2561111/.

[43] F. A. Shepherd, J. Dancey, R. Ramlau, *et al.*, "Prospective randomized trial of docetaxel versus best supportive care in patients with non-small-cell lung cancer previously treated with platinum-based chemotherapy," *Journal of clinical oncology : official journal of the American Society of Clinical Oncology*, vol. 18, no. 10, pp. 2095–2103, 2000, ISSN: 0732-183X. DOI: 10.1200/JCO.2000.18.10.2095. [Online]. Available: https://pubmed.ncbi.nlm.nih.gov/10811675/.

[44] I. F. Tannock, R. de Wit, W. R. Berry, *et al.*, "Docetaxel plus prednisone or mitoxantrone plus prednisone for advanced prostate cancer," *The New England journal of medicine*, vol. 351, no. 15, pp. 1502–1512, Oct. 2004, ISSN: 1533-4406. DOI: 10.1056/NEJMOA040720. [Online]. Available: https://pubmed.ncbi.nlm.nih.gov/15470213/.

[45] S. B. Park, D. Goldstein, A. V. Krishnan, *et al.*, "Chemotherapy-induced peripheral neurotoxicity: a critical analysis," *CA: a cancer journal for clinicians*, vol. 63, no. 6, pp. 419–437, Nov. 2013, ISSN: 1542-4863. DOI: 10.3322/CAAC.21204. [Online]. Available: https://pubmed.ncbi.nlm.nih.gov/24590861/.

[46] N. M. Kuderer, D. C. Dale, J. Crawford, and G. H. Lyman, "Impact of primary prophylaxis with granulocyte colony-stimulating factor on febrile neutropenia and mortality in adult cancer patients receiving chemotherapy: A systematic review," *Journal of Clinical Oncology*, vol. 25, no. 21, pp. 3158–3167, Jul. 2007, ISSN: 0732183X. DOI: 10.1200/JCO.2006.08.8823. [Online]. Available: https://www.researchgate.net/publication/6204906_Impact_of_Primary_Prophylaxis_With_Granulocyte_Colony-Stimulating_Factor_on_Febrile_Neutropenia_and_Mortality_in_Adult_Cancer_Patients_Receiving_Chemotherapy_A_Systematic_Review.

[47] K. E. Yoo, R. Y. Kang, J. Y. Lee, *et al.*, "Awareness of the adverse effects associated with prophylactic corticosteroid use during docetaxel therapy," *Supportive Care in Cancer*, vol. 23, no. 7, pp. 1969–1977, Dec. 2015, ISSN: 14337339. DOI: 10.1007/S00520-014-2547-Y.

[48] S. Jiralerspong, E. S. Kim, W. Dong, L. Feng, G. N. Hortobagyi, and S. H. Giordano, "Obesity, diabetes, and survival outcomes in a large cohort of early-stage breast cancer patients," *Annals of Oncology*, vol. 24, no. 10, pp. 2506–2514, 2013, ISSN: 15698041. DOI: 10.1093/ANNONC/MDT224.

[49] D. Lebwohl and R. Canetta, "Clinical development of platinum complexes in cancer therapy: an historical perspective and an update," *European Journal of Cancer*, vol. 34, no. 10, pp. 1522–1534, Sep. 1998, ISSN: 0959-8049. DOI: 10.1016/S0959-8049(98)00224-X.

[50] R. S. Go and A. A. Adjei, "Review of the Comparative Pharmacology and Clinical Activity of Cisplatin and Carboplatin," *https://doi.org/10.1200/JCO.1999.17.1.409*, vol. 17, no. 1, pp. 409–422, Sep. 2016, ISSN: 0732183X. DOI: 10.1200/JCO.1999.17.1.409. [Online]. Available: https://ascopubs.org/doi/10.1200/JCO.1999.17.1.409.

[51] J. M. Rademaker-Lakhai, M. Crul, L. Zuur, *et al.*, "Relationship between cisplatin administration and the development of ototoxicity," *Journal of Clinical Oncology*, vol. 24, no. 6, pp. 918–924, Feb. 2006, ISSN: 0732183X. DOI: 10.1200/JCO.2006.10.077.

[52] Y. Kidani, K. Inagaki, and S. Tsukagoshi, "Examination of antitumor activities of platinum complexes of 1,2-diaminocyclohexane isomers and their related complexes," *Gann*, vol. 67, no. 6, pp. 921–922, Jan. 1976, ISSN: 0016-450X. DOI: 10.20772/cancersci1959.67.6{_}921.

[53] A. Eastman, "Cross-linking of glutathione to DNA by cancer chemotherapeutic platinum coordination complexes," *Chemico-Biological Interactions*, vol. 61, no. 3, pp. 241–248, 1987, ISSN: 00092797. DOI: 10.1016/0009-2797(87)90004-4.

[54] W. J. van der Vijgh, "Clinical Pharmacokinetics of Carboplatin," *Clinical Pharmacokinetics*, vol. 21, no. 4, pp. 242–261, Nov. 1991, ISSN: 11791926. DOI: 10.2165/00003088-199121040-00002/METRICS. [Online]. Available: https://link.springer.com/article/10.2165/00003088-199121040-00002.

[55] G. Y. Ho, N. Woodward, and J. I. Coward, "Cisplatin versus carboplatin: comparative review of therapeutic management in solid malignancies," *Critical reviews in oncology/hematology*, vol. 102, pp. 37–46, Jun. 2016, ISSN: 1879-0461. DOI: 10.1016/J.CRITREVONC.2016.03.014. [Online]. Available: https://pubmed.ncbi.nlm.nih.gov/27105947/.

[56] C. Ekhart, M. E. De Jonge, A. D. Huitema, J. H. Schellens, S. Rodenhuis, and J. H. Beijnen, "Flat dosing of carboplatin is justified in adult patients with normal renal function," *Clinical Cancer Research*, vol. 12, no. 21, pp. 6502–6508, Nov. 2006, ISSN: 10780432. DOI: 10.1158/1078-0432.CCR-05-1076.

[57] G. G. Plnter and J. L. Shohet, "Two fluid compartments in the renal inner medulla: A view through the keyhole of the concentrating process," *Philosophical Transactions of the Royal Society A: Mathematical, Physical and Engineering Sciences*, vol. 364, no. 1843, pp. 1551–1561, Jun. 2006, ISSN: 1364503X. DOI: 10.1098/RSTA.2006.1774.

[58] D. Lorusso, F. Petrelli, A. Coinu, F. Raspagliesi, and S. Barni, "A systematic review comparing cisplatin and carboplatin plus paclitaxel-based chemotherapy for recurrent or metastatic cervical cancer," *Gynecologic oncology*, vol. 133, no. 1, pp. 117–123, 2014, ISSN: 1095-6859. DOI: 10.1016/J.YGYNO.2014.01.042. [Online]. Available: https://pubmed.ncbi.nlm.nih.gov/24486604/.

[59] R. Kitagawa, N. Katsumata, T. Shibata, *et al.*, "Paclitaxel plus carboplatin versus paclitaxel plus cisplatin in metastatic or recurrent cervical cancer: The open-label randomized phase III trial JCOG0505," *Journal of Clinical Oncology*, vol. 33, no. 19, pp. 2129–2135, Jul. 2015, ISSN: 15277755. DOI: 10.1200/JCO.2014.58.4391.

[60] J. K. Duong, G. J. Veal, C. E. Nath, *et al.*, "Population pharmacokinetics of carboplatin, etoposide and melphalan in children: a re-evaluation of paediatric dosing formulas for carboplatin in patients with normal or mild impairment of renal function," *British Journal of Clinical Pharmacology*, vol. 85, no. 1, p. 136, Jan. 2019, ISSN: 13652125. DOI: 10.1111/BCP.13774. [Online]. Available: /pmc/articles/PMC6303207/%20/pmc/articles/PMC6303207/?report=abstract%20https://www.ncbi.nlm.nih.gov/pmc/articles/PMC6303207/.

[61] L. E. Friberg, A. Henningsson, H. Maas, L. Nguyen, and M. O. Karlsson, "Model of chemotherapy-induced myelosuppression with parameter consistency across drugs," *Journal of Clinical Oncology*, vol. 20, no. 24, pp. 4713–4721, Dec. 2002, ISSN: 0732183X. DOI: 10.1200/JCO.2002.02.140.

[62] J. W. T. Yates and D. A. Fairman, "How translational modeling in oncology needs to get the mechanism just right," *Clinical and Translational Science*, vol. 15, no. 3, pp. 588–600, Mar. 2022, ISSN: 1752-8054. DOI: 10.1111/cts.13183.

[63] A. Nasim, J. Yates, G. Derks, and C. Dunlop, "A Spatially Resolved Mechanistic Growth Law for Cancer Drug Development Predicting Tumor Growing Fractions," *Cancer Research Communications*, vol. 2, no. 8, pp. 754–761, Aug. 2022. DOI: 10.1158/2767-9764.crc-22-0032.

[64] *What Is MATLAB? - MATLAB & Simulink*. [Online]. Available: https://uk.mathworks.com/discovery/what-is-matlab.html#.

[65] LIXOFT, *Population parameter using SAEM algorithm*. [Online]. Available: https://monolix.lixoft.com/tasks/population-parameter-estimation-using-saem/.

[66] LIXOFT, *Monolix documentation*. [Online]. Available: https://monolix.lixoft.com/.

[67] WOLFRAM, *Wolfram Language & System Documentation Center*. [Online]. Available: https://reference.wolfram.com/language/.

[68] N. D. Evans, R. J. Dimelow, and J. W. Yates, "Modelling of tumour growth and cytotoxic effect of docetaxel in xenografts," *Computer Methods and Programs in Biomedicine*, vol. 114, no. 3, e3–e13, May 2014, ISSN: 0169-2607. DOI: 10.1016/J.CMPB.2013.06.014.

[69] A. S. Zandvliet, J. H. M. Schellens, C. Dittrich, J. Wanders, J. H. Beijnen, and A. D. R. Huitema, "Population pharmacokinetic and pharmacodynamic analysis to support treatment optimization of combination chemotherapy with indisulam and carboplatin," *Br J Clin Pharmacol*, vol. 66, 2008. DOI: 10.1111/j.1365-2125.2008.03230.x.

[70] W. J. Aston, D. E. Hope, A. K. Nowak, B. W. Robinson, R. A. Lake, and W. J. Lesterhuis, "A systematic investigation of the maximum tolerated dose of cytotoxic chemotherapy with and without supportive care in mice," *BMC Cancer*, vol. 17, no. 1, pp. 1–10, Oct. 2017, ISSN: 14712407. DOI: 10.1186/S12885-017-3677-7/FIGURES/4. [Online]. Available: https://bmccancer.biomedcentral.com/articles/10.1186/s12885-017-3677-7.

[71] PETA, *"The Silver Spring Monkeys: The Case That Launched PETA,"*. [Online]. Available: https://www.peta.org/issues/animals-used-for-experimentation/silver-spring-monkeys/..

[72] N. Henrique Franco, "Animal Experiments in Biomedical Research: A Historical Perspective," *Animals : an Open Access Journal from MDPI*, vol. 3, no. 1, p. 238, Mar. 2013, ISSN: 20762615. DOI: 10.3390/ANI3010238. [Online]. Available: /pmc/articles/PMC4495509/%20/pmc/articles/PMC4495509/?report=abstract%20https://www.ncbi.nlm.nih.gov/pmc/articles/PMC4495509/.

[73] J. Tannenbaum and B. T. Bennett, "Russell and Burch's 3Rs Then and Now: The Need for Clarity in Definition and Purpose," *Journal of the American Association for Laboratory Animal Science : JAALAS*, vol. 54, no. 2, p. 120, Mar. 2015, ISSN: 15596109. [Online]. Available: /pmc/articles/PMC4382615/%20/pmc/articles/PMC4382615/?report=abstract%20https://www.ncbi.nlm.nih.gov/pmc/articles/PMC4382615/.

[74] *Guide for the Care and Use of Laboratory Animals*. Washington, D.C.: National Academies Press, Dec. 2011, ISBN: 978-0-309-15400-0. DOI: 10.17226/12910.

[75] Cancer Research UK, *"Invasive Breast Carcinoma Statistics"*. [Online]. Available: https://www.cancerresearchuk.org/health-professional/cancer-statistics/statistics-by-cancer-type/breast-cancer.

[76] Union for International Cancer Control, *New Global Cancer Data (Breast): GLOBOCAN 2022*. [Online]. Available: https://gco.iarc.who.int/media/globocan/factsheets/cancers/20-breast-fact-sheet.pdf.

[77] S. Díaz-Seoane, X. R. Barreiro, and A. F. Villaverde, "STRIKE-GOLDD 4.0: user-friendly, efficient analysis of structural identifiability and observability," *Bioinformatics (Oxford, England)*, vol. 39, no. 1, Jan. 2023, ISSN: 1367-4811. DOI: 10.1093/BIOINFORMATICS/BTAC748. [Online]. Available: https://pubmed.ncbi.nlm.nih.gov/36398887/.

[78] K. P. Burnham and D. R. Anderson, Eds., *Model Selection and Multimodel Inference*. New York, NY: Springer New York, 2004, ISBN: 978-0-387-95364-9. DOI: 10.1007/b97636.

[79] C. J. Beavers, J. E. Rodgers, A. J. Bagnola, *et al.*, "Cardio-Oncology Drug Interactions: A Scientific Statement From the American Heart Association," *Circulation*, vol. 145, no. 15, E811–E838, Apr. 2022, ISSN: 1524-4539. DOI: 10.1161/CIR.0000000000001056. [Online]. Available: https://pubmed.ncbi.nlm.nih.gov/35249373/.

[80] U. Campia, J. J. Moslehi, L. Amiri-Kordestani, *et al.*, "Cardio-Oncology: Vascular and Metabolic Perspectives: A Scientific Statement From the American Heart Association," *Circulation*, vol. 139, no. 13, E579–E602, Mar. 2019, ISSN: 15244539. DOI: 10.1161/CIR.0000000000000641/ASSET/C7C96481-E277-41A0-A5EA-06642EE1D0DD/

ASSETS / IMAGES / LARGE / E579FIG03 . JPG. [Online]. Available: https : / / www.ahajournals.org/doi/10.1161/CIR.0000000000000641.

[81] L. Montégut, C. López-Otín, and G. Kroemer, "Aging and cancer," *Molecular Cancer 2024 23:1*, vol. 23, no. 1, pp. 1–16, May 2024, ISSN: 1476-4598. DOI: 10 . 1186 / S12943-024-02020-Z. [Online]. Available: https://molecular-cancer.biomedcentral.com/articles/10.1186/s12943-024-02020-z.

Appendix A

Supplementary Material

A.1 Additional Data

A.1.1 The Regressor

Sorting for Initial Tumour Weight

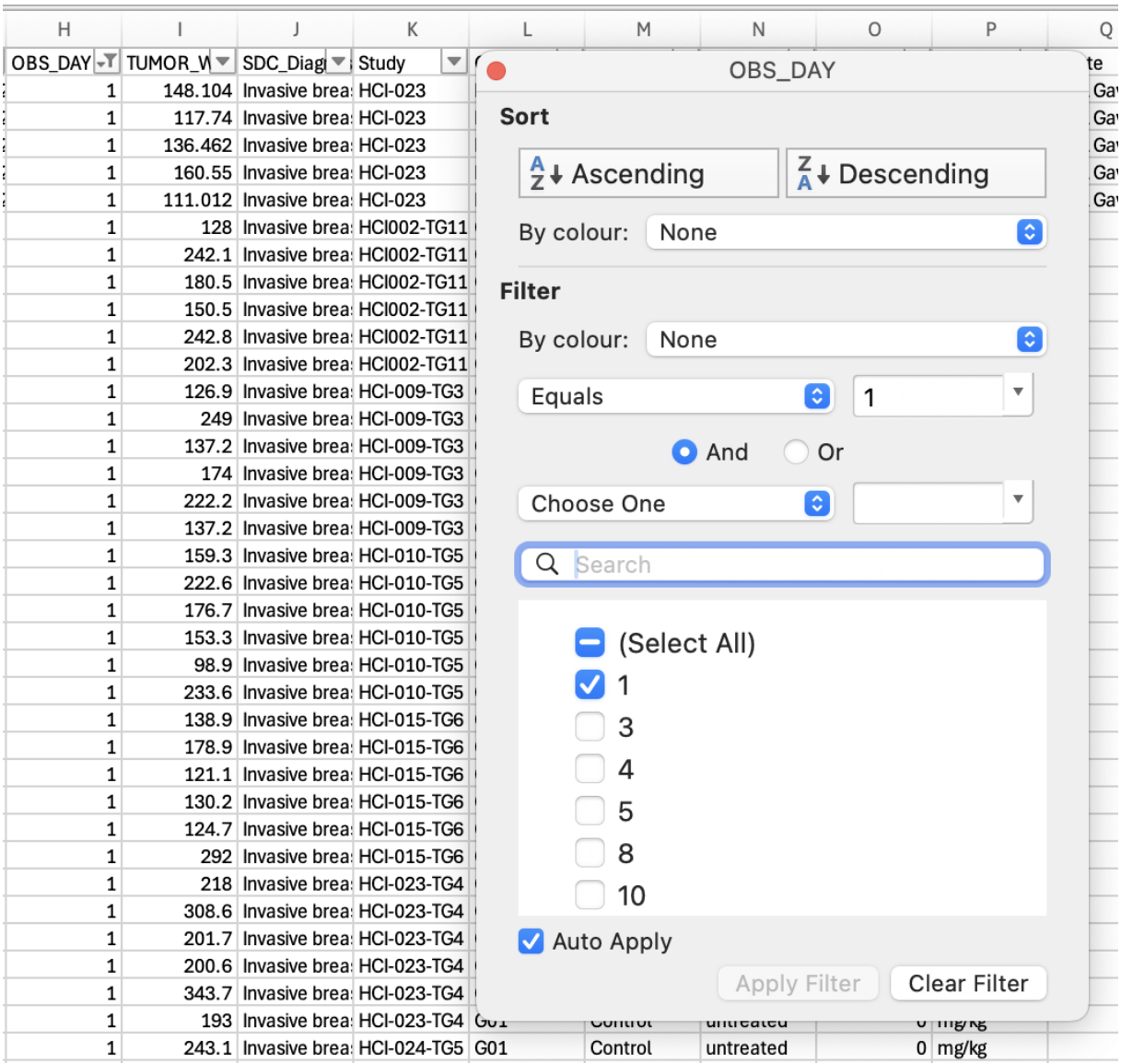

OBS_DAY	TUMOR_W	SDC_Diagi	Study					
1	148.104	Invasive brea	HCI-023					
1	117.74	Invasive brea	HCI-023					
1	136.462	Invasive brea	HCI-023					
1	160.55	Invasive brea	HCI-023					
1	111.012	Invasive brea	HCI-023					
1	128	Invasive brea	HCI002-TG11					
1	242.1	Invasive brea	HCI002-TG11					
1	180.5	Invasive brea	HCI002-TG11					
1	150.5	Invasive brea	HCI002-TG11					
1	242.8	Invasive brea	HCI002-TG11					
1	202.3	Invasive brea	HCI002-TG11					
1	126.9	Invasive brea	HCI-009-TG3					
1	249	Invasive brea	HCI-009-TG3					
1	137.2	Invasive brea	HCI-009-TG3					
1	174	Invasive brea	HCI-009-TG3					
1	222.2	Invasive brea	HCI-009-TG3					
1	137.2	Invasive brea	HCI-009-TG3					
1	159.3	Invasive brea	HCI-010-TG5					
1	222.6	Invasive brea	HCI-010-TG5					
1	176.7	Invasive brea	HCI-010-TG5					
1	153.3	Invasive brea	HCI-010-TG5					
1	98.9	Invasive brea	HCI-010-TG5					
1	233.6	Invasive brea	HCI-010-TG5					
1	138.9	Invasive brea	HCI-015-TG6					
1	178.9	Invasive brea	HCI-015-TG6					
1	121.1	Invasive brea	HCI-015-TG6					
1	130.2	Invasive brea	HCI-015-TG6					
1	124.7	Invasive brea	HCI-015-TG6					
1	292	Invasive brea	HCI-015-TG6					
1	218	Invasive brea	HCI-023-TG4					
1	308.6	Invasive brea	HCI-023-TG4					
1	201.7	Invasive brea	HCI-023-TG4					
1	200.6	Invasive brea	HCI-023-TG4					
1	343.7	Invasive brea	HCI-023-TG4					
1	193	Invasive brea	HCI-023-TG4	G01	Control	untreated	0	mg/kg
1	243.1	Invasive brea	HCI-024-TG5	G01	Control	untreated	0	mg/kg

Figure A.1. *Utilisation of the built-in filter function to identify all tumour weights for observation day 1.*

Creation of "Regressor" Column to Perform Regression

ID	OBS_DAY	TUMOR_V	Regressor
010-1068	1	159.3	159.3
010-1068	4	214	0
010-1068	8	197.7	0
010-1068	11	250.3	0
010-1068	15	209	0
010-1068	18	261.8	0
010-1068	22	313.7	0
010-1068	25	432.9	0
010-1068	29	290.7	0
010-1081	1	222.6	222.6
010-1081	4	328.3	0
010-1081	8	345.3	0
010-1081	11	364.4	0
010-1081	15	416.9	0
010-1081	18	475.2	0
010-1081	22	429	0
010-1081	25	554	0
010-1081	29	724.7	0
010-1105	1	176.7	176.7
010-1105	4	273.5	0
010-1105	8	236.1	0
010-1105	11	299.4	0
010-1105	15	341.9	0
010-1105	18	353.8	0
010-1105	22	535.7	0
010-1105	25	737.4	0
010-1105	29	564.4	0
010-1111	1	153.3	153.3

Figure A.2. *Tumour weights over time for control data, figure 2.*

A.2 Preclinical Patient-Derived Xenograft Data

A.2.1 Control Data

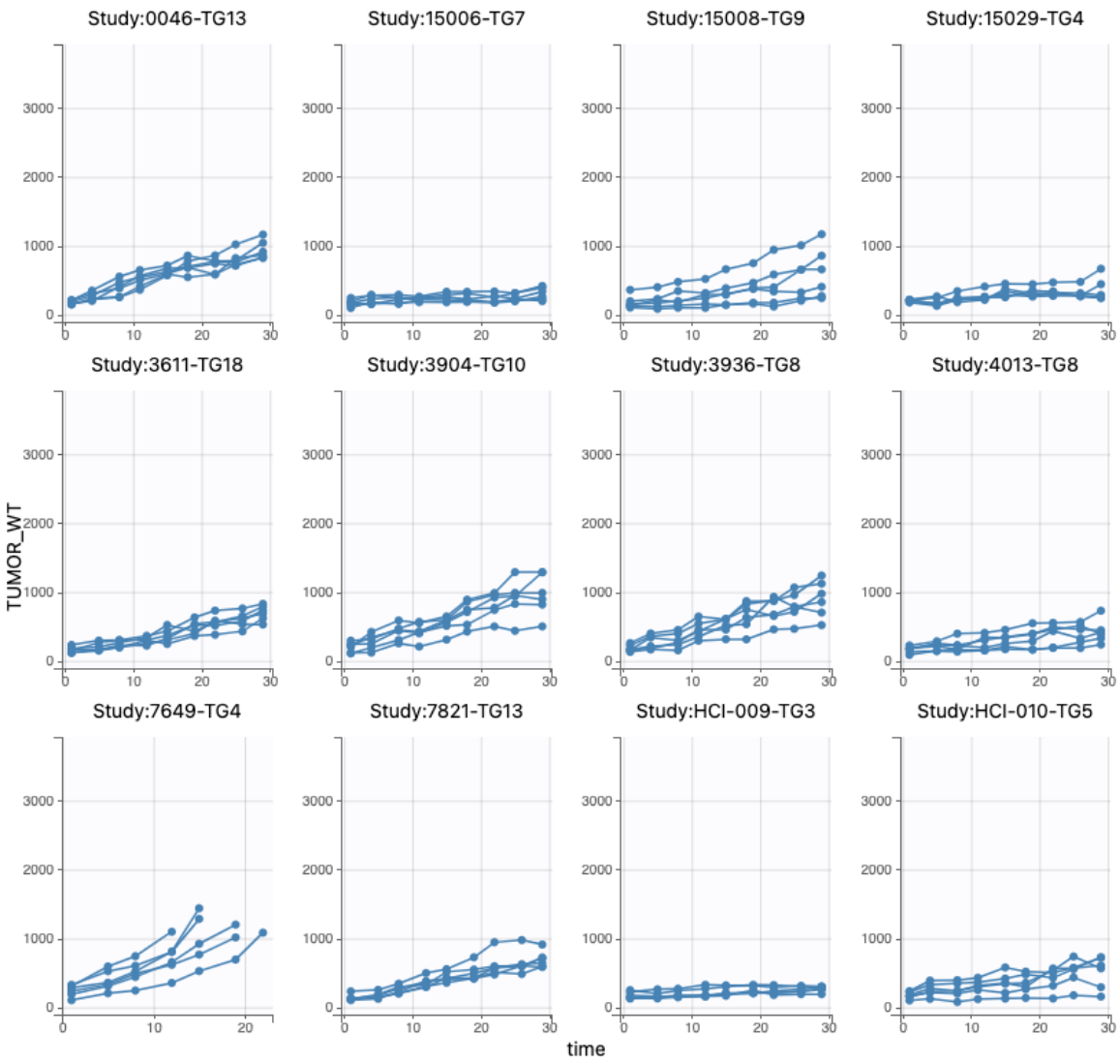

Figure A.3. *Tumour weights over time for control data, figure 1.*

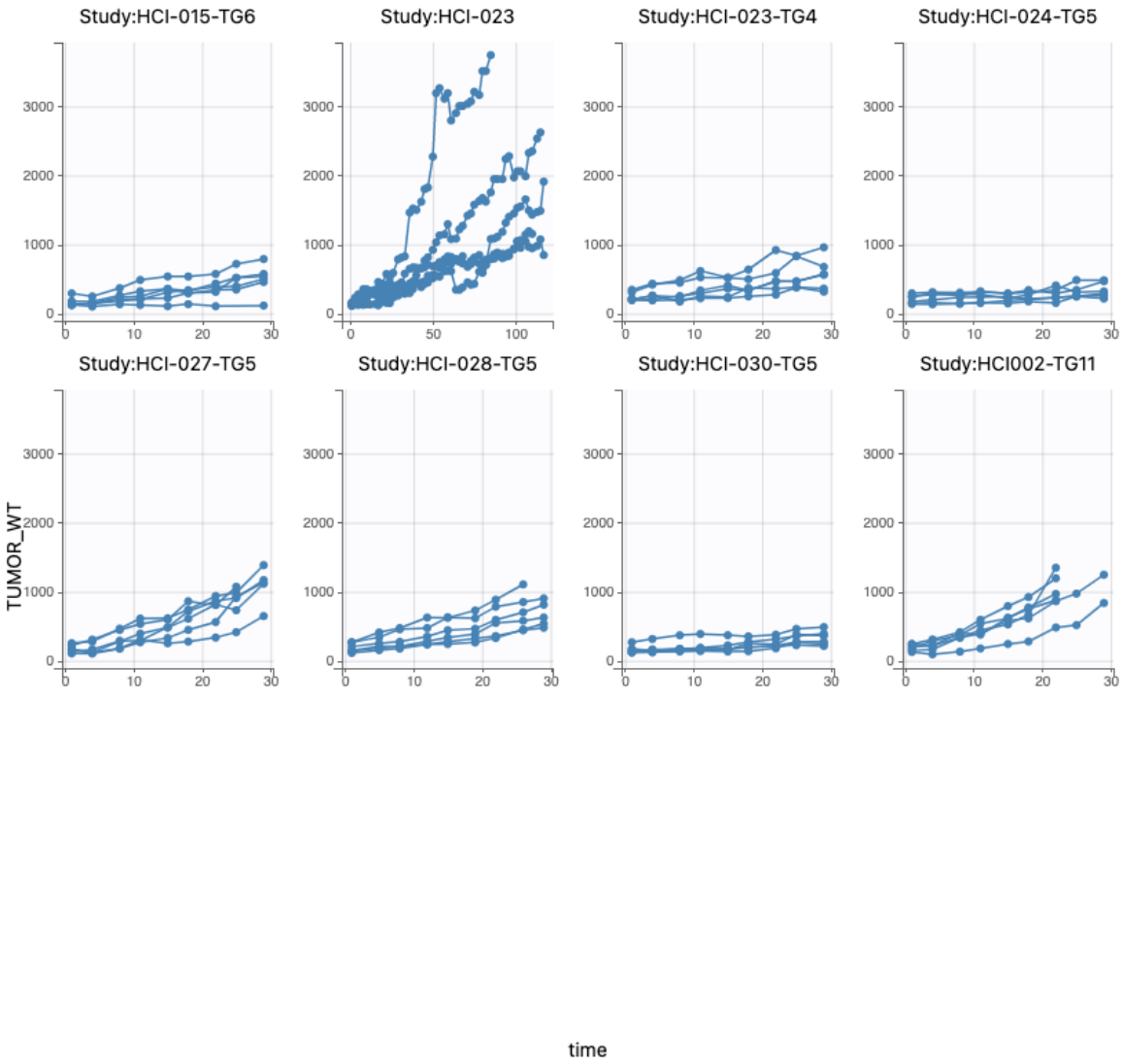

Figure A.4. *Tumour weights over time for control data, figure 2.*

A.2.2 Docetaxel Treatment Data

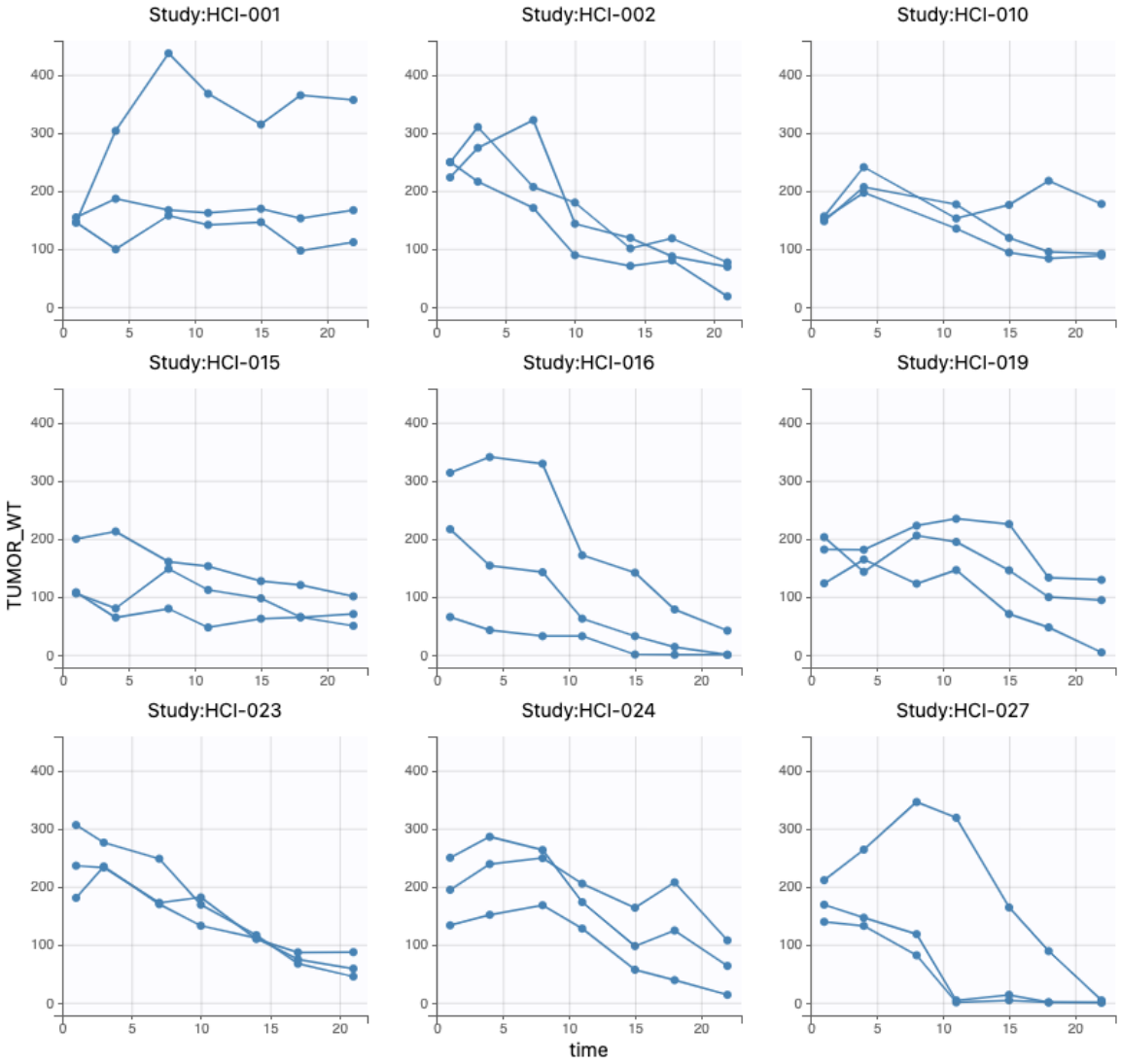

Figure A.5. *Tumour weights over time for docetaxel treatment data, figure 1.*

A.2.3 Carboplatin Treatment Data

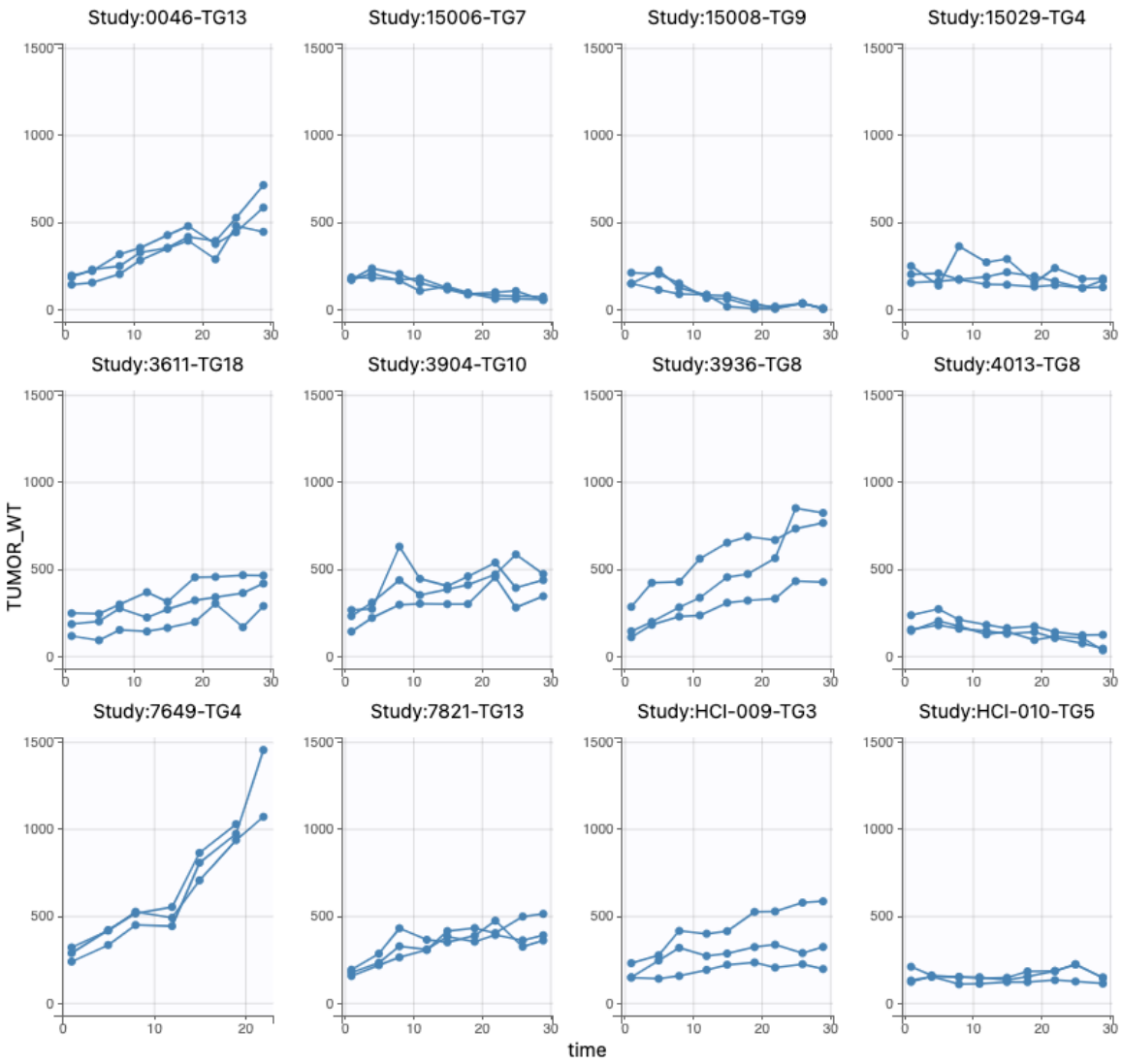

Figure A.6. *Tumour weights over time for carboplatin treatment data, figure 1.*

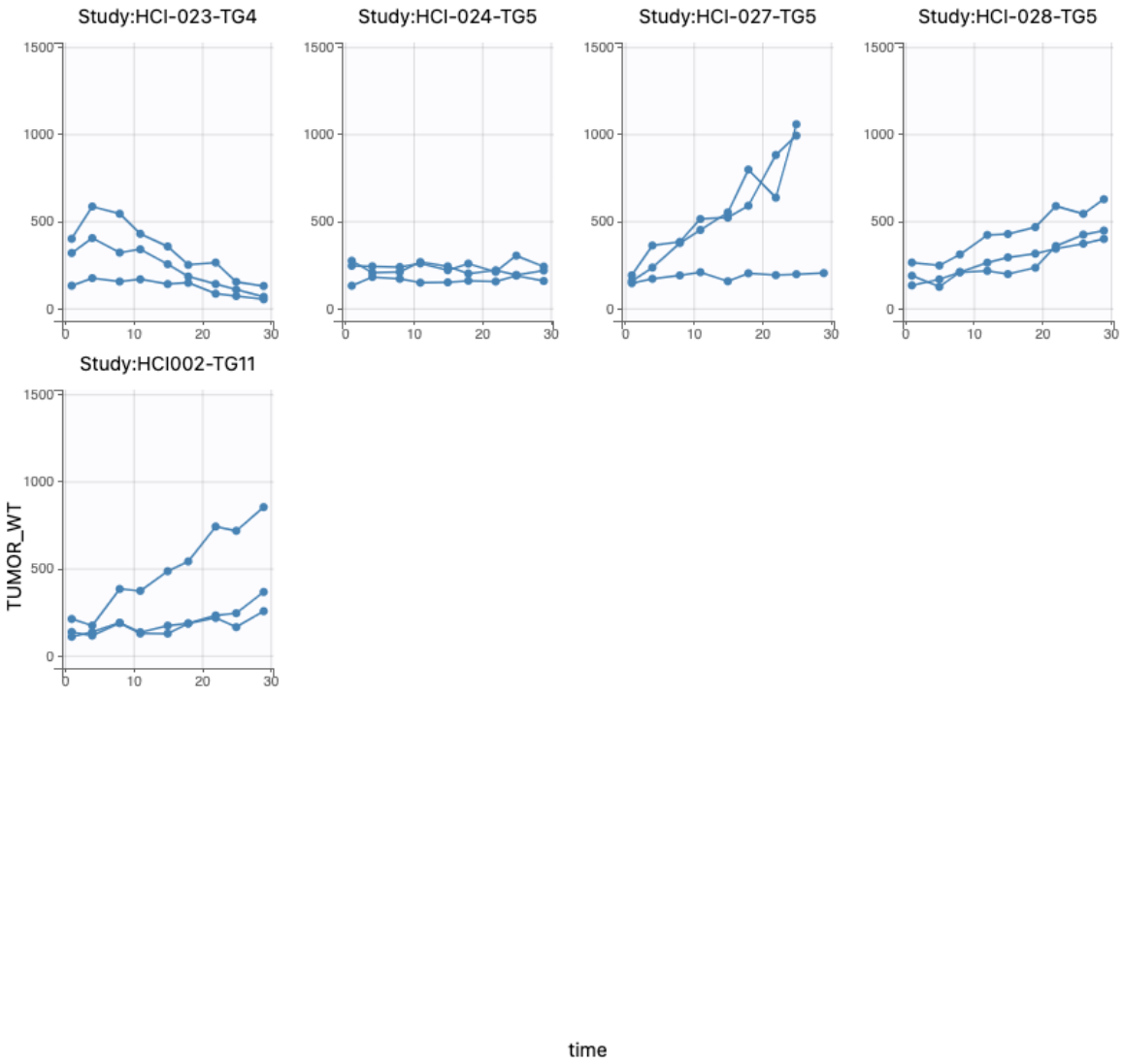

Figure A.7. *Tumour weights over time for docetaxel treatment data, figure 2.*

A.2.4 Docetaxel and Carboplatin in Combination Treatment Data (Doc20+Carbo)

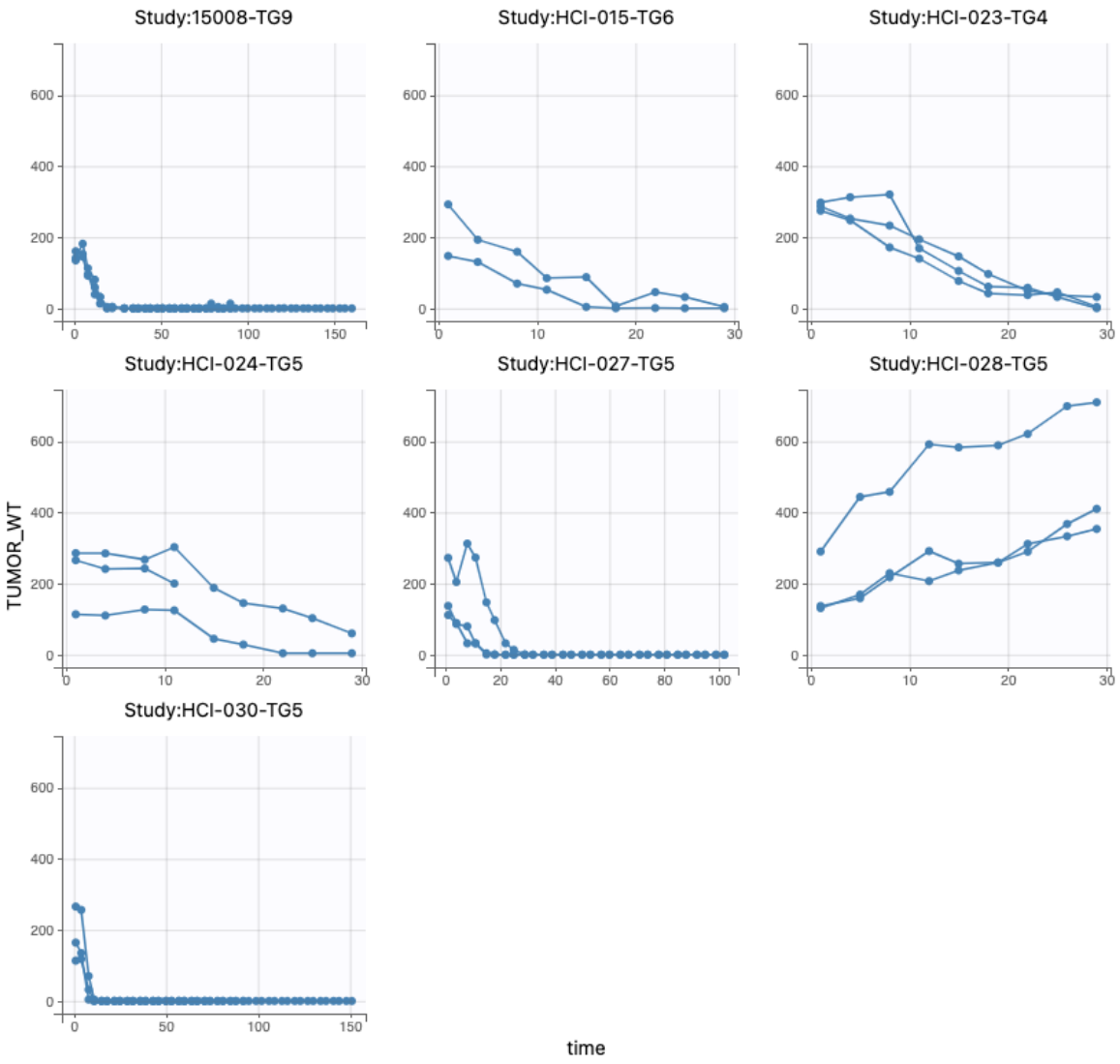

Figure A.8. *Tumour weights over time for docetaxel and carboplatin in combination treatment data.*

Appendix B

Code

B.1 Mlxtran

B.1.1 Control

```
DESCRIPTION:
;;;;;;;;;;;; Control ;;;;;;;;;;;;
Two ODEs which describe tumour volume and growth factor respectively.
[LONGITUDINAL]
input = {beta, muP, muQ, ITV}
ITV = {use = regressor};

EQUATION:
; Initial conditions
t0 = 0
Vt_0 = ITV
GF_0 = 0.5

;;;;;; Tumour Growth Model ;;;;;;
m = beta - muP + muQ
; Proliferation and cell death rates
GF_inf = muQ / m
; ODE for tumour volume
ddt_Vt = m*Vt*(GF - GF_inf)
; ODE for growth fraction
ddt_GF = m * (GF - GF_inf) * ((1 - GF) - (1 - GF)^(2/3))

OUTPUT:
output = {Vt}
```

Listing B.1: Tumour Growth Model for the control in Mlxtran.

B.1.2 Docetaxel

```
DESCRIPTION:
;;;;;;;;;;;; DOCTAXEL ;;;;;;;;;;;;;
```

```
A script delineating the pharmacokinetics of Carboplatin coupled
   with the effect this therapeutic has upon tumour volume which has
   been characterised with various effects such as
a Hill type effect, Michaelis-Menten effect, Linear effect or
   quadratic effect

[LONGITUDINAL]
input = {beta, muP, muQ, K_kill, ITV

; depending on the effect used
; A ; Linear
; A, B ; M-M
n ; Hill Type

ITV = {use = regressor};

PK:
effect(target=Qp)

EQUATION:
; Initial conditions
t0 = 0 ; ITV; for tumour volume
Vt_0 = ITV ; for starting time
GF_0 = 0.5 ; for the growth factor

;;;;;;;;;;; Docetaxels Compartmental model ;;;;;;;;;;;
; inital conditions of Docetaxel
Cp_0 = 0 ; in plasma
Q_0 = 0 ; in tissue

; values obtained through literature
Kpe = 0.382
KpT = 0.523
Ktp = 0.196
Vp = 1.30

; ODEs for docetaxel compartments
ddt_qP = -(Kpe + Ktp) * qP + Ktp * qT
ddt_qT = KpT * qP - Ktp * qT
Cp = qP/Vp

```

```
;;;;;;;;;;;; Revised m parameter for drug effect ;;;;;;;;;;;;
; Michaelis-Menten
m = beta*(1 - A*(Cp)/(B+Cp)) - muP - K_kill*Cp +muQ;

; Hill type
m = beta*(1 - A*(Cp^n)/(B+Cp^n)) - muP - K_kill*Cp + muQ;

; Linear effect
m = beta*(1 - A*Cp) - muP - muQ + muQ - K_kill*Cp;

; Quadratic effect
m = beta*(1 - A*Cp^2) - muP - K_kill*Cp +muQ;

;;;;;;;;;;;; Tumour Growth Model with Growth Factor ODE ;;;;;;;;;;;;
; Proliferation and cell death rates
GF_inf = muQ / m

; ODE for tumour volume
ddt_Vt = m*Vt*(GF - GF_inf)

; ODE for growth factor
ddt_GF = m * (GF - GF_inf) * ((1 - GF) - (1 - GF)^(2/3))

OUTPUT:
output = Vt
```

Listing B.2: Docetaxel Tumour Growth Model in Mlxtran.

B.1.3 Carboplatin

```
DESCRIPTION:
;;;;;;;;;;;; CARBOPLATIN ;;;;;;;;;;;;;
A script delineating the pharmacokinetics of Carboplatin coupled
   with the effect this therapeutic will have upon tumour volume
   which has been characterised with various effects such as Hill
type effect, Linear effect, quadratic effect and Michaelis-Menten
   effect

[LONGITUDINAL]
input = {beta, muP, muQ, K_kill, ITV,
        ; depending on the effect used
        A ; Linear
```

```
        A, B, n ; Hill Type }

ITV = {use = regressor};

PK:
depot(target=Qp)

EQUATION:
; Initial conditions
Vt_0 = ITV
t0 = 0
GF_0 = 0.5

;;;;;;;;;;;; Carboplatins Compartmental model ;;;;;;;;;;;;
; inital conditions of Carboplatin
qP_0 = 0 ; in plasma
qT_0 = 0 ; in tissue

; values obtained through literature
V_plasma = 15.5
V_tissue = 9.86
CL = 76.5
Inter_CL = 3.46

; putting clearance and volumes in terms of rates
Kpe = CL / V_plasma
Kpt = Inter_CL / V_plasma
Ktp = Inter_CL / V_tissue

; ODEs for Carboplatin's Compartments
ddt_qP = -(Kpe + Kpt) * qP + Ktp * qT
ddt_qT = Kpt * qP - Ktp * qT
Cp = qP/V_plasma

;;;;;;;;;;;; Revised m value for drug effect ;;;;;;;;;;;;
; For MM
m = beta*(1 - A*(Cp)/(B+Cp)) - muP - K_kill*Cp +muQ;

; Hill type effect
m = beta*(1 - A*(Cp^n)/(B+Cp^n)) - muP - K_kill*Cp + muQ;

```

```
; Linear effect
m = beta*(1 - A*Cp) - muP - K_kill*Cp + muQ;

; Quadratic effect
m = beta*(1 - A*Cp^2) - muP - K_kill*Cp +muQ;

;;;;;;;;;;;; Tumour Growth Model with Growth Factor ODE ;;;;;;;;;;;;
; Proliferation and cell death rates
GF_inf = muQ / m

; ODE for tumour volume
ddt_Vt = m*Vt*(GF - GF_inf)

; ODE for growth fraction
ddt_GF = m * (GF - GF_inf) * ((1 - GF) - (1 - GF)^(2/3))

OUTPUT:
output = Vt
```

Listing B.3: Carboplatin Tumour Growth Model in Mlxtran.

B.1.4 Docetaxel and Carboplatin in Combination

```
DESCRIPTION:
;;;;;;;;;;;; DOCETAXEL & CARBOPLATIN IN COMBINATION ;;;;;;;;;;;;
A script delineating the pharmacokinetics of Docetaxel and
   Carboplatin in combination coupled with the effect this
therapeutic will have upon tumour volume which has been
   characterised with various effects such as Hill type effect,
   linear effect,
quadratic effect and Michaelis-Menten effect

[LONGITUDINAL]
input = {beta, muP, muQ, ITV, K_kill,
        ; depending on the effect used
        A ; Linear
        A, B, n ; Hill Type }
ITV = {use = regressor};

PK:
depot(target=Qp)

```

```
EQUATION:
GF_0 = 0.5
t0 = 0
Vt_0 = ITV
; For Docetaxel
qP_0 = 0 ; for Docetaxel
qT_0 = 0 ; for Docetaxel
C_cent_0 = 0 ; For Carboplatin
qPer_0 = 0 ; For Carboplatin

;;;;;;;;;;;; Known Parameter Values of Docetaxel ;;;;;;;;;;;;
Kpe = 0.382
KpT = 0.523
Ktp = 0.196
Vp = 1.30

; ODEs for Docetaxels compartments
ddt_qP = -(Kpe + Ktp) * qP + Ktp * qT
ddt_qT = KpT * qP - Ktp * qT
Cp = qP/Vp

;;;;;;;;;;;; Known Parameter Values of Carboplatin ;;;;;;;;;;;;
V_Cent = 15.5
V_Per = 9.86
CL = 76.5
Inter_CL = 3.46

; putting clearance and volumes in terms of rates
K10 = CL / V_Cent
K12 = Inter_CL / V_Cent
K21 = Inter_CL / V_Per

; ODEs for Carboplatin's Compartments
ddt_qP = -(K10 + K12) * qCent + K21 * qPer
ddt_qPer = K12 * qCent - K21 * qPer
Cp_C = qCent/V_Cent

;;;;;;;;;;;; The Combined Effect ;;;;;;;;;;;;
Eff_C = Cp_d + Cp_C ; Additive

;;;;;;;;;;;; Revised m variable for drug effect ;;;;;;;;;;;;
```

```
; Linear effect
m = beta*(1 + A*Eff_C) - muP - K_kill*Eff_C;

; Quadratic effect
m = beta*(1 + A*Eff_C^2) - muP - muQ - K_kill*Eff_C;

; Michaelis-Menten effect
m = beta*(1 + A*Eff_Cn/(B+Eff_Cn)) - muP - K_kill*Eff_C;

; Hill type effect
m = beta*(1 + A*Eff_Cn)/(B+Eff_Cn)) - muP - K_kill*Eff_C + muQ;

;;;;;;;;;;;; Tumour Growth SECOND Model ;;;;;;;;;;;;
; Proliferation and cell death rates
GF_inf = muQ / m

; ODE for tumour volume
ddt_Vt = m*Vt*(GF - GF_inf)

; ODE for growth fraction
ddt_GF = m * (GF - GF_inf) * ((1 - GF) - (1 - GF)^(2/3))

OUTPUT:
output = Vt
```

Listing B.4: Docetaxel Carboplatin Combined Tumour Growth Model in Mlxtran.

B.2 MATLAB

The inspector property interface was utilised to enhance the graphics of visuals delineated in this report. For instance, the inclusion and editing of units and legends was performed in this interface.

B.2.1 Forward Simulations

The Control

```
function simulate_growth_model()
    % params
    beta = 0.5;
```

```
    muQ = 0.04;
    muP = 0.34;

    % Initial conditions
    Vt0 = 190; % Initial Vt
    GF0 = 0.5; % Initial GF
    tspan = [0 840];

    [T, Y] = ode45(@(t, y) odes(t, y, beta, muQ, muP), tspan, [Vt0
    GF0]);

    %Plots
    figure;
    subplot(2,1,1);
    plot(T, Y(:,1), 'LineWidth', 2);
    xlabel('Time');
    ylabel('V_t');
    title('Tumor Volume Over Time');

    subplot(2,1,2);
    plot(T, Y(:,2), 'LineWidth', 2);
    xlabel('Time');
    ylabel('GF');
    title('Growth Fraction Over Time');
end

function dydt = odes(~, y, beta, muQ, muP)
    Vt = y(1);
    GF = y(2);

    % m for the control
    m = beta - muP + muQ;

    GF_inf = muQ / m;

    % ODEs
    dVt_dt = m * Vt * (GF - GF_inf);
    dGF_dt = m * (GF - GF_inf) * ((1 - GF) - (1 - GF)^(2/3));

    dydt = [dVt_dt; dGF_dt];
end
```

Listing B.5: Simulation of forward prediction for the tumour volume dynamics for the control group in MATLAB.

Treatment at Multiple Dosing Levels for Carboplatin

```
%%% Params %%%
Beta = 0.26;
muP = 0.19;
muQ = 0.037;
K_kill = 0.013;
A = 0.48;
B = 0.07;

V_Cent = 15.5;
V_Per = 9.86;

CL = 0.76 * 1.5;
Inter_CL = 3.46;
K10 = CL / V_Cent;
K12 = Inter_CL / V_Cent;
K21 = Inter_CL / V_Per;

%%% Initial conditions %%%
qCent_0 = 0.5;
qPer_0 = 0;
Vt0 = 190; % Average of the initial values for Carboplatin
GF0 = 0.19;
injection_interval = 72; % dataset delineates drug injected weekly
    is 168
total_time = 840; % changed to 840 as full injection is a month

doses = [0.25, 0.5, 0.75, 1.0];
colors = {'r', 'g', 'b', 'k'};

for d = 1:length(doses)
    injection_amount = doses(d);
    intervals = total_time / injection_interval;
    y0 = [qCent_0, qPer_0, Vt0, GF0];

    %%% Sets up injection times %%%
```

```
    for i = 1:intervals
        tspan = [(i-1)*injection_interval i*injection_interval];
        [t, y] = ode45(@(t, y) tumor_growth_model(t, y, Beta, muP,
    muQ, K_kill, A, B, K10, K12, K21, V_Cent, V_Per), tspan, y0);

        y0 = y(end, :) + injection_amount;
    end

    qCent = y(:,1);
    qPer = y(:,2);
    Vt = y(:,3);
    GF = y(:,4);
    Cp_c = qCent ./ V_Cent; % Effects central
    Cp_p = qPer ./ V_Per; % Effects peripheral

    subplot(1,2,1);
    hold on;
    plot(t, Vt, 'Color', colors{d});
    xlabel('Time');
    ylabel('Tumor Volume');
    title('Tumor Volume Over Time');

    subplot(1,2,2);
    hold on;
    plot(t, GF, 'Color', colors{d});
    xlabel('Time');
    ylabel('Growth Fraction');
    title('Growth Fraction Over Time');
end

legend('Dose 0.25', 'Dose 0.5', 'Dose 0.75', 'Dose 1.0');

function dydt = tumor_growth_model(t, y, Beta, muP, muQ, K_kill, A,
    B, K10, K12, K21, V_Cent, V_Per)
    qCent = y(1);
    qPer = y(2);
    Vt = y(3);
    GF = y(4);

    Cp_c = qCent / V_Cent;
    Cp_p = qPer / V_Per;
```

```
74
75      ddt_qCent = -(K10 + K12) * qCent + K21 * qPer;
76      ddt_qPer = K12 * qCent - K21 * qPer;
77
78      m = Beta * (1 - A * (Cp_c) / (B + Cp_c)) - muP - K_kill * Cp_c;
79
80      GF_inf = muQ / m;
81      ddt_Vt = m * Vt * (GF - GF_inf);
82      ddt_GF = m * (GF - GF_inf) * ((1 - GF) - (1 - GF)^(2/3));
83
84      dydt = [ddt_qCent; ddt_qPer; ddt_Vt; ddt_GF];
85  end
```

Listing B.6: Simulation of the tumour volume dynamics for the therapeutic carboplatin in MATLAB.

Multiple Dosing Levels Observing Carboplatin's Pharmacokinetic Model

```
1  %%% Params %%%
2  Beta = 0.26;
3  muP = 0.19;
4  muQ = 0.037;
5  K_kill = 0.013;
6  A = 0.48;
7  B = 0.07;
8
9  V_Cent = 15.5;
10 V_Per = 9.86;
11
12 CL = 0.76 * 1.5;
13 Inter_CL = 3.46;
14 K10 = CL / V_Cent;
15 K12 = Inter_CL / V_Cent;
16 K21 = Inter_CL / V_Per;
17
18 %%% Initial conditions %%%
19 qCent_0 = 0.5;
20 qPer_0 = 0;
21 Vt_0 = 190; % Average of the initial values for Carboplatin
22 GF_0 = 0.19;
23 injection_interval = 168;
24 total_time = 840;
```

```
25
26 doses = [0.25, 0.5, 0.75, 1.0];
27 colors = {'r', 'g', 'b', 'k'};
28
29 for d = 1:length(doses)
30     injection_amount = doses(d);
31     intervals = total_time / injection_interval;
32     y0 = [qCent_0, qPer_0, Vt_0, GF_0];
33
34     %%% Sets up injection times %%%
35     for i = 1:intervals
36         tspan = [(i-1)*injection_interval i*injection_interval];
37         [t, y] = ode45(@(t, y) tumor_growth_model(t, y, Beta, muP,
    muQ, K_kill, A, B, K10, K12, K21, V_Cent, V_Per), tspan, y0);
38
39         y0 = y(end, :) + injection_amount;
40     end
41
42     qCent = y(:,1);
43     qPer = y(:,2);
44     Vt = y(:,3);
45     GF = y(:,4);
46     Cp_c = qCent ./ V_Cent; % Effect on central
47     Cp_p = qPer ./ V_Per; % Effect on peripheral
48
49     subplot(1,2,1); % Subplot for Central Compartment
50     hold on;
51     plot(t_total, Cp_c, 'Color', colors(d));
52     xlabel('Time');
53     ylabel('Concentration (Central)');
54     title(['Central Compartment - Dose ', num2str(doses(d))]);
55
56     subplot(1,2,2); % Subplot for Peripheral Compartment
57     hold on;
58     plot(t_total, Cp_p, 'Color', colors(d));
59     xlabel('Time');
60     ylabel('Concentration (Peripheral)');
61     title(['Peripheral Compartment - Dose ', num2str(doses(d))]);
62 end
63
64 legend('Dose 0.25', 'Dose 0.5', 'Dose 0.75', 'Dose 1.0');
```

```
65
66 %%% Tumor Growth and PK Model %%%
67 function dydt = tumor_growth_model(t, y, Beta, muP, muQ, K_kill, A,
       B, K10, K12, K21, V_Cent, V_Per)
68     qCent = y(1);
69     qPer = y(2);
70     Vt = y(3);
71     GF = y(4);
72
73     Cp_c = qCent / V_Cent;
74     Cp_p = qPer / V_Per;
75
76     ddt_qCent = -(K10 + K12) * qCent + K21 * qPer;
77     ddt_qPer = K12 * qCent - K21 * qPer;
78
79     m = Beta * (1 - A * (Cp_c) / (B + Cp_c)) - muP - K_kill * Cp_c;
80
81     GF_inf = muQ / m;
82     ddt_Vt = m * Vt * (GF - GF_inf);
83     ddt_GF = m * (GF - GF_inf) * ((1 - GF) - (1 - GF)^(2/3));
84
85     dydt = [ddt_qCent; ddt_qPer; ddt_Vt; ddt_GF];
86 end
```

Listing B.7: Simulation of the PK model for the therapeutic carboplatin in MATLAB.

B.3 Mathmatica

B.3.1 Structural Identfiability Analysis for the Control

```
1 (*Control Model*)
2 \[Beta] = Symbol["\[Beta]"];
3 \[Mu]P = Symbol["\[Mu]P"];
4 \[Mu]Q = Symbol["\[Mu]Q"];
5 Rdiff = Symbol["Rdiff"];
6
7 MControl = \[Beta] - \[Mu]P + \[Mu]Q;
8 fControl[V_] := MControl V (1 - (1 - (Rdiff/((3 V)/(4
     \[Pi]))^(1/3))) - \[Mu]Q/MControl)
9
10 (*Initial condition*)
```

```
V0 = V0;

(*Taylor Series Coefficients*)
fControl[V0]

y1 = D[fControl[V], V];
coeffs = {fControl[V] /. V -> V0};
coeffs = Append[coeffs, y1 /. V -> V0]

y2 = D[y1, V];
coeffs = Append[coeffs, y2 /. V -> V0]

y3 = D[y2, V];
coeffs = Append[coeffs, y3 /. V -> V0]
```

Listing B.8: Taylor series coefficents of the TGM for the control group computed in Mathematica.

B.3.2 Structural Identfiability Analysis for the Treatment

```
(*Treatment Model*)
\[Beta] = Symbol["\[Beta]"];
\[Mu]P = Symbol["\[Mu]P"];
\[Mu]Q = Symbol["\[Mu]Q"];
Rdiff = Symbol["Rdiff"];
Imax = Symbol["Imax"];
Cp = Symbol["Cp"];
IC50 = Symbol["IC50"];
Kkill = Symbol["Kkill"];

Mtreatment = \[Beta] (1 - (Imax Cp) / (IC50 + Cp)) - \[Mu]P + Kkill
    Cp + \[Mu]Q;
fTreatment[V_] := Mtreatment V (1 - (1 - (Rdiff / ((3 V) / (4
    \[Pi]))) ^ (1/3))) - \[Mu]Q / Mtreatment);

(*Initial condition*)
V0 = V0;

(*Taylor Series Coefficients*)
fTreatment[V0]

y1 = D[fTreatment[V], V];
```

```
coeffs = {fTreatment[V] /. V -> V0};
coeffs = Append[coeffs, y1 /. V -> V0]

y2 = D[y1, V];
coeffs = Append[coeffs, y2 /. V -> V0]

y3 = D[y2, V];
coeffs = Append[coeffs, y3 /. V -> V0]
```

Listing B.9: Taylor series coefficents of the TGM for the treatment group computed in Mathematica.

Appendix C

MATLAB Outputs

C.1 Forward Simulations of Carboplatin

C.1.1 Pharmacokinetic Analysis of Carboplatin

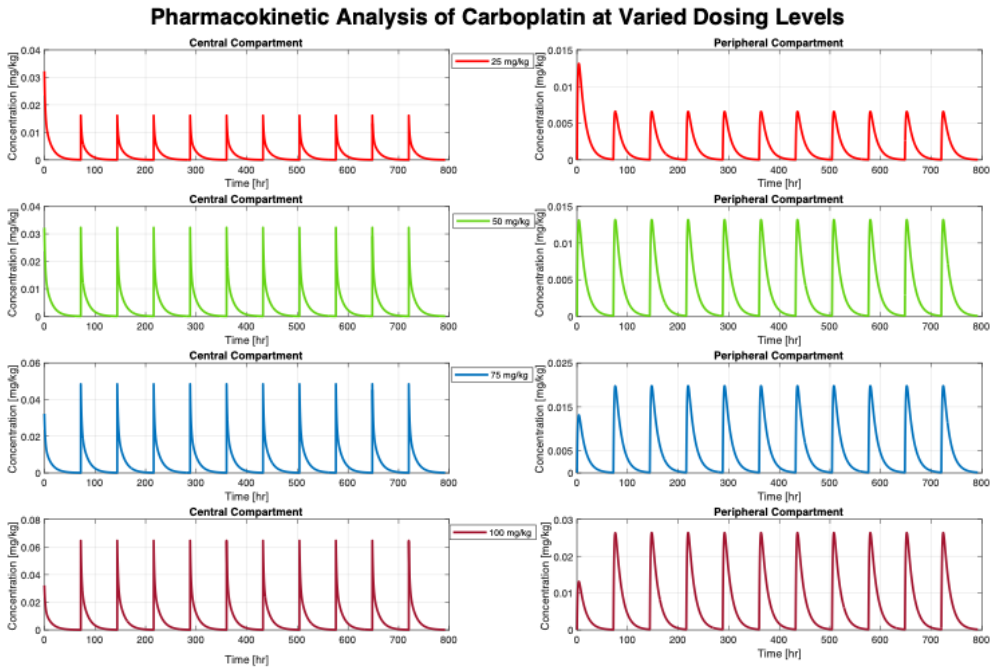

Figure C.1. *PK simulation for carboplatin at various dose levels with a dose being administered every three days.*

C.1.2 Analysis of the Growth Factor and Tumour Volume when Carboplatin is Administered

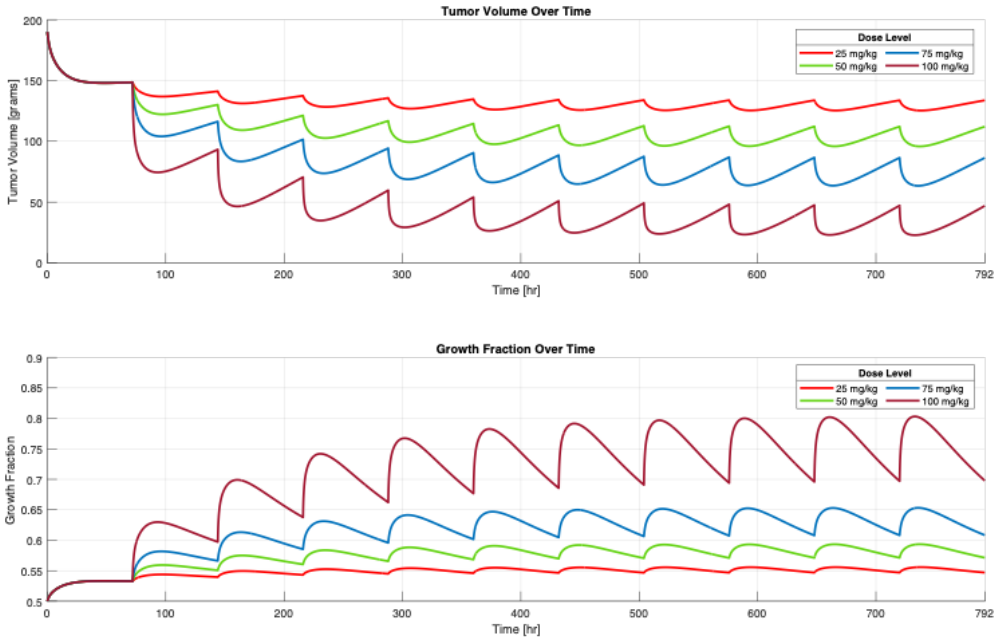

Figure C.2. *Simulation of tumour volume dynamics and growth fraction when carboplatin is administered at various dose levels; where a dose is administered every three days.*

Appendix D

Monolix Outputs

D.1 Individual Fits

D.1.1 Control Group for Docetaxel and Carboplatin

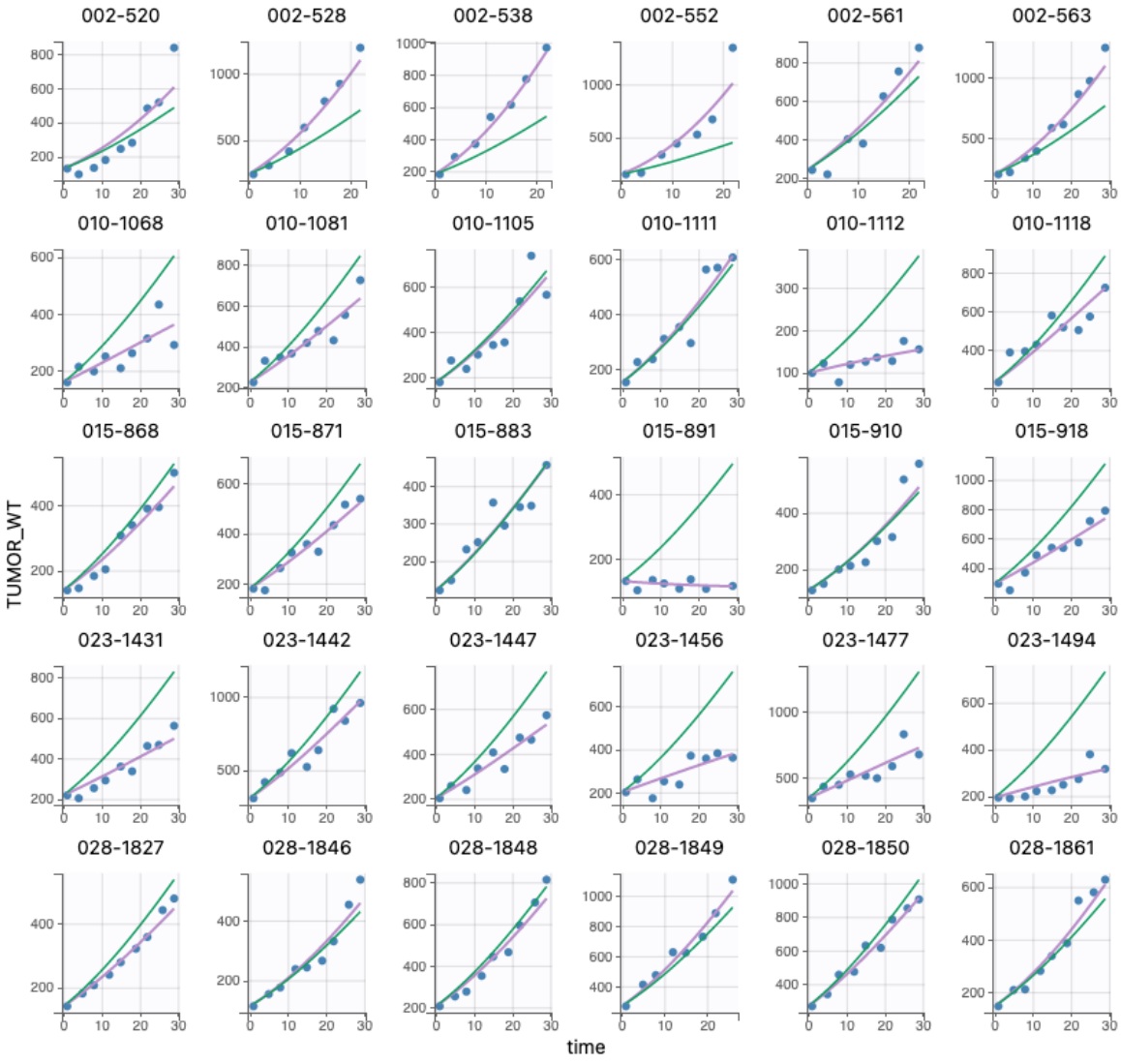

Figure D.1. *Individual fits of the control group simulated in Monolix, figure 1 [66].*

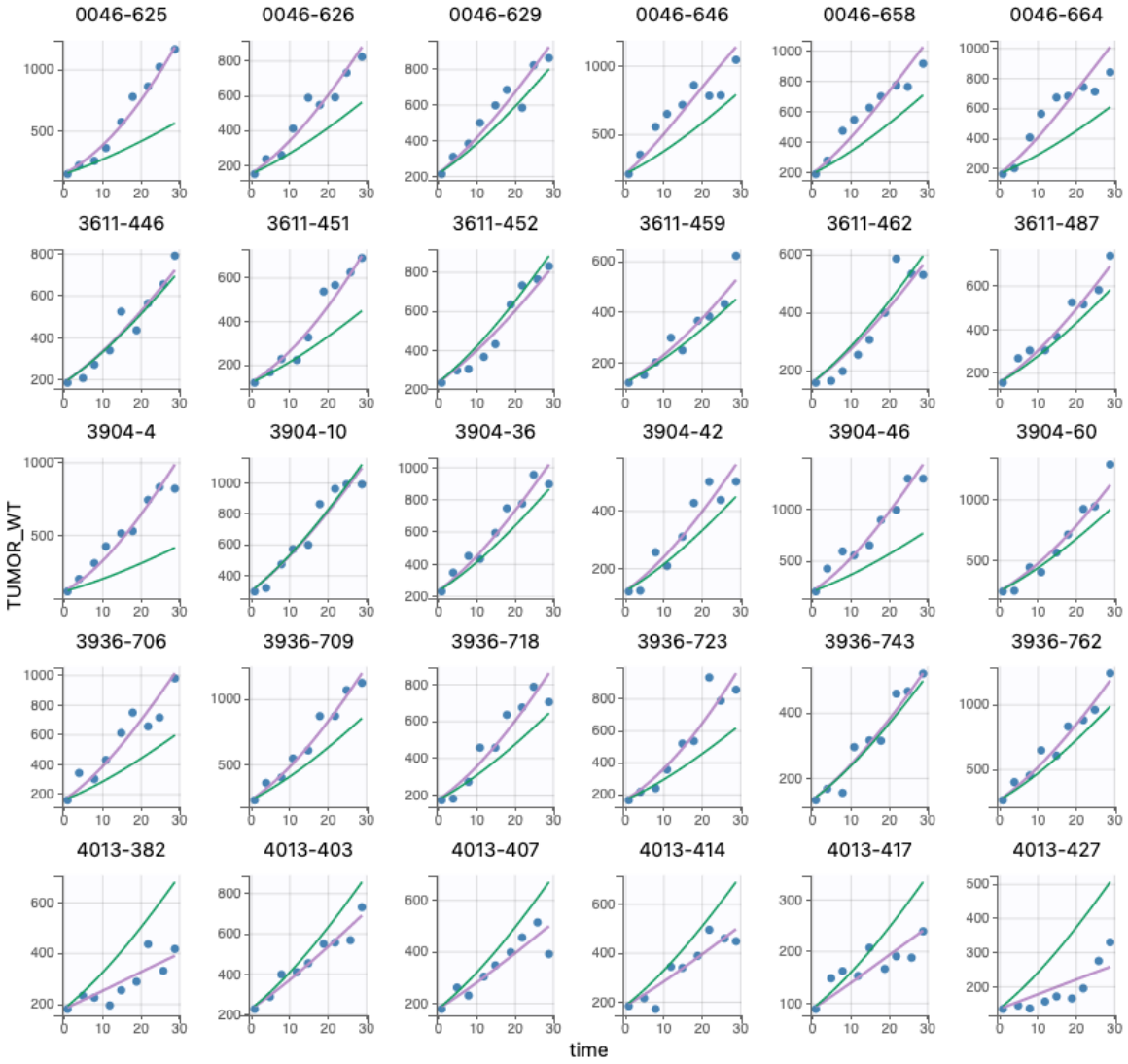

Figure D.2. *Individual fits of the control group simulated in Monolix, figure 2 [66].*

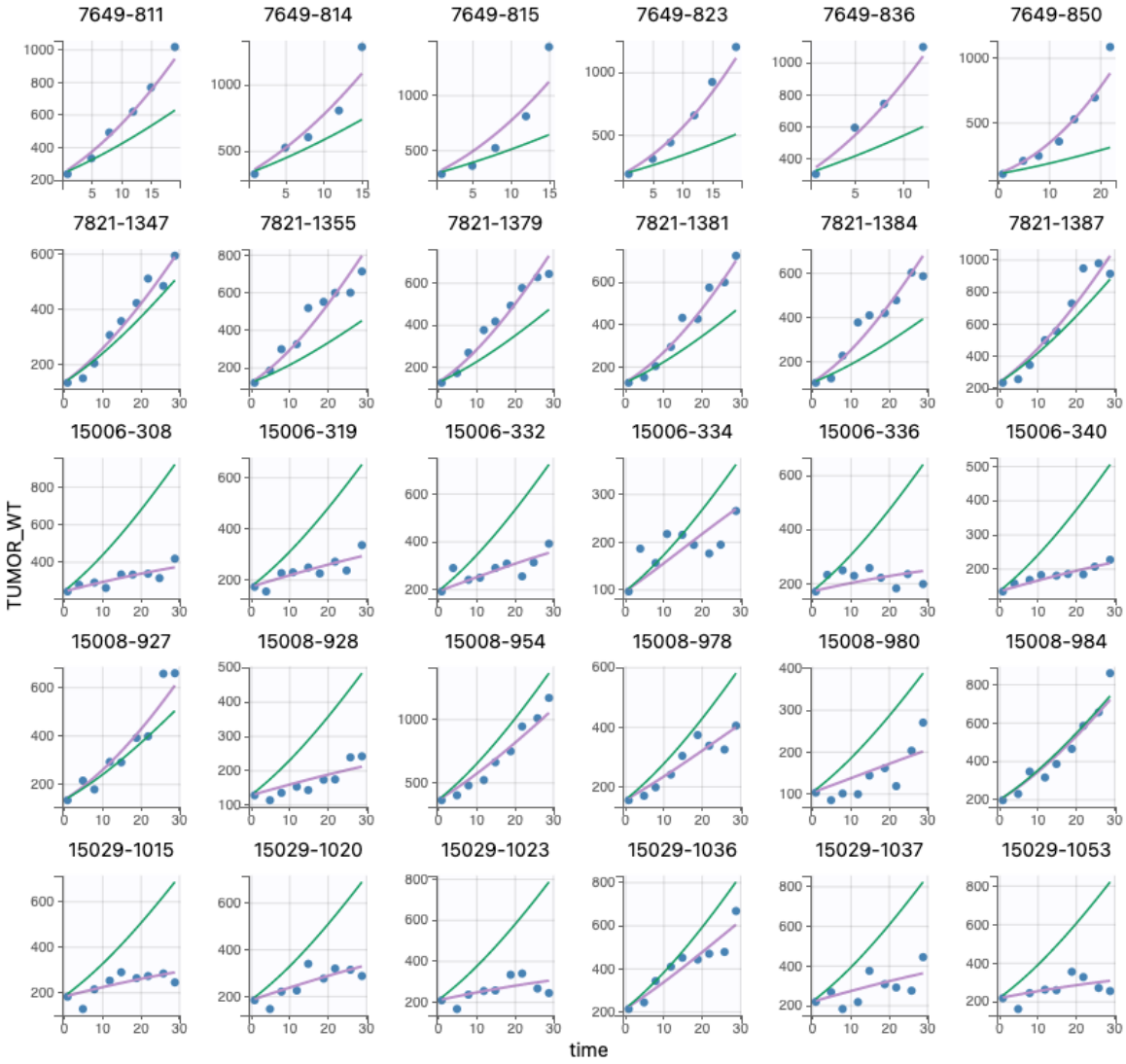

Figure D.3. *Individual fits of the control group simulated in Monolix, figure 3 [66].*

D.1.2 Linear Effect for Docetaxel Treatment

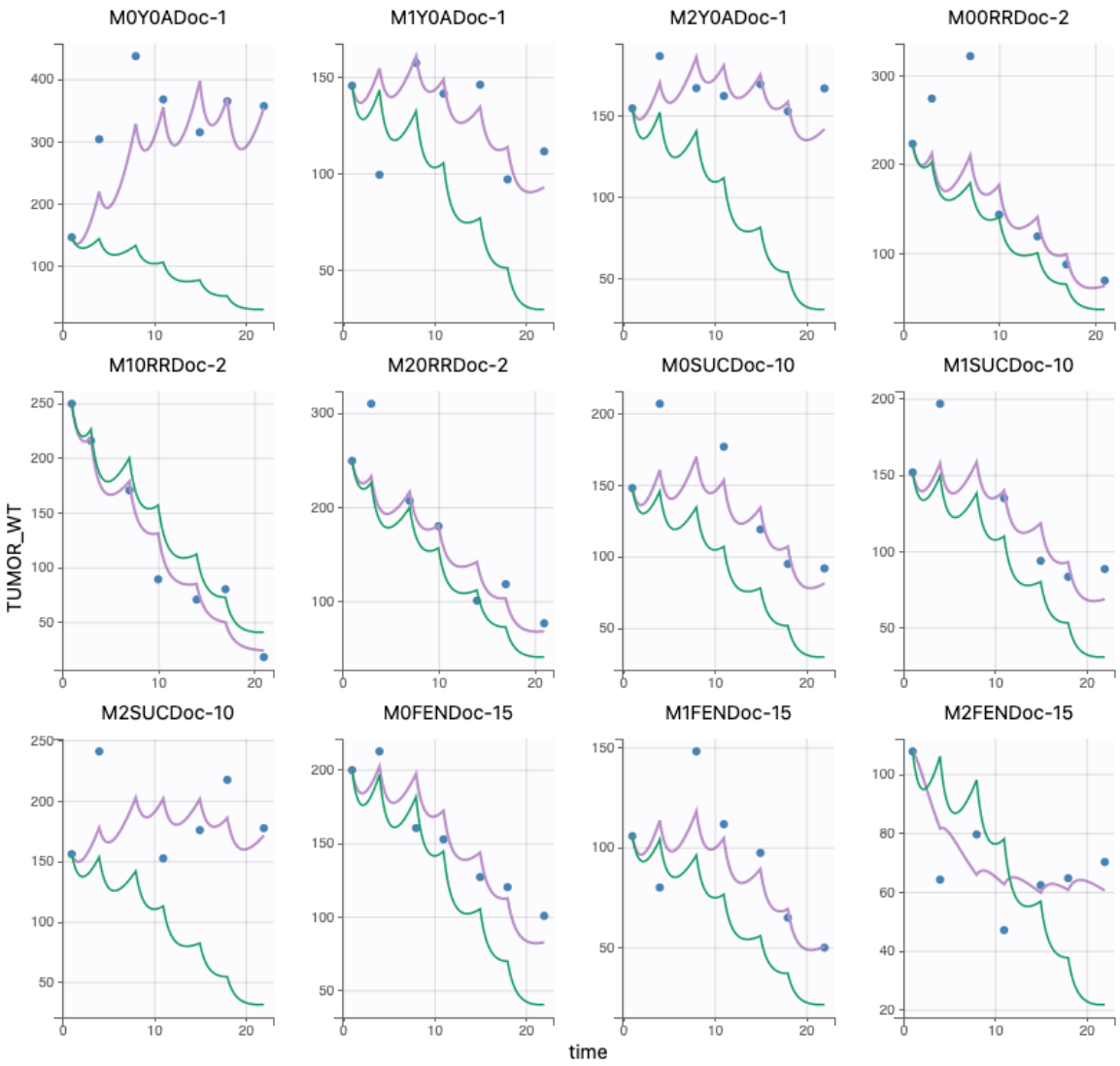

Figure D.4. *Individual fits of the docetaxel treatment group with the linear effect simulated in Monolix, figure 1 [66].*

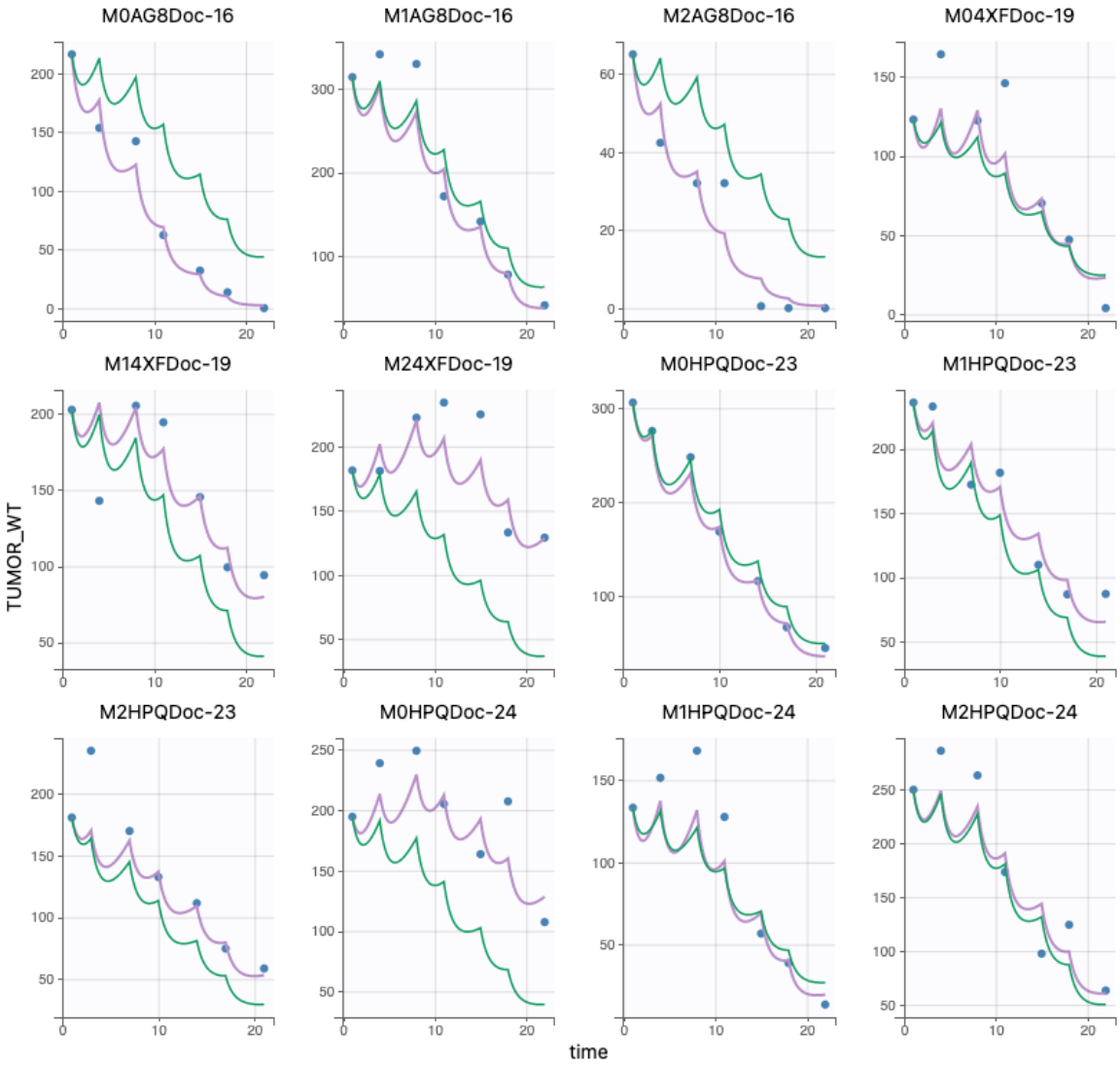

Figure D.5. *Individual fits of the docetaxel treatment group with the linear effect simulated in Monolix, figure 2 [66].*

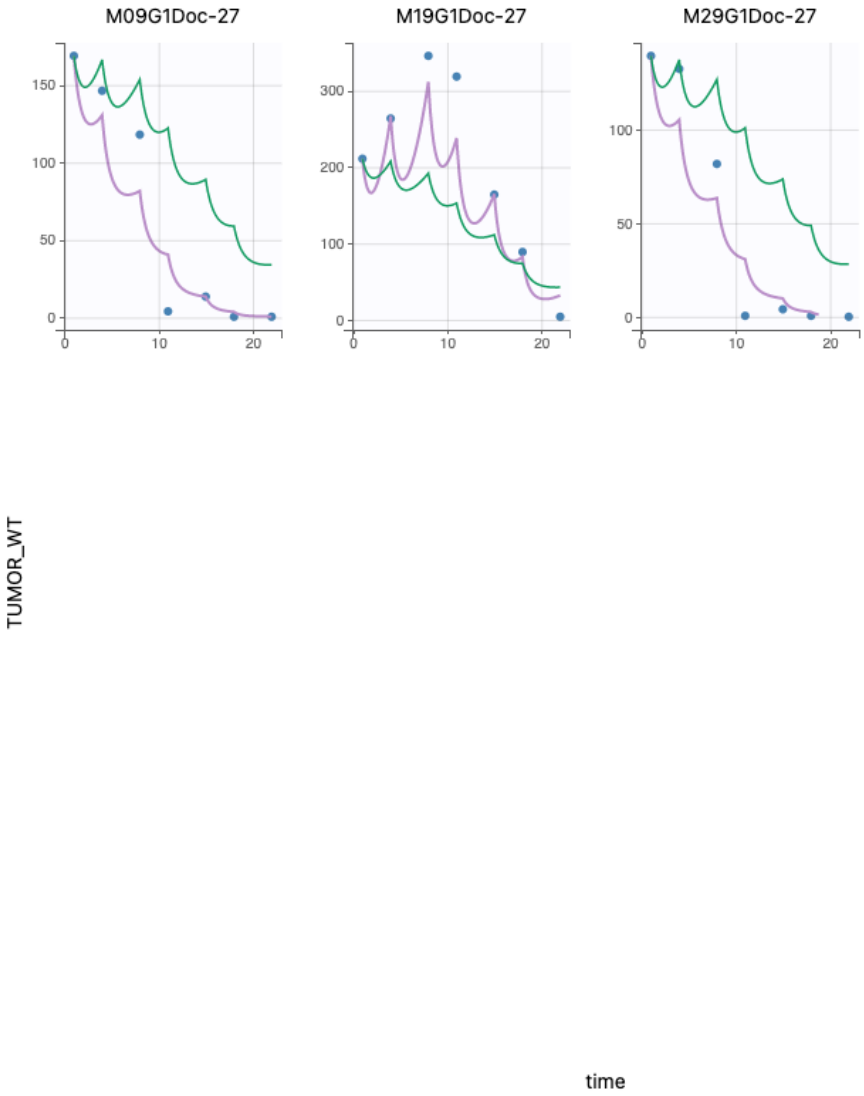

Figure D.6. *Individual fits of the docetaxel treatment group with the linear effect simulated in Monolix, figure 3 [66].*

D.1.3 Michaelis-Menten Effect for Docetaxel Treatment

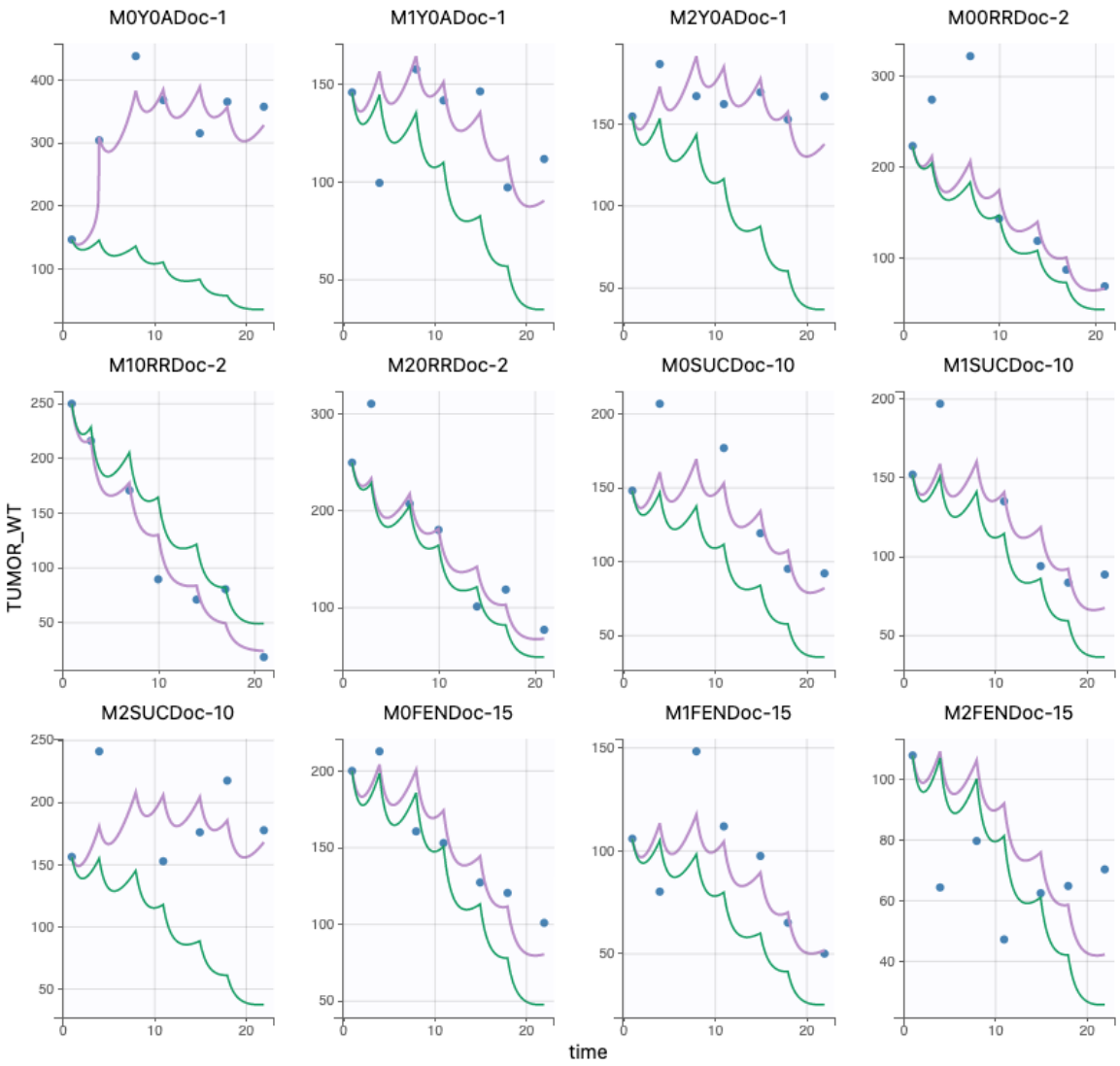

Figure D.7. *Individual fits of the docetaxel treatment group with the Michaelis-Menten effect simulated in Monolix, figure 1 [66].*

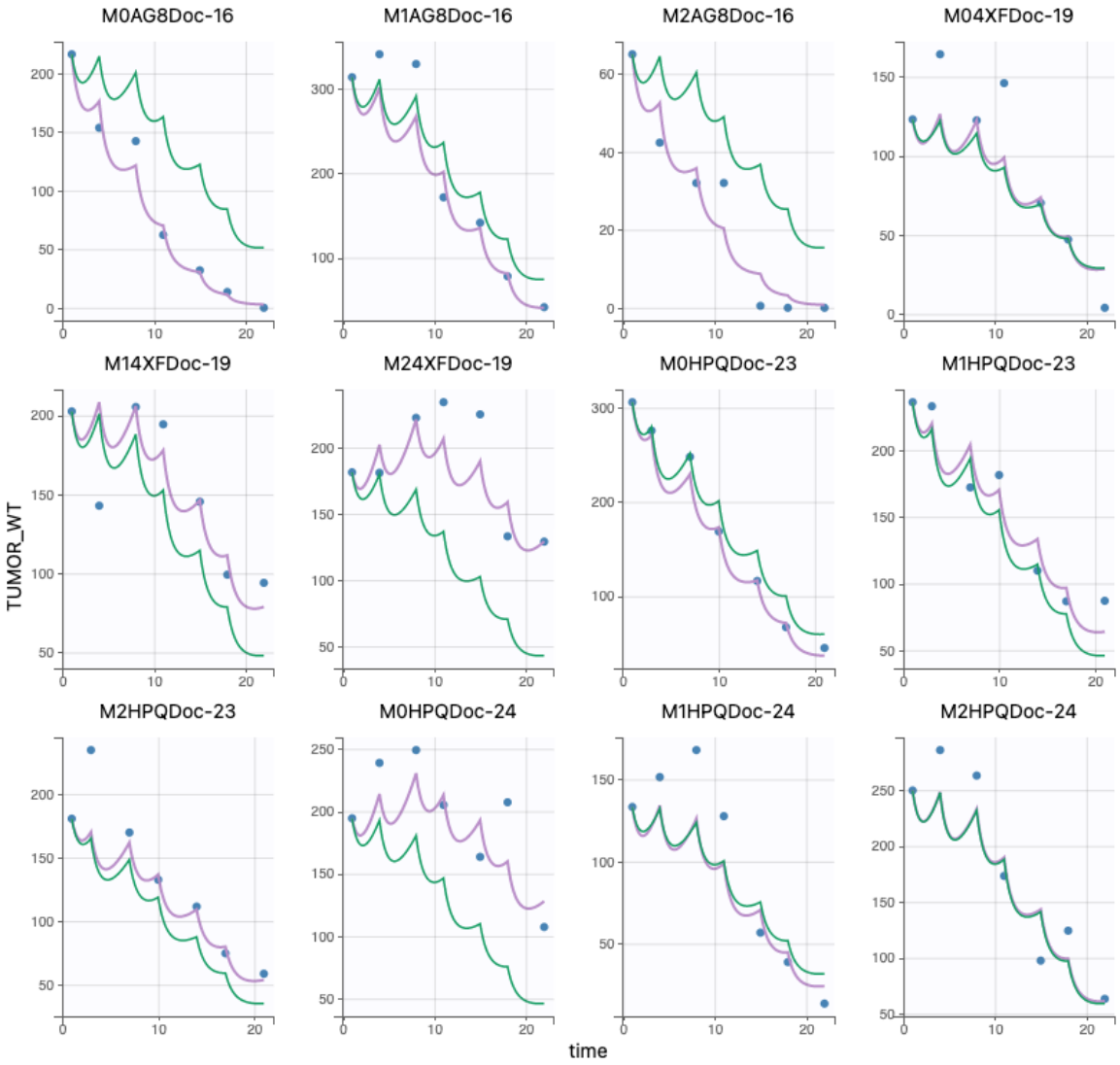

Figure D.8. *Individual fits of the docetaxel treatment group with the Michaelis-Menten effect simulated in Monolix, figure 2 [66].*

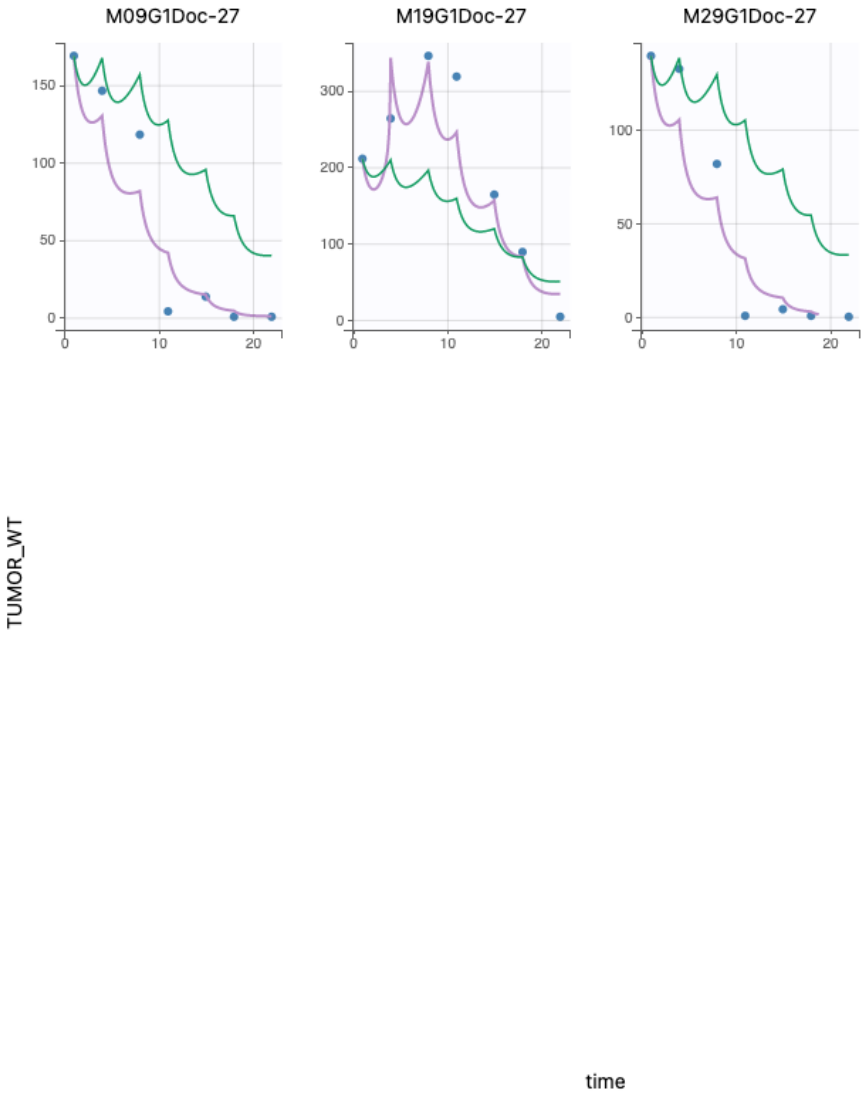

Figure D.9. *Individual fits of the docetaxel treatment group with the Michaelis-Menten effect simulated in Monolix, figure 3 [66].*

D.1.4 Hill Type Effect for Docetaxel Treatment

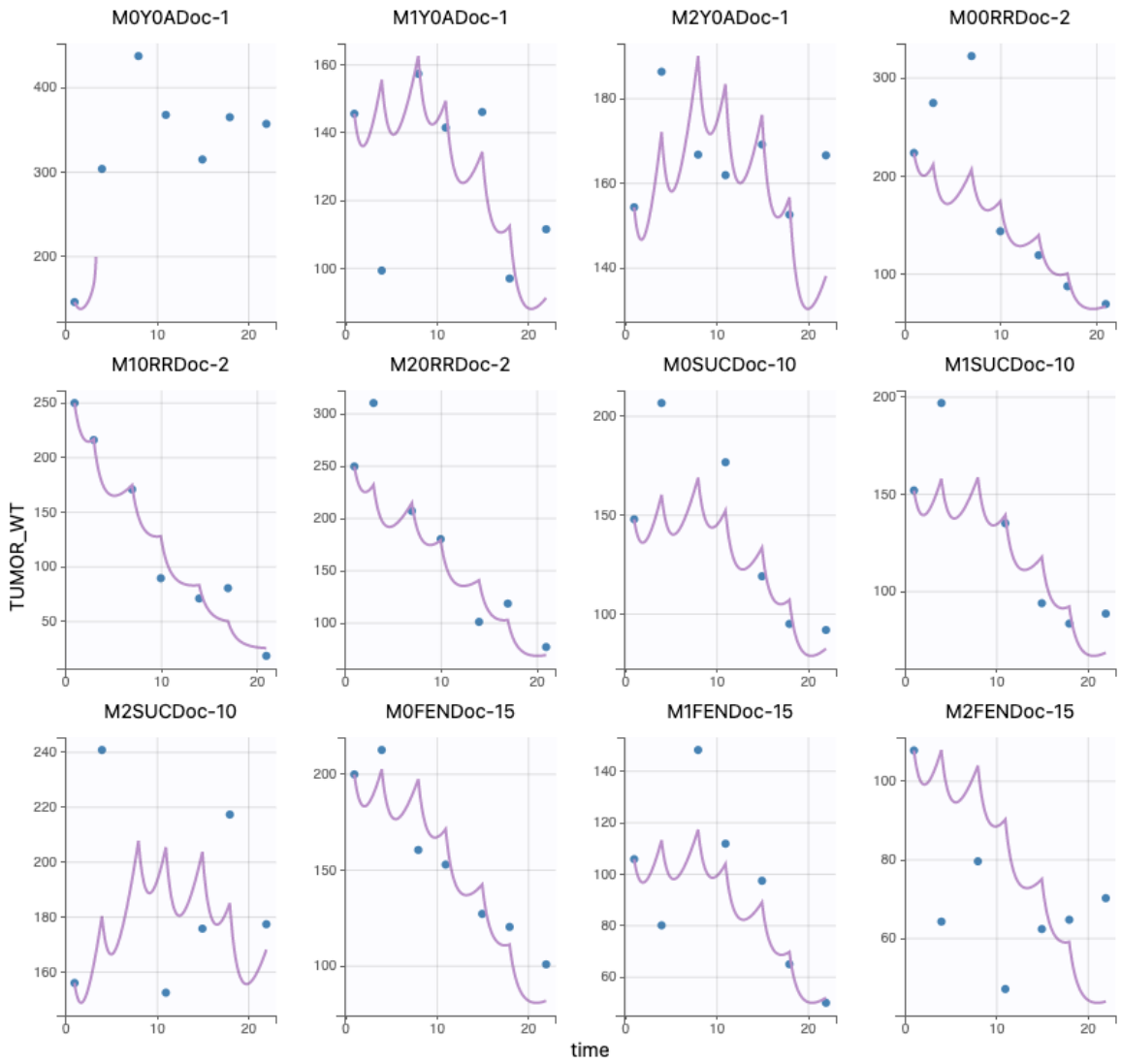

Figure D.10. *Individual fits of the docetaxel treatment group with the Hill type effect simulated in Monolix, figure 1 [66].*

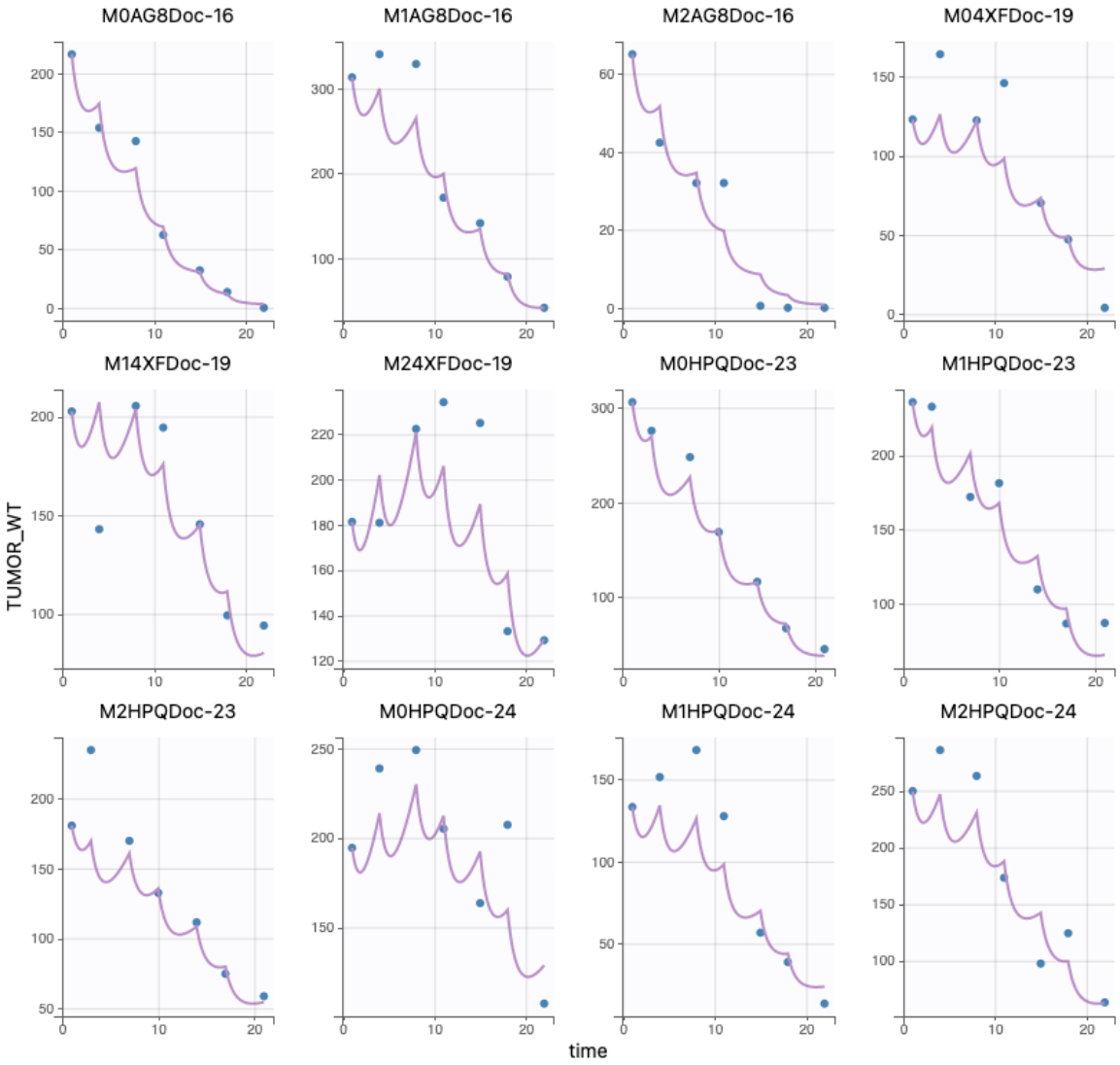

Figure D.11. *Individual fits of the docetaxel treatment group with the Hill type effect simulated in Monolix, figure 2 [66].*

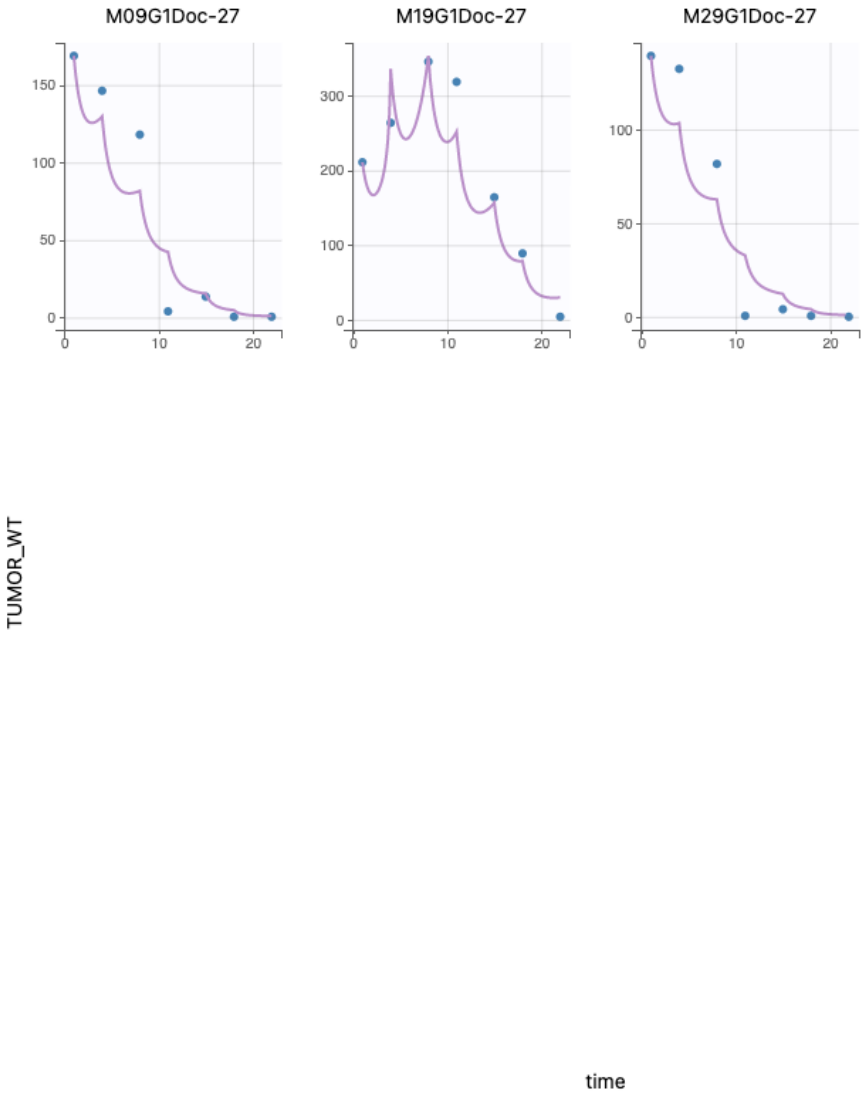

Figure D.12. *Individual fits of the docetaxel treatment group with the Hill type effect simulated in Monolix, figure 3 [66].*

D.1.5 Linear Effect for Carboplatin Treatment

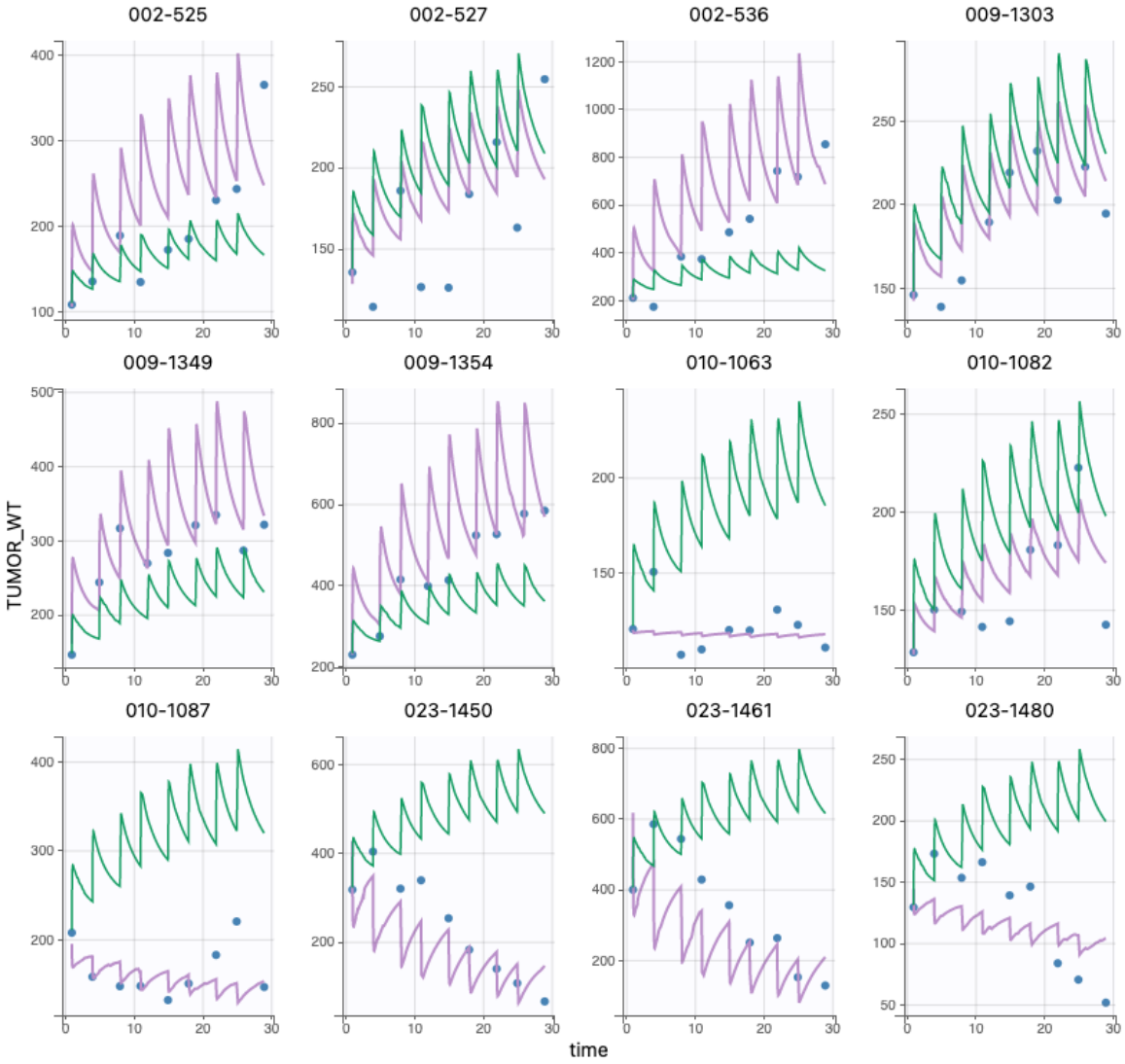

Figure D.13. *Individual fits of the carboplatin treatment group with the linear effect simulated in Monolix, figure 1 [66].*

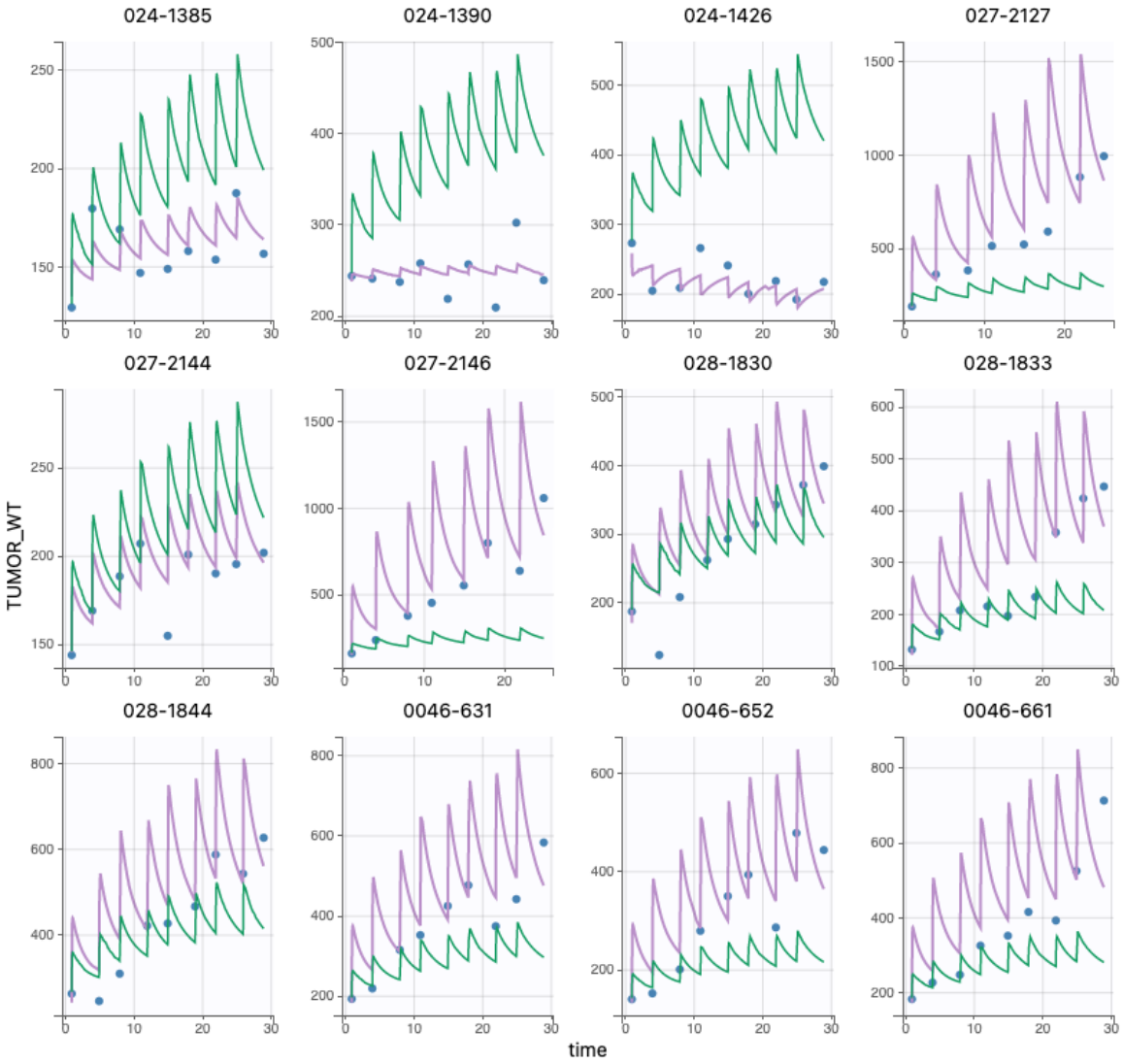

Figure D.14. *Individual fits of the carboplatin treatment group with the linear effect simulated in Monolix, figure 2 [66].*

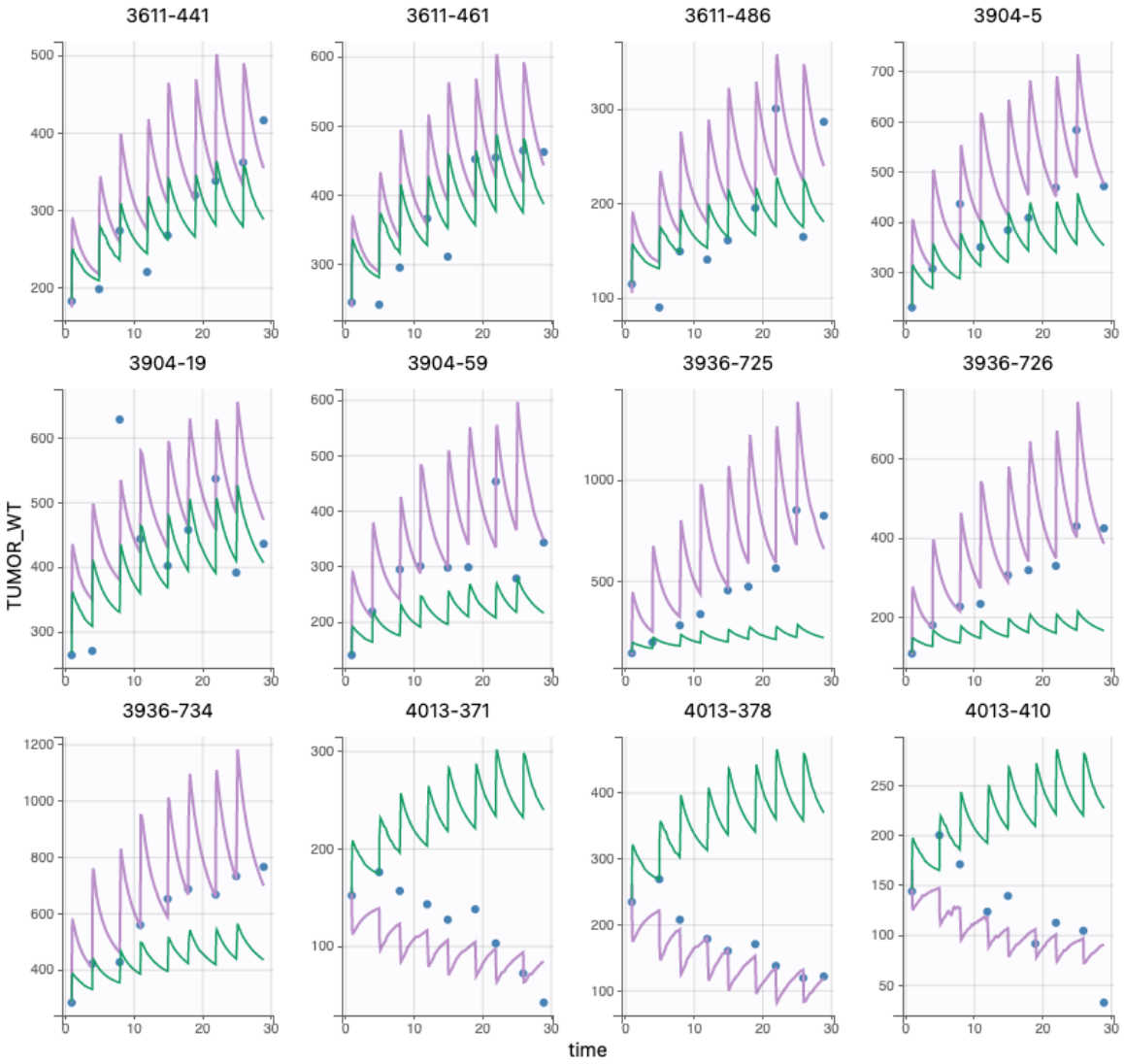

Figure D.15. *Individual fits of the carboplatin treatment group with the linear effect simulated in Monolix, figure 3 [66].*

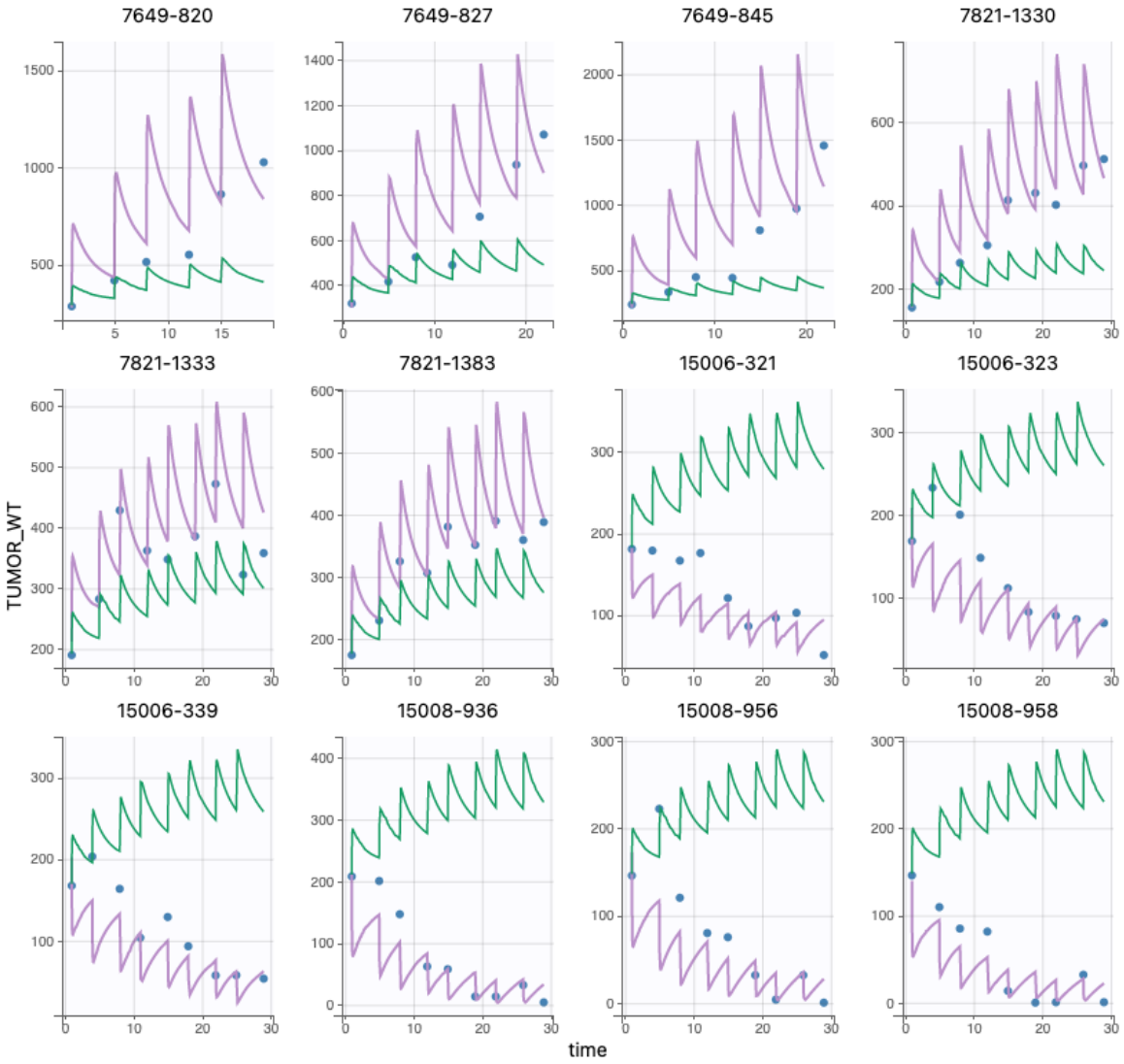

Figure D.16. *Individual fits of the carboplatin treatment group with the linear effect simulated in Monolix, figure 4 [66].*

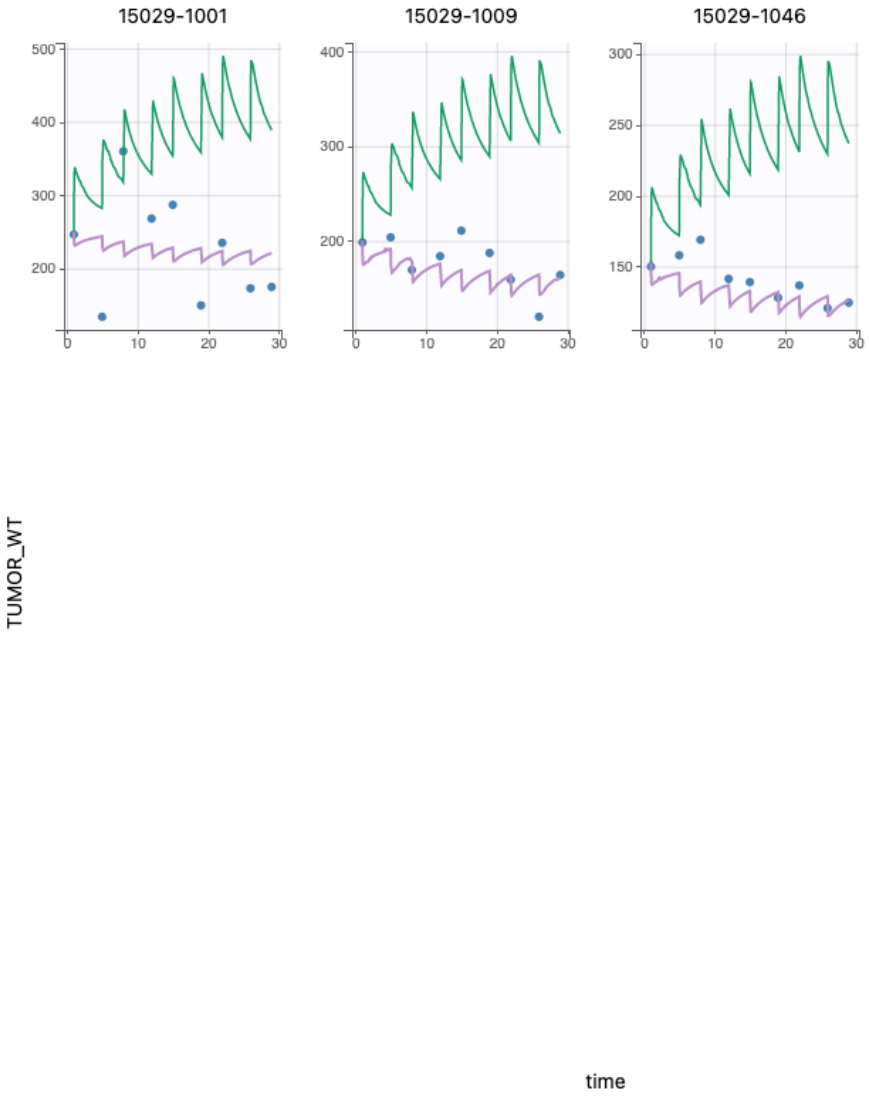

Figure D.17. *Individual fits of the carboplatin treatment group with the linear effect simulated in Monolix, figure 5 [66].*

D.1.6 Michaelis-Menten Effect for Carboplatin Treatment

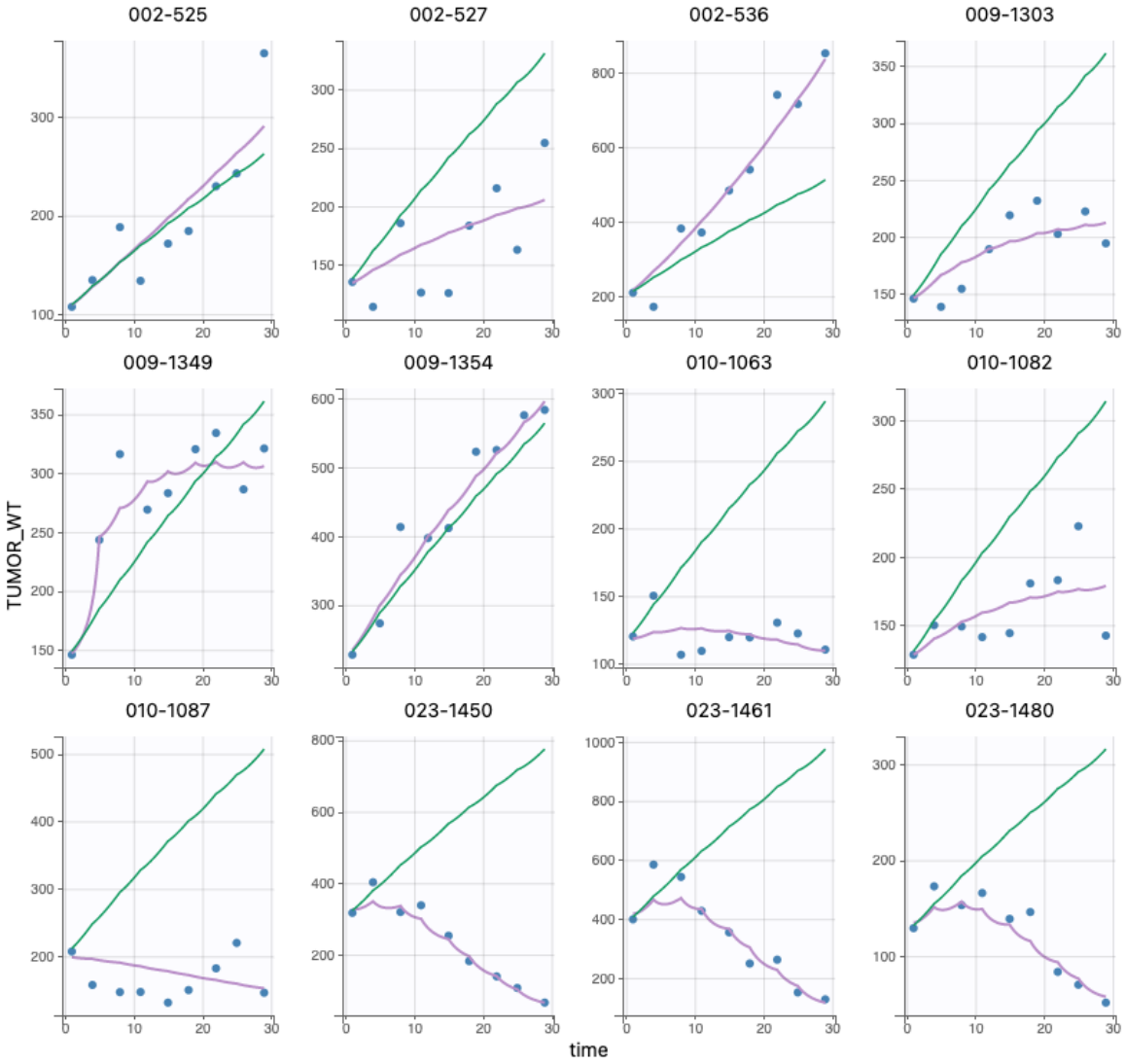

Figure D.18. *Individual fits of the carboplatin treatment group with the Michaelis-Menten effect simulated in Monolix, figure 1 [66].*

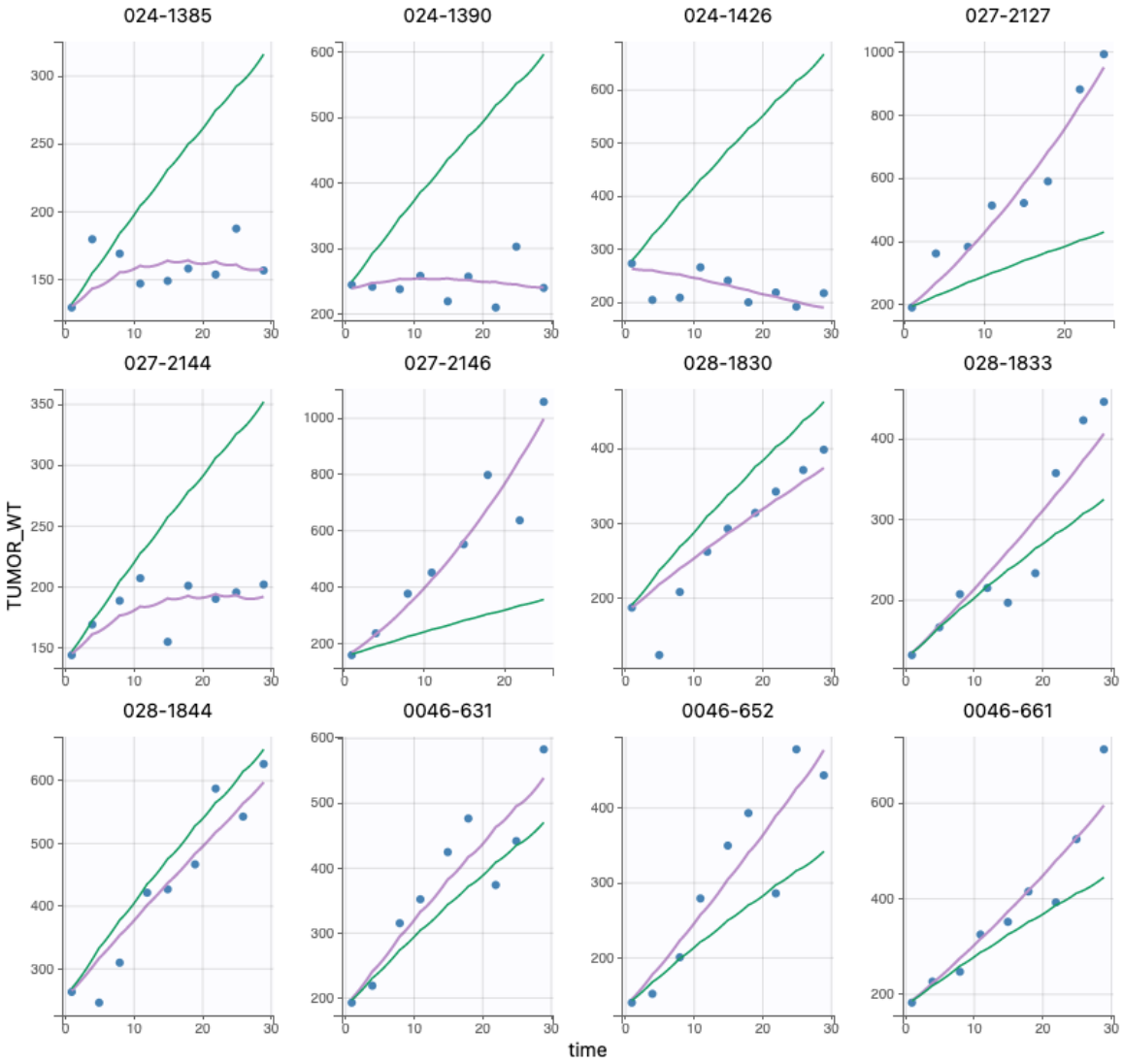

Figure D.19. *Individual fits of the carboplatin treatment group with the Michaelis-Menten effect simulated in Monolix, figure 2 [66].*

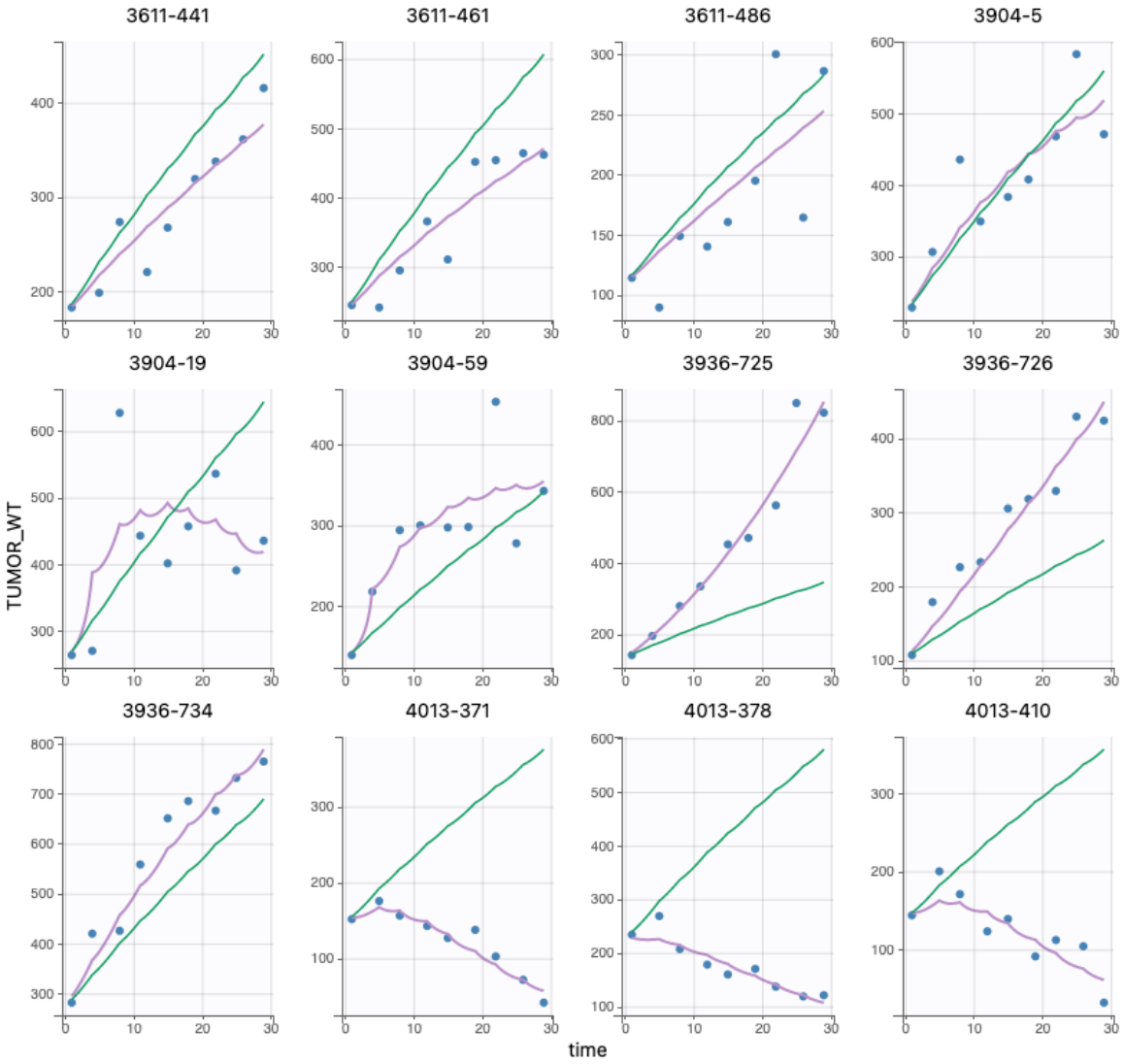

Figure D.20. *Individual fits of the carboplatin treatment group with the Michaelis-Menten effect simulated in Monolix, figure 3 [66].*

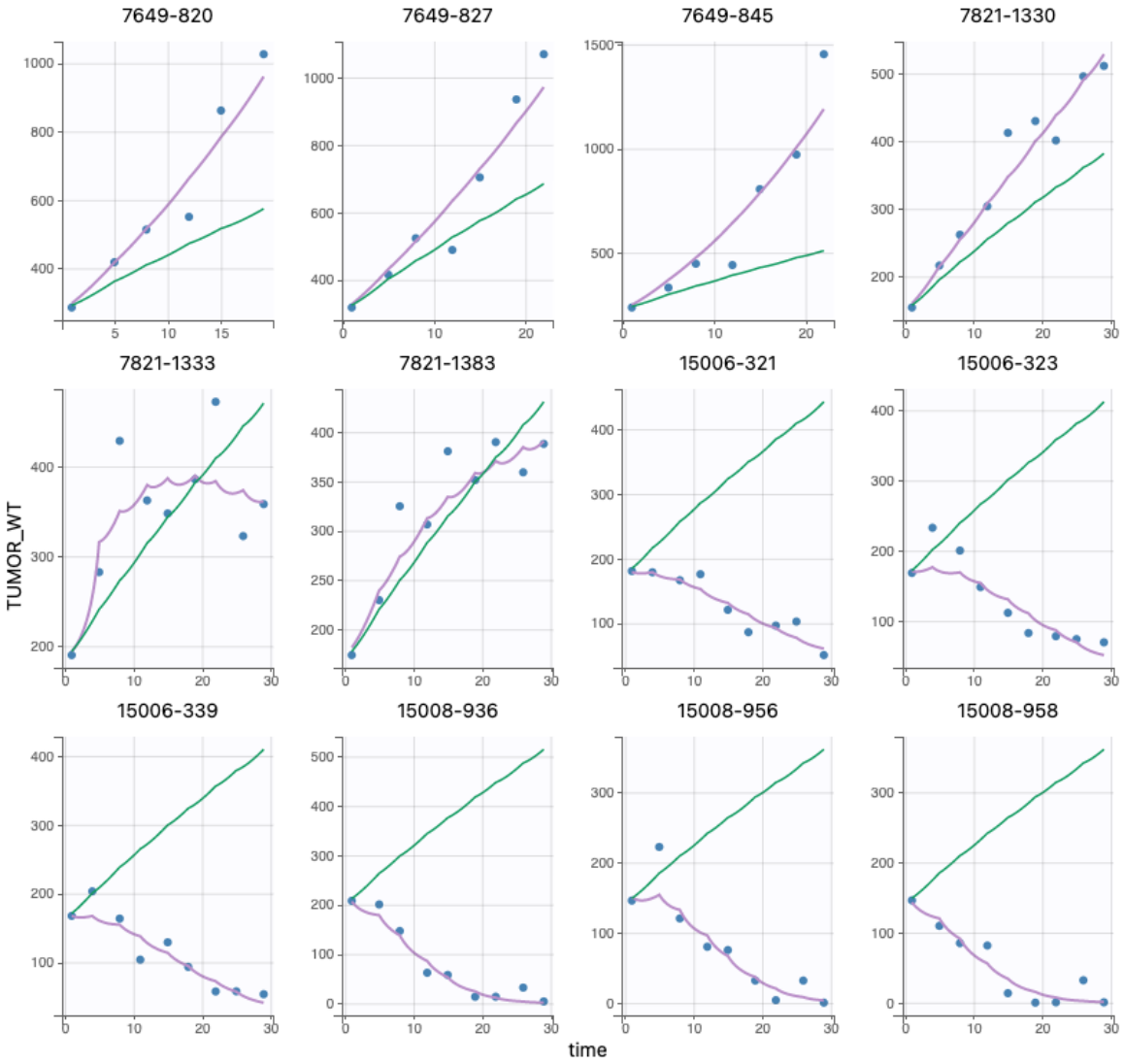

Figure D.21. *Individual fits of the carboplatin treatment group with the Michaelis-Menten effect simulated in Monolix, figure 4 [66].*

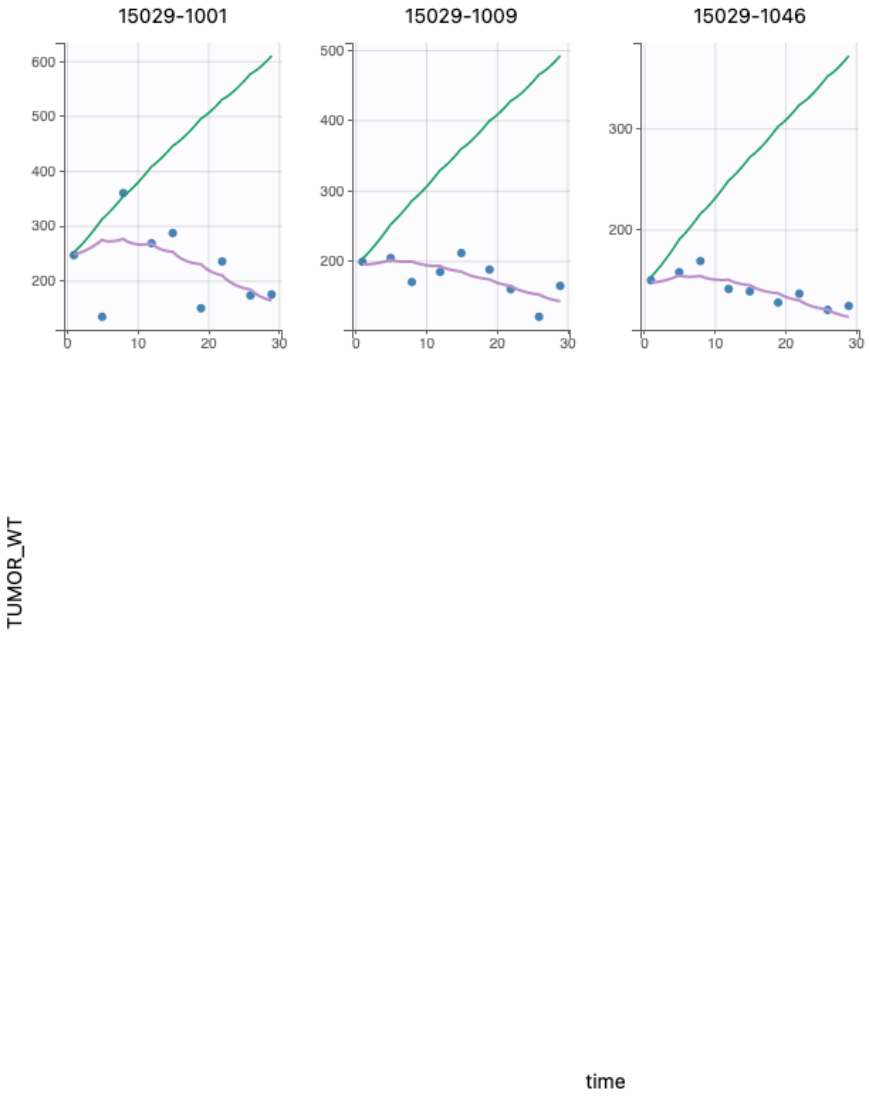

Figure D.22. *Individual fits of the carboplatin treatment group with the Michaelis-Menten effect simulated in Monolix, figure 5 [66].*

D.1.7 Quadratic Effect for Carboplatin

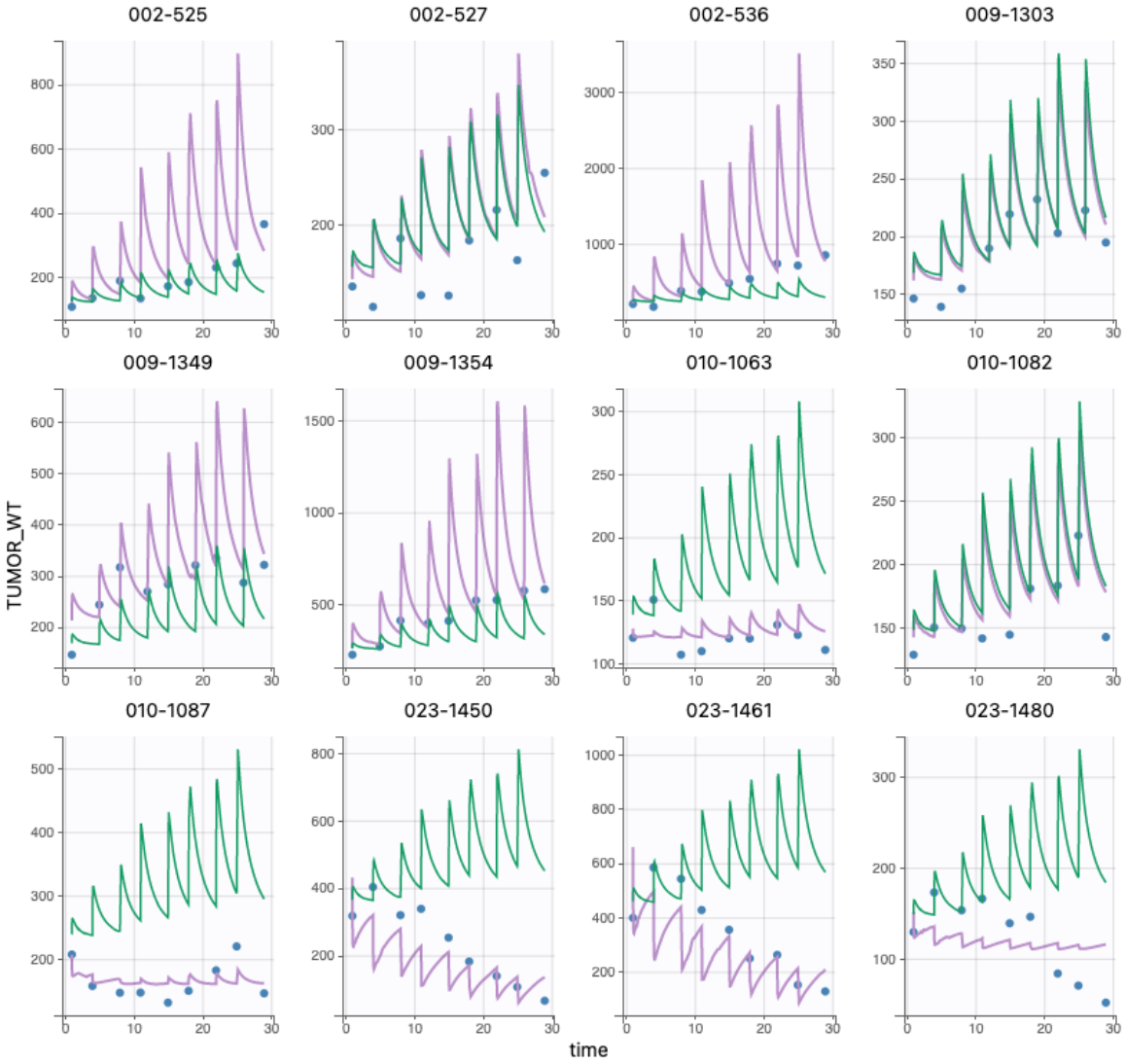

Figure D.23. *Individual fits of the carboplatin treatment group with the quadratic effect simulated in Monolix, figure 1 [66].*

D.1.8 Carboplatin and Docetaxel in Combination with Linear Effect

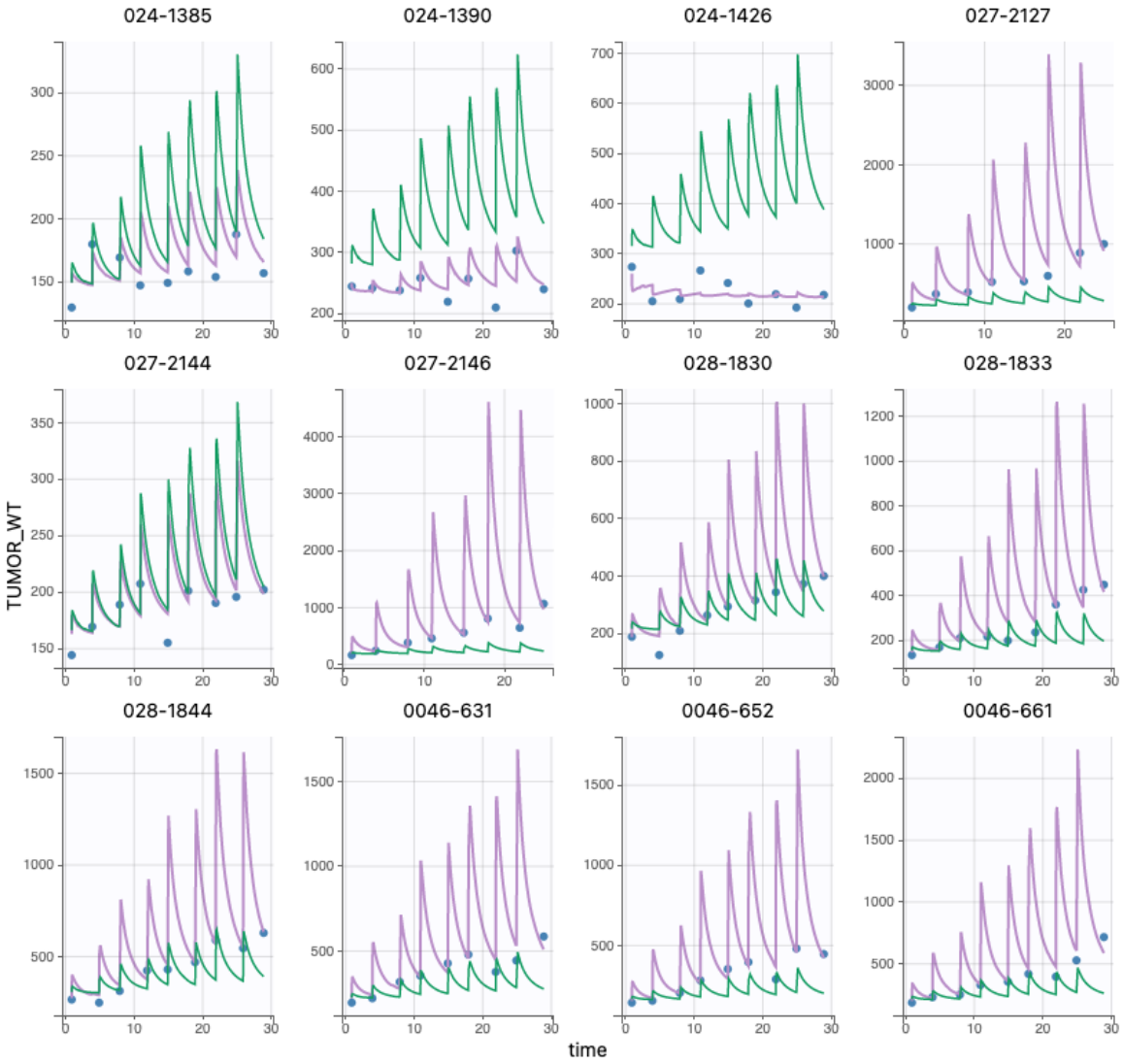

Figure D.24. *Individual fits of the carboplatin treatment group with the quadratic effect simulated in Monolix, figure 2 [66].*

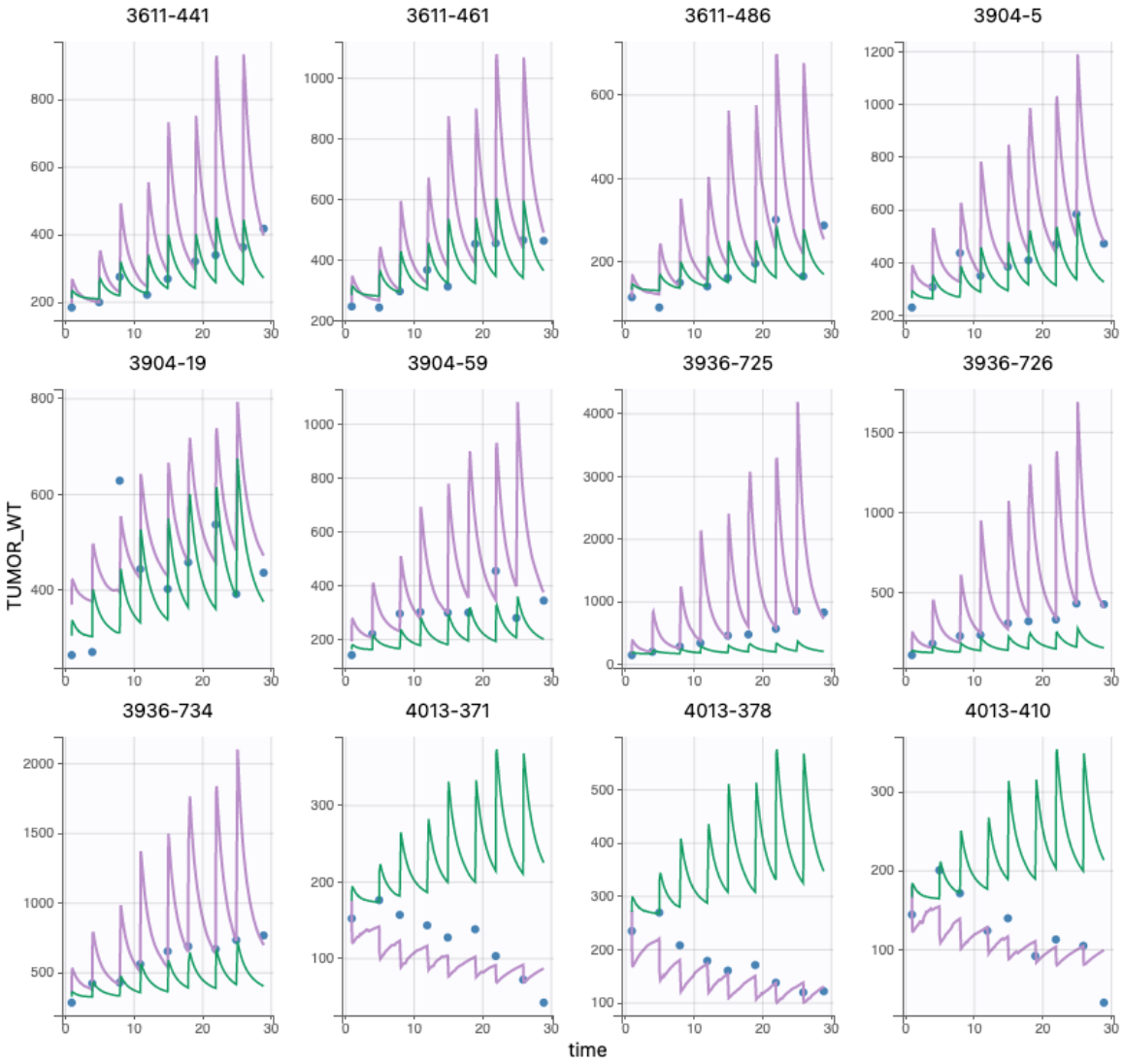

Figure D.25. *Individual fits of the carboplatin treatment group with the quadratic effect simulated in Monolix, figure 3 [66].*

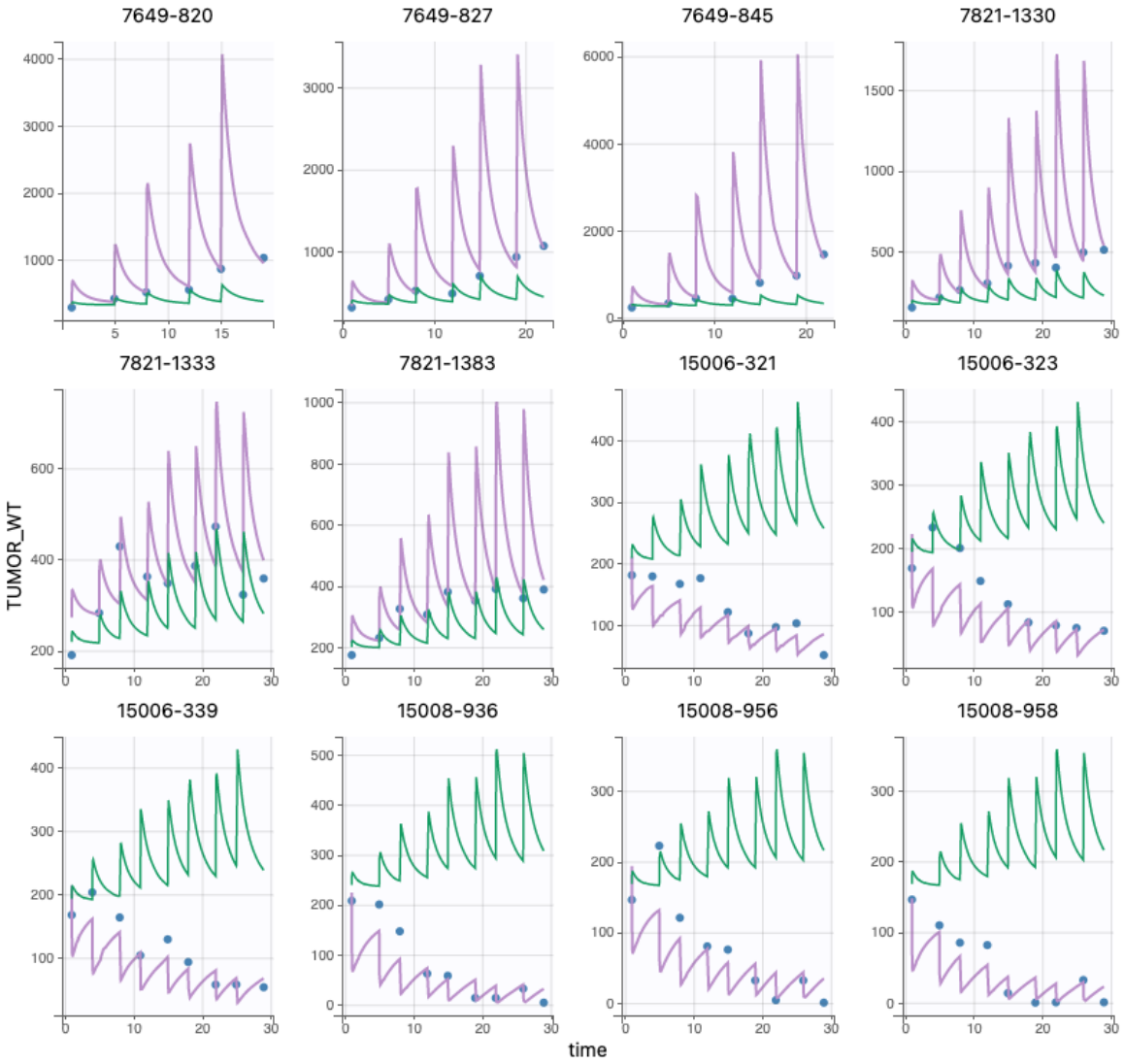

Figure D.26. *Individual fits of the carboplatin treatment group with the quadratic effect simulated in Monolix, figure 4 [66].*

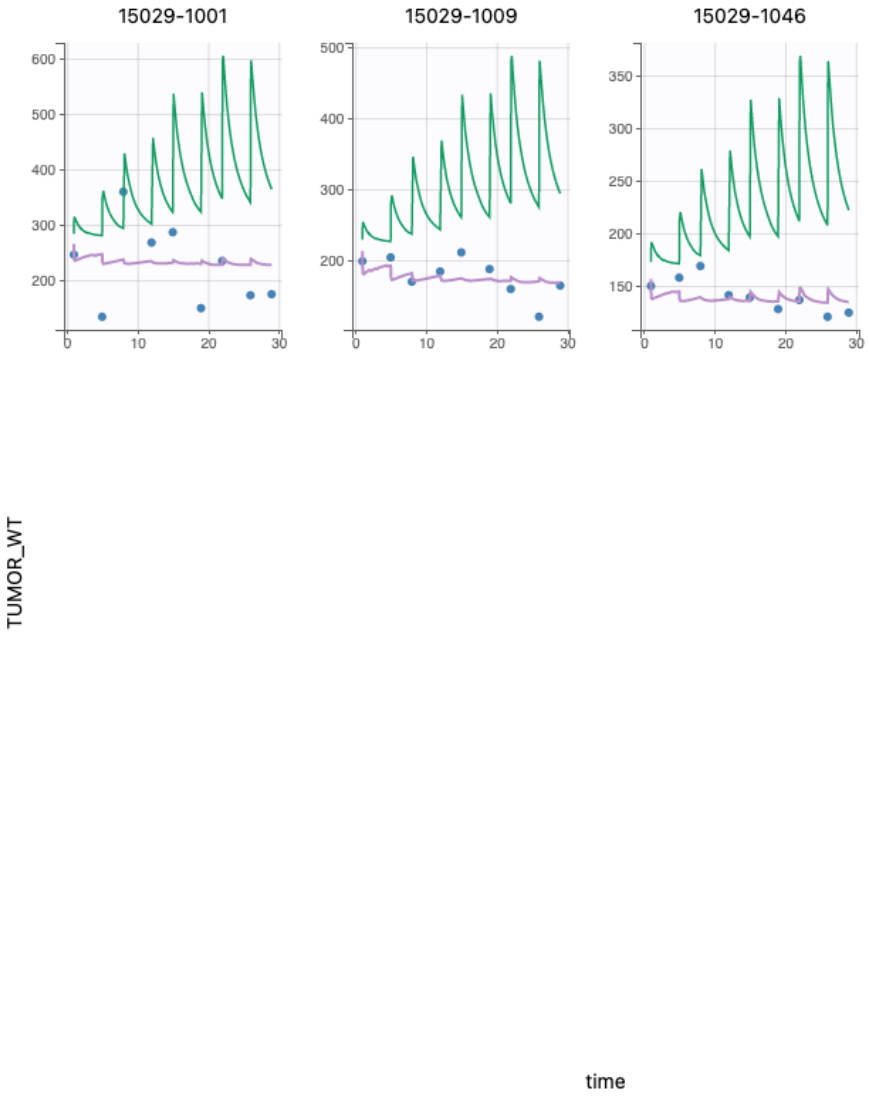

Figure D.27. *Individual fits of the carboplatin treatment group with the quadratic effect simulated in Monolix, figure 5 [66].*

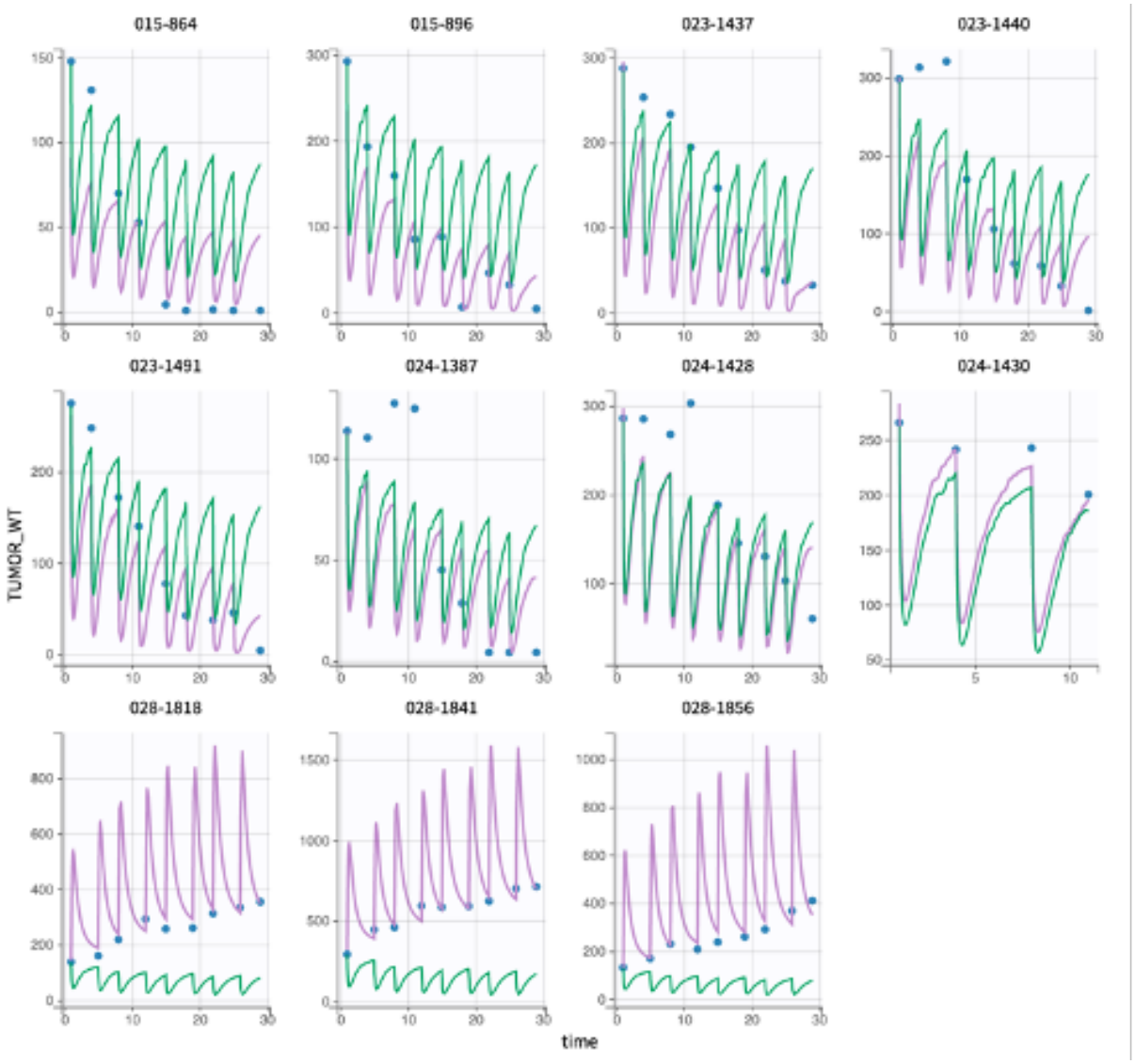

Figure D.28. *Individual fits of the additive combination of docetaxel and carboplatin treatment group with the linear effect simulated in Monolix[66].*

D.1.9 Carboplatin and Docetaxel in Combination with Quadratic Effect

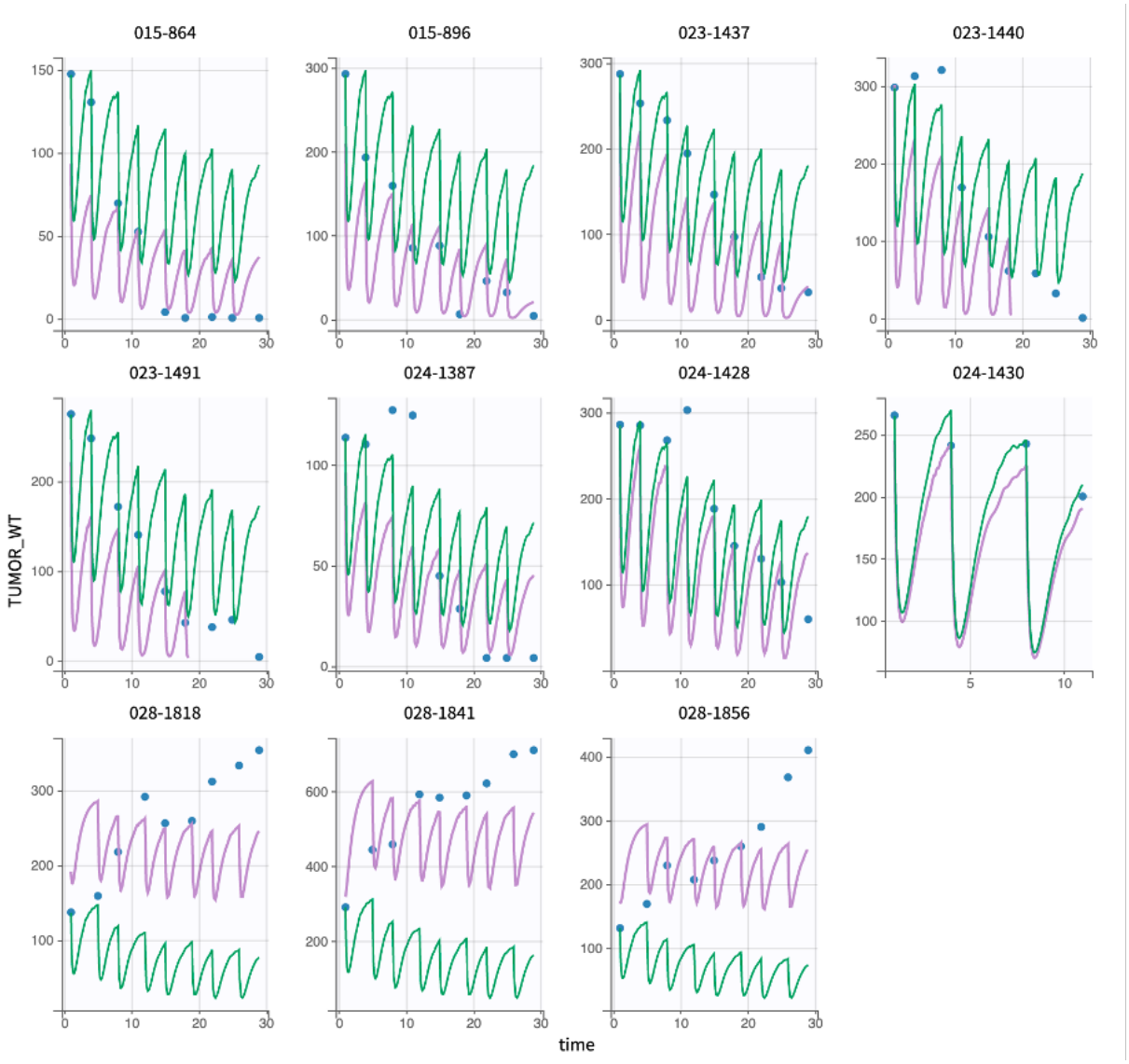

Figure D.29. *Individual fits of the additive combination of docetaxel and carboplatin treatment group with the quadratic effect simulated in Monolix[66].*

D.1.10 Carboplatin and Docetaxel in Combination with Michaelis-Menten Effect

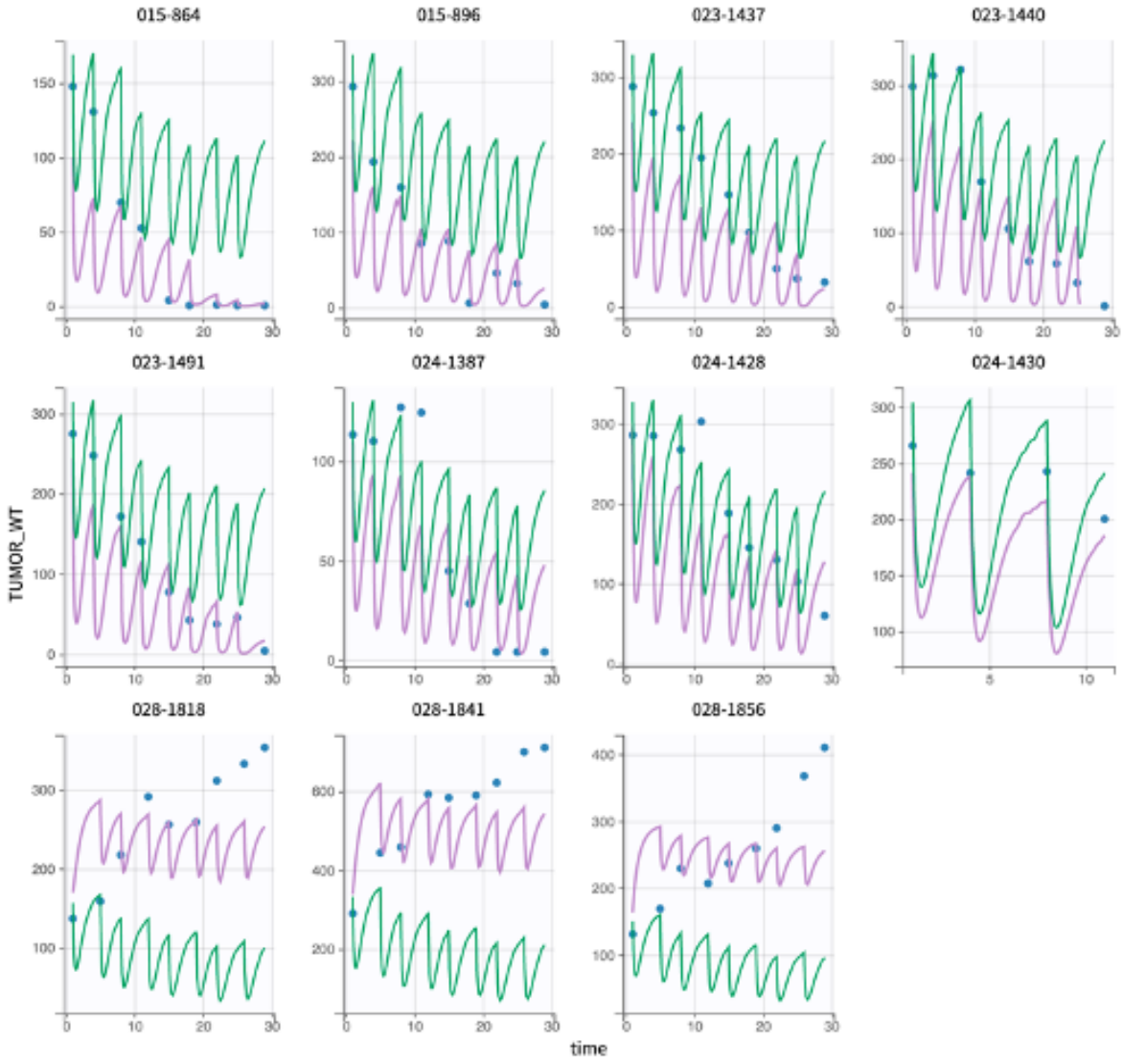

Figure D.30. *Individual fits of the additive combination of docetaxel and carboplatin treatment group with the Michaelis-Menten effect simulated in Monolix[66].*

D.2 Visual Predictive Check (VPC)

D.2.1 Control

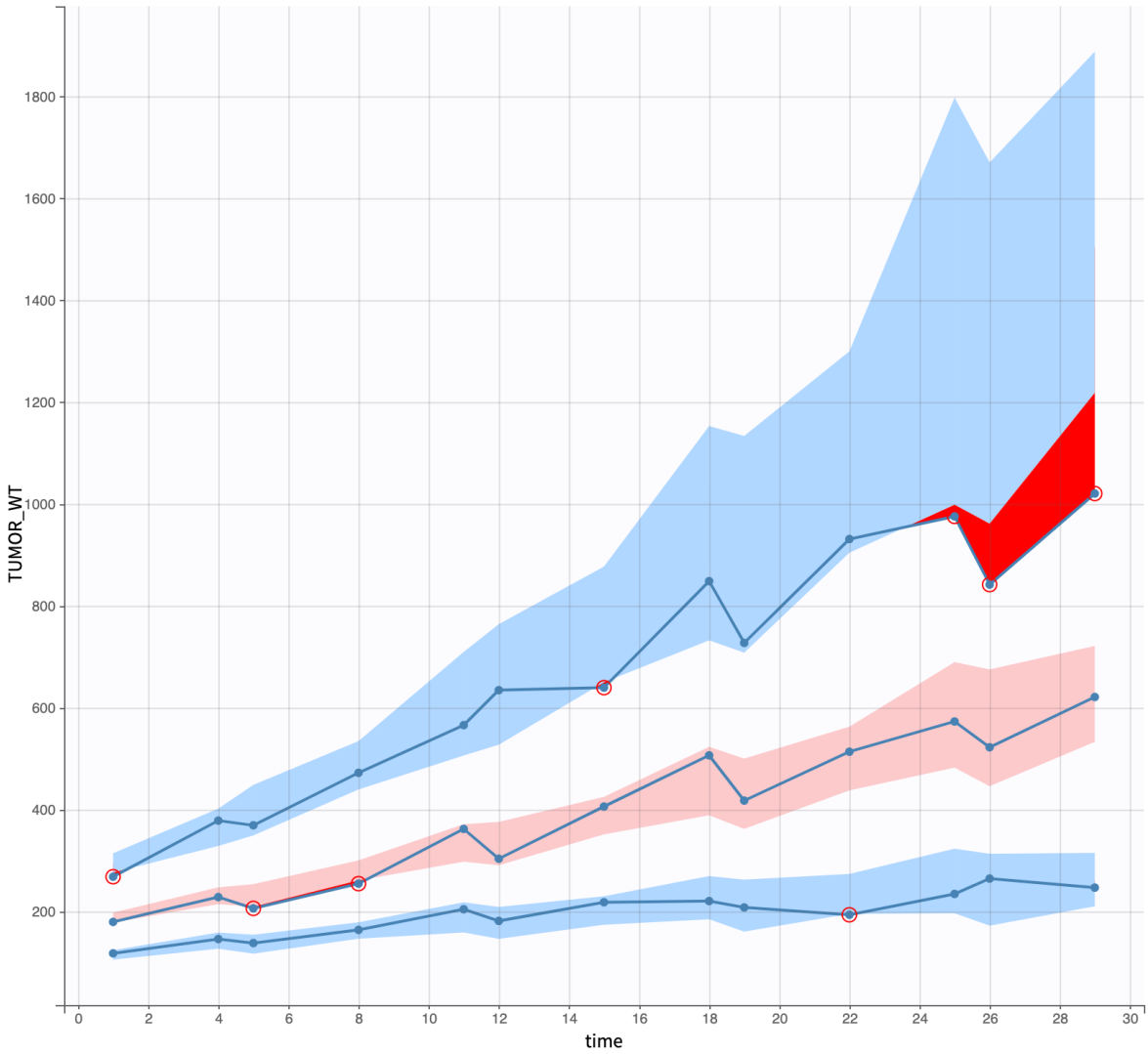

Figure D.31. *Visual predictive check for the control group simulated in Monolix [66].*

D.2.2 Carboplatin and Docetaxel in Combination with Linear

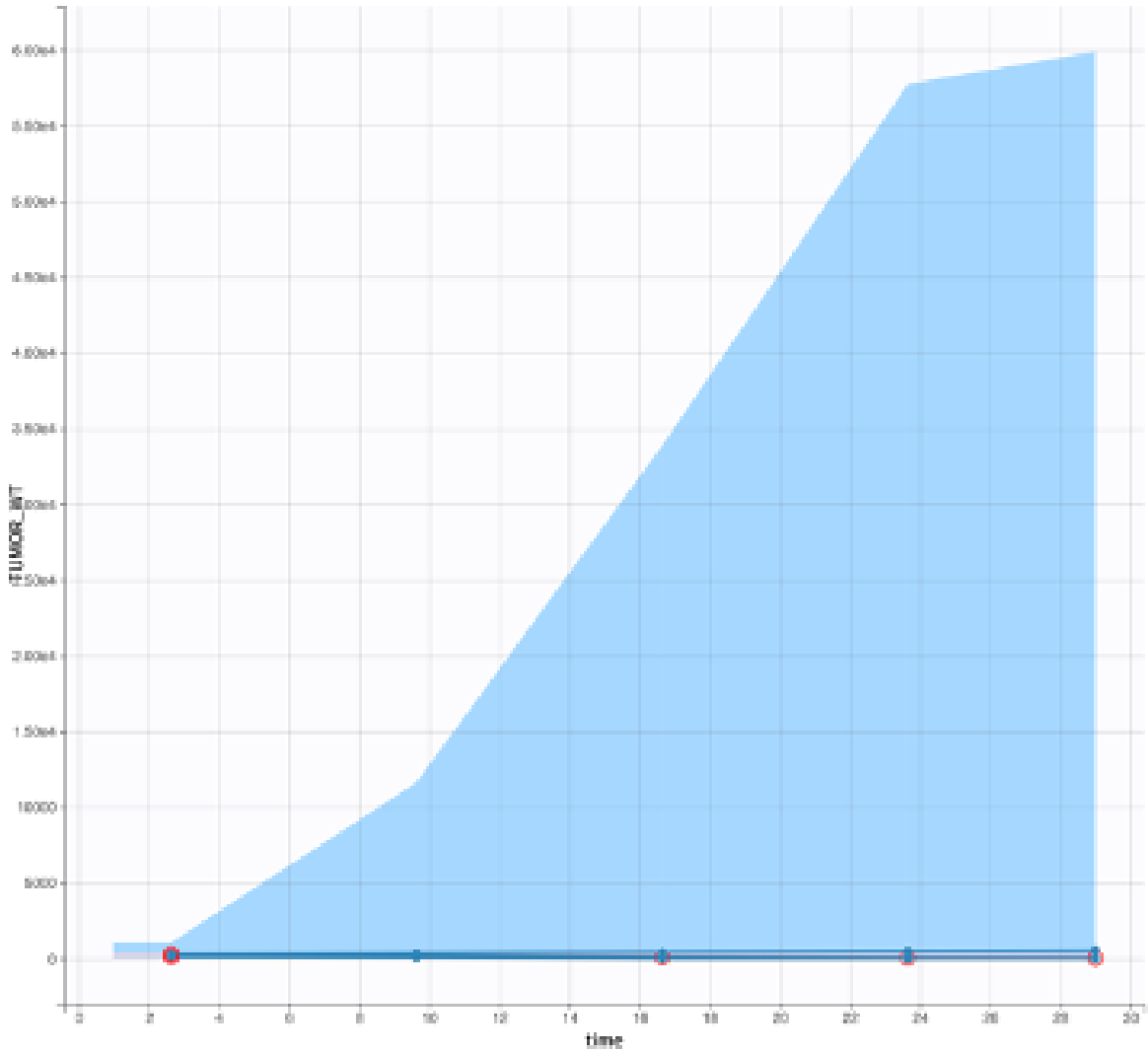

Figure D.32. *Visual predictive check for carboplatin and docetaxel in combination with the linear effect simulated in Monolix [66].*

Appendix E

Results Tables

E.1 Docetaxel Group

E.1.1 Hill Type Effect

Parameter	VALUE		S.E.	R.S.E. (%)
Fixed Effects				
beta_pop	0.44		0.14	31.9
muP_pop	0.12		0.11	92.0
muQ_pop	0.023		0.051	222
K_kill_pop	0.05		0.0068	13.7
A_pop	0.011		0.018	164
B_pop	0.98		0.48	49.1
n_pop	1.49		1.12	75.2
Parameter	**VALUE**	**C.V.(%)**	**S.E.**	**R.S.E. (%)**
Standard Deviation of the Random Effects				
omega_beta	0.26	25.96	0.17	67.7
omega_muP	0.4	41.57	1.21	304
omega_muQ	0.67	75.78	5.34	792
omega_K_kill	0.33	33.4	0.091	28.0
omega_A	1.68	396.43	1.31	78.3
omega_B	0.92	115.48	0.35	37.9
omega_n	1.08	148.17	0.54	49.8
Error Model Parameters				
a	9.42		2.66	28.3
b	0.13		0.21	162

Table E.1. *Parameter estimates of docetaxel group with the Hill type effect simulated in Monolix [66].*

E.2 Carboplatin Group

E.2.1 Hill Type Effect

Parameter	VALUE		S.E.	R.S.E. (%)
Fixed Effects				
beta_pop	0.27		0.14	51.7
muP_pop	0.18		0.13	75.0
muQ_pop	0.04		0.028	71.3
K_kill_pop	0.013		0.004	30.0
A_pop	0.28		0.5	178
B_pop	0.019		0.87	4.61e+3
n_pop	0.78		139.37	1.79e+4
Parameter	**VALUE**	**C.V.(%)**	**S.E.**	**R.S.E. (%)**
Standard Deviation of the Random Effects				
omega_beta	0.14	13.59	0.33	244
omega_muP	0.16	16.59	0.75	455
omega_muQ	0.65	72.36	0.63	323
omega_K_kill	1.08	148.07	0.16	14.6
omega_A	0.48	50.36	1.45	306
omega_B	1.82	515.84	557.06	3.06e+4
omega_n	0.72	83.02	14192.37	1.96e+6
Error Model Parameters				
a	10.87		1.83	16.8
b	0.1		0.0098	9.40

Table E.2. *Parameter estimates of carboplatin group with the Hill type effect term simulated in Monolix [66].*

Appendix F

Mathematical Formulae

F.1 Error Models

F.1.1 Constant Error Model

$$y = f + a\varepsilon \tag{F.1}$$

where:

- a: Magnitude of the error.
- f: True value
- ϵ: Random error term

F.1.2 Proportional Error Model

$$y = f + bf\varepsilon \tag{F.2}$$

where:

- f: True value
- b: Proportionality constant
- ϵ: Random error term

F.1.3 Combined Error Models

Combination of Constant and Proportional Errors

$$y = f + (a + bf)\varepsilon. \tag{F.3}$$

where:

- f: True value
- a: Magnitude of the error.
- b: Proportionality constant
- ϵ: Random error term

Combination with Square Root Formulation

$$y = f + \sqrt{a^2 + b^2 f^2}\varepsilon. \tag{F.4}$$

where:

- f: True value
- a: Magnitude of the error.
- b: Proportionality constant
- ϵ: Random error term

F.2 Performance Metrics

F.2.1 Standard Error

$$SE = \frac{s}{\sqrt{n}} \tag{F.5}$$

where:

- s: Sample standard deviation
- n: Sample size

F.2.2 Residual Standard Error

$$RSE = \frac{SE}{\overline{X}} \times 100 \tag{F.6}$$

where:

- SE: Standard error, Eq F.5.
- $\overline{X}$: Sample mean

F.2.3 Coefficent of Variation

$$CV = \frac{\sigma}{\mu} \times 100 \tag{F.7}$$

where:

- σ: Standard deviation of the dataset.
- μ: Mean of the dataset.

F.2.4 Akaike Information Criterion

$$\text{AIC} = 2k - 2\ln(L) \tag{F.8}$$

- n: Sample size.
- k: Number of parameters in the model.
- L: The likelihood.

F.2.5 Bayesian Information Criterion

$$\text{BIC} = \ln(n) \cdot k - 2\ln(L) \tag{F.9}$$

- n: Sample size.
- k: Number of parameters in the model.
- L: The likelihood.